

# **DAMMSÄKERHET**

Internal Erosion Detection at the Røsvatn Test Site Experiences from blind test using Resistivity, Self Potential, Temperature, and Visual inspection

Sam Johansson and Åke Nilsson (ed)

**Rapport 05:42** 

### **DAMMSÄKERHET**

# Internal Erosion Detection at the Røsvatn Test Site -

Experiences from blind test using Resistivity, Self Potential, Temperature, and Visual inspection

#### Part A - Assessment report

Sam Johansson and Åke Nilsson

# Part B - Design and construction of the dam and the defects

Åke Nilsson and Steve Garner

# Part C - Pre-Study and Field Measurements using Resistivity, Self Potential, and Temperature

Torleif Dahlin, Johan Friborg, Sam Johansson, and Pontus Sjödahl

Elforsk rapport 05:42

#### Context

The opportunity to perform a genuine blind test of any dam surveillance technique on a full scale dam is extremely rare. Field tests for dam breach studies have been carried out by EBL at the unique test site at Røsvatn in Norway since 2001. The possibility to use one of their test dams was therefore appreciated, and of fundamental importance for the project.

The test program described in this report is unique and focused on addressing the important question of the extent to which Self Potential and Resistivity monitoring techniques can be relied on in the investigation/monitoring of unexpected leakages in earth and rockfill dams. The blind test was designed specifically to address this question and any interpretation and/or conclusions only apply to the reliance on Self Potential and Resistivity methods to investigate unexpected leakages. Other conclusions may be drawn by inference, but these inferences must be treated as such. Two other methods (temperature and visual inspections) were also added to the test set-up to maximise the value of this unique opportunity to also test their usefulness, and to improve data collection in the light of the pre-study results.

This blind testing was designed to present a severe but fair challenge to the SP/resistivity technology during first filling and initial saturation, and like most blind tests for technologies and methods that have not been subjected to such testing, the probability of the technology passing the test is low. This was known at the outset, especially given the results of the earlier theoretical study (i.e. the "Pre-study"), the results of which were so pessimistic that the project was almost abandoned. However, the decision to proceed was made on the understanding that the blind test also provided an opportunity to test the theory and underlying assumptions.

The test was only made possible by the willingness of HydroResearch and its associates to perform the field measurements and interpretations in an objective way in the best interests of advancing scientific knowledge.

The project was divided in separate parts, all co-funded by Elforsk and BCHydro.

Lars Hammar Elforsk AB Des Hartford BCHydro

#### **Executive Summary**

#### General

Resistivity, Self Potential, and Temperature are three indirect methods for leakage monitoring in embankment dams. The interpretation of the result is however sometimes uncertain, and furthermore often difficult to verify with other methods. BC Hydro (Canada), Elforsk AB (Sweden) and EBL represented by Statkraft Grøner (Norway) jointly conducted a research project in order to test the performance of those methods at the unique test site at Røsvatn in Norway. Defects were constructed in the test embankment dam 2003-1, built in July 2003. The project team was separated into a "defect design group", and a "monitoring group". This arrangement allowed making the monitoring as a blind test, in order to test the capability of these different methods. A reference group was also created for the project.

#### **Pre-study and Design**

A pre-study was carried out by the "monitoring group" in order to estimate the detection level of the electrical methods. The sensitivity for different defect sizes, materials, and locations were simulated by numerical modelling. The need of temperature measurements was obvious, and was therefore added. The simulations showed that surely detectably defects for both resistivity and SP must be in the order of one m<sup>2</sup>. The soil properties are important to verify and several laboratory tests should be done.

The dam, with a height of 5.25m and a length of 37m, was built with a central core of moraine with supporting rock fill. Three defects were constructed with a cross-section of 0.16m<sup>2</sup>, i.e. about six times smaller than the smallest detectable size found in the pre-study for defects located at 3m depth. According to the pre-study none of the real defects should be possible to detect with the electrical methods, using an investigation approach. The fact that none of the designed defects were going to be detected according to the pre-study was considered in the "reference group". No changes were suggested because the designed defects were considered to be possible sizes of defects of interest to detect in real full scale dams. It was also assumed that the report from the "monitoring group" might indicate a conservative position, and the optimum design was judged to be achieved if some of the defects were going to be detected and some not.

## Field Measurements (extracted from the summary written by "the monitoring group" before the location of the defects were revealed)

Measurements were made with empty reservoir at three occasions and at five reservoir water levels. The original methods (Resistivity, Self Potential and Temperature) were used together with IP (Induced Polarization) and Visual Inspection at the dam toe. In total 61 electrodes for resistivity measurements were installed along the exposed dam core. Excellent data quality was achieved due to good electrode contact and short electrode separations. For the time-series SP measurements 49 non-polarizable Cu-CuSO<sub>4</sub> electrodes were installed. SP was also measured manually in three cross-sections, and along the shore-line. Temperature measurements were carried out along the dam toe, using 23 temperature sensors.

Transient thermal impact due to short time temperature changes and temporal resistivity changes in the core material were found to be more complicated than what was foreseen in the Pre-Study. The resistivity of the reservoir water was also lower than assumed, which reduced the contrast between materials. The conditions for the SP measurements were

found to be more complicated than assumed in the pre-study. Furthermore, the resistivity of the core material and the reservoir water was lower than expected, causing lower SP anomalies than predicted in the pre-study. The collected final information from all methods shows three main defect areas. The most significant defect is found around section 22m, which is shown by all methods. The elevation is more uncertain varying from elevation 365 to 368m. A second significant defect is observed at section 27m at elevation 365-367m. The SP anomaly is however weak and interpreted only as possible defect. A third area is probably somewhere around chainage 5m, and at any level between 365 and 369m.

#### Assessment

All defects built in the dam were small, and none should have been detected according to the predictions made in the Pre-Study. However, the pre-study assumed an investigation approach where anomalies due to material differences should be able to detect. Due to the different water levels in the reservoir a monitoring approach could be adopted that increased the detection level of the methods. Three defects (Defect A, B and C) were constructed carefully, but an undesired leakage area occurred around the drainage pipes (called Defect D below), with a similar leakage flow as the other three defects. All those four defects were detected by temperature measurements and by visual inspections, if we allow a deviation of two meter along the dam. Both these methods are performed from the downstream toe, and cannot exactly locate the defects in the core, neither along the dam nor at the level. The conditions at the site were however favorable for both methods compared to normal conditions at a typical embankment dam.

The section for Defect D was probably detected by resistivity measurements based on the investigation approach alone. If a two meter deviation can be accepted also the section for Defect A was found by the same approach. These defects were confirmed using the monitoring approach, by which also Defect B was detected. In total, this result is well above the expectations given in the pre-study, although defect C should have been detected. The conditions for the SP-measurements were much more complicated than indicated in the pre-study, and none of the defects should be detected by the method. However, using the monitoring approach defect B was indicated as a weak anomaly, close to the monitoring accuracy. Another indication of a defect was given 2m to the right of Defect A. The other defects were not detected, while two other areas were pointed out.

No final conclusion about the general application of resistivity and SP can be made until the electrical properties of the soil material have been determined. The experience from these tests indicates that resistivity and SP seems less sensitive than temperature and visual inspections, but the conditions at the test were in some aspects favorable to the latter methods. Both resistivity and SP will give information in the core, in opposite to the other methods that just give information at the dam toe. The information given by the resistivity measurements was in this test more informative than the SP measurements.

The test show that temperature, resistivity, and SP may be used at investigations, but result from single or short time investigations are complicated to evaluate, and less accurate than result from long time monitoring. All methods are expected to be more suitable methods for long time monitoring. This was indicated in the pre-study, proved in the field test, and agrees with the experience gained from the ongoing long term monitoring tests in Sweden.

# Internal Erosion Detection at the Røsvatn Test Site PART A Assessment report

Sam Johansson HydroResearch Sam Johansson AB Åke Nilsson Swedpower AB

#### **Summary**

The result from the blind test at unique test site at Røsvatn has given valuable experience of the detection ability for geophysical methods as temperature, resistivity and self potential, compared to visual inspections. Although some important material data still is missing, some conclusions have been drawn for the extensive data material.

All defects built in the dam were small, and none should have been detected according to the predictions made in the Pre-Study. However, the pre-study assumed an investigation approach where anomalies due to material differences should be able to detect. Due to the different water levels in the reservoir a monitoring approach could be adopted that increased the detection level of the methods. Three defects (Defect A, B and C) were constructed carefully, but an undesired leakage area occurred around the drainage pipes (called Defect D below), with a similar leakage flow as the other three defects.

All four defects were detected by temperature measurements and by visual inspections, if we allow a deviation of two meter along the dam. Both these methods are performed from the downstream toe, and cannot exactly locate the defects in the core, neither along the dam nor at the level. The conditions at the site were however favorable for both methods compared to normal conditions at a typical embankment dam.

Defect D was detected by resistivity measurements based on the investigation approach alone. If a two meter deviation can be accepted also Defect B was found by the same approach. This is better than expected, based on the result from the pre-study. These defects were confirmed using the monitoring approach. Defect A was also detected using the monitoring approach. Defect C was not detected. In total, this result is well above the expectations given in the pre-study.

The conditions for the SP-measurements were much more complicated than indicated in the pre-study, and none of the defects should be detected by the method. However, using the monitoring approach defect B was indicated as a weak anomaly, close to the monitoring accuracy. Another indication of a defect was given two meter to the right of Defect A. The other defects were not detected, while two other areas were pointed out.

No final conclusion about the general application of resistivity and SP can be made until the electrical properties of the soil material have been determined. The experience from these tests indicates that resistivity and SP seems less sensitive than temperature and visual inspections, but the conditions at the test were in some aspects favorable to the latter methods. Both resistivity and SP will give information in the core, in opposite to the other methods that just give information at the dam toe. The information given by the resistivity measurements was in this test more informative than the SP measurements.

The test show that temperature, resistivity, and SP may be used at investigations, but result from single or short time investigations are complicated to evaluate, and less accurate than result from long time monitoring. All methods are expected to be more suitable methods for long time monitoring. This was indicated in the pre-study, proved in the field test, and agrees with the experience gained from the ongoing long term monitoring tests in Sweden.

# Part A - Assessment report

#### SUMMARY

#### CONTENT

1	11	NTRODUCTION	
2	D	ESIGN AND CONSTRUCTION OF THE DAM AND THE DEFECTS	2
3	E	XPERIENCES FROM PRE-STUDY	4
	3.1 3.2	BACKGROUND AND MODELING ASSUMPTIONS  RESULT  POST-DISCUSSION	4 4
4	Т	EMPERATURE	7
	4.1 4.2 4.3	MONITORING AND EVALUATION	7
5	R	ESISTIVITY – FIELD MEASUREMENTS	9
	5.1 5.2 5.3	MONITORING AND EVALUATION	9
6	S	P SURVEYS – FIELD MEASUREMENTS	12
		MONITORING AND EVALUATION  RESULT  DISCUSSION	12 14
7	٧	ISUAL OBSERVATIONS- FIELD MEASUREMENTS	15
		MONITORING AND EVALUATION RESULTS DISCUSSION	15 16
8	11	NTEGRATION OF MEASUREMENTS RESULTS	20
^	_	DONOLLISIONS AND DECOMMENDATIONS	04

#### 1 INTRODUCTION

Resistivity, Self Potential, and Temperature are three indirect methods for leakage monitoring in embankment dams. The methods have been used in several embankment dams for investigation and monitoring at research applications and practical use. The interpretation of the result is however sometimes uncertain, and furthermore often difficult to verify with other methods. BC Hydro (Canada), Elforsk AB (Sweden) and EBL represented by Statkraft Grøner (Norway) jointly conducted a research project in order to test the performance of those methods at the unique test site at Røsvatn in Norway.

The test embankment dam "2003-1" was built in July 2003. Defects, consisting of permeable material, were constructed though the impervious core in order to test the expected ranges of capabilities of the geo-electrical techniques to detect leakage in embankment dams. Field measurements using temperature, resistivity and self potential were tested. In addition, "visual observations" of leakage water along the toe of the dam during the test period were used as a method to determine the locations of the defects in the core.

The project team was separated into a "defect design group" which did not participate in the monitoring, and a "monitoring group" which had no knowledge of the locations and sizes of the zones of high seepage. This arrangement allowed making the monitoring as a blind test, in order to test the capability of these different methods. A reference group was also created for the project. The members in the groups are shown in the table below.

Defect design group	Monitoring group	Reference group
Steve Garner, BC Hydro	Torleif Dahlin. LTH (Resistivity,	Des Hartford, BC Hydro
Åke Nilsson, SwedPower	IP)	Lars Hammar, Elforsk
	Johan Friborg, HydroResearch (SP)	Aslak Lövoll, EBL
	Sam Johansson, HydroResearch (Project leader, temperature, and visual inspection)	Einar Ødemark, Statkraft- Grøner,
	* '	Tina Fridolf, Svenska Kraftnät,
	Pontus Sjödahl, LTH (Resistivity, IP, and visual inspection)	Malte Cederström, Vattenfall Vattenkraft.

The following part is an assessment report presenting a comparison of the results of the field measurements with the geometric locations of the defects.

Reference is given to the following PARTS in this research project.

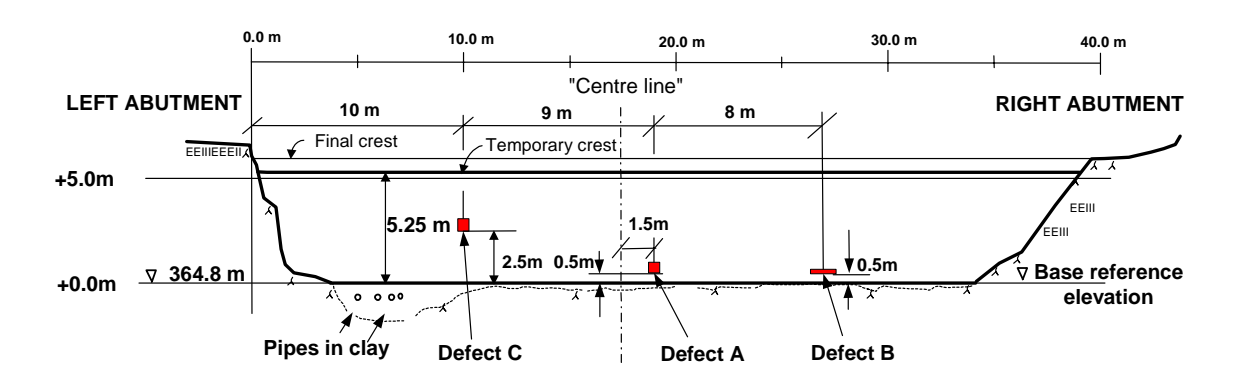
- A. Assessment report
- B. Design and construction of the dam and the defects
- C. Pre-study and Field measurements, as delivered in October 2003. (A preliminary version of the Pre-study was delivered in June 2003, and a draft in May 2003).

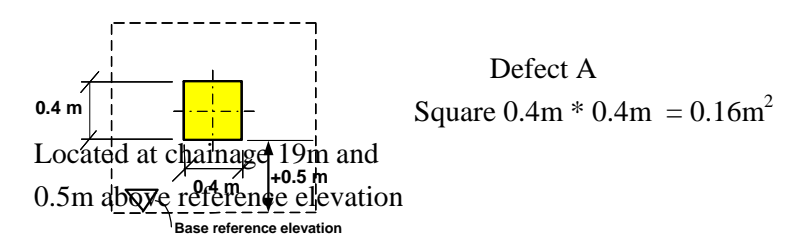
This assessment report should be read together with the part B and C where are all details are shown.

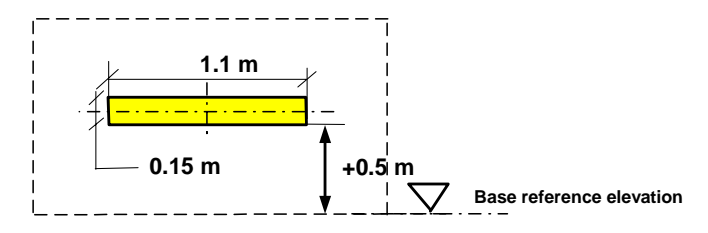
# 2 DESIGN AND CONSTRUCTION OF THE DAM AND THE DEFECTS

The core was constructed by moraine with a low content of boulders. The content of fines was approximately 28% calculated on the material less than 20 mm.

The location and geometry of the defects are shown in **figure 1**. The three defects (called A, B and C) are also shown relative to the cross-sectional geometry of the core, as well as upstream and downstream shells in **figure 2**, **3** and **4**. The material in the defects was a sandy gravel from a natural deposit. Most of the minus 2mm material was washed out from the natural material before it was used for the construction of the defects.







Defect B
Rectangular 0.15m \* 1.1m = 0.16m<sup>2</sup>
Located at chainage 27m, and 0.5m above reference elevation

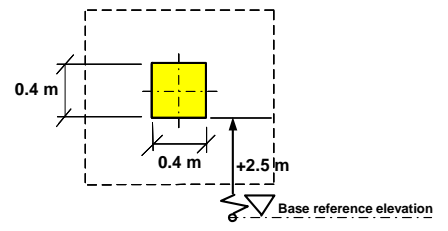


Figure 1 Location and sizes of defects.

Base reference elevation

Defect C Square  $0.4m * 0.4m = 0.16 m^2$ 

Located at chainage 10m, and 2.5m above reference

elevation

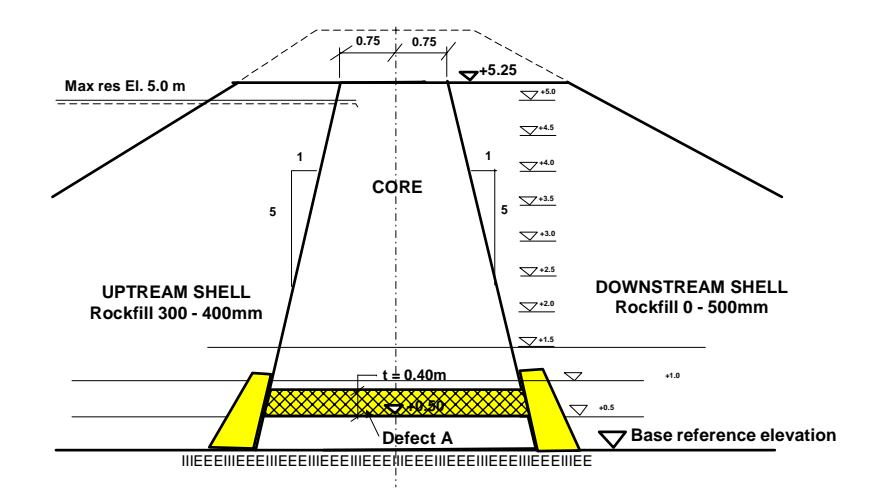


Figure 2 Defect A.

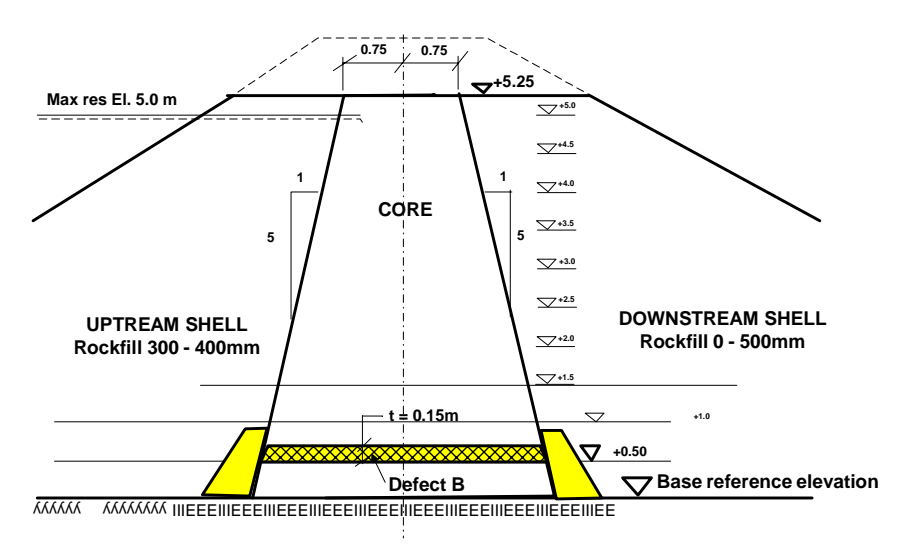


Figure 3 Defect B.

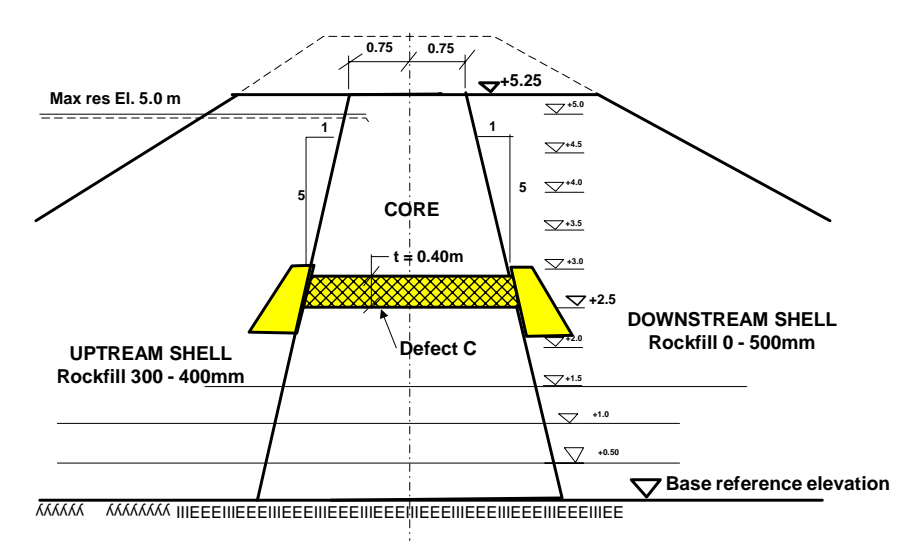


Figure 4 Defect C.

#### 3 EXPERIENCES FROM PRE-STUDY

#### 3.1 Background and modeling assumptions

A pre-study was carried out by the "monitoring group" in order to estimate the detection level of the electrical methods. The sensitivity for different defect sizes and locations were simulated by numerical modelling. The importance of different parameters was also studied.

The dam used in the pre-modelling was 40m long and 6m high funded on rock, with steep abutments also of rock. Extensive modelling was made for resistivity and SP, which was the two primary methods in the initial phase of the pre-study. Since those methods are temperature dependent, preliminary thermal simulations were performed. No sensitivity simulations were made for temperature measurements. The pre-study indicated, however, a clear need of temperature measurements, and it was decided to include such measurements in the field test.

Soil properties data for this application are rare, especially for the cross-coupling coefficient, which is important for the SP measurements. The values used in the simulations were assumed based on literature data and experience from dam monitoring in Sweden. These parameters have a large variation in soils, and laboratory tests of the real materials in the test dam were recommended.

In order to estimate the detectable defects, sensitivity analysis was made for two square and two rectangular defects. Two different areas,  $0.25m^2$  and  $1.0m^2$ , were studied. The defects were placed at three different depths (1m, 3m, and 5m). Three different defect materials were also studied: fine sand, coarse sand, and gravel. Thus, 36 different simulations were performed.

#### 3.2 Result

Single investigations or long term monitoring using geophysical methods give different possibilities for seepage detection. Single investigations are less powerful because just absolute values and relative values in space could be used for evaluation. Long term monitoring provides also evaluation of relative changes in time, which often can be related to anomalous seepage flow. The situation at the test site is more like investigation than long term monitoring. The calculated sensitivity may be improved if relative evaluation techniques can be applied. The results of this study will not be valid for long-term monitoring.

The thermal simulations showed that the temperature change in the soil may have the same impact on the resistivity as the resistivity change between the proposed materials in the defects. A detected resistivity anomaly will thus have two unknowns (resistivity of the soil and temperature). It was therefore suggested that temperature measurement should be performed, preferably inside the dam, but at least at the dam toe during the field tests.

The simulations showed that surely detectably defects for both resistivity and SP must be in the order of one m<sup>2</sup> for defects located in the middle of the dam. Defects in the lower part will be difficult to detect. Defects should not be placed close to the abutments due to boundary influence. Avoid the area closer than 5-10m from the abutments (1-2H) especially for deep located defects (this is valid both for resistivity and SP).

The soil properties are important to verify and several laboratory tests should be done. Drainage of excess water from construction and from precipitation may also affect the result. The variation in compaction during construction may in this case be seen as resistivity variations caused by temperature changes between the soil and the water in the reservoir.

#### 3.3 Post-discussion

The size of the dam and the geometry used in the pre-study agrees well with the real test dam. The result should, in that aspect, be valid.

The results in the pre-study from the "monitoring group" were discussed in the "reference group" before the construction commenced. The fact that none of the designed defects were going to be detected according to the pre-study was considered. Anyway it was agreed that the design was going to be kept in principle as it was. The reason why it was agreed not to enlarge the permeable zones was that the designed defects were considered to be possible sizes of defects of interest to detect in real full scale dams. It was also assumed that the report from the "monitoring group" might indicate a conservative position, and the optimum design was judged to be achieved if some of the defects were going to be detected and some not.

Hence, all defects in the dam got an area of  $0.16m^2$ , i.e. about six times smaller than the smallest detectable size found in the pre-study for defects located at 3m depth. Two defects were also located at larger depth. According to the pre-study none of the real defects should be possible to detect with the electrical methods, using an investigation approach. Evaluation based on relative changes (i.e. using a monitoring approach) at different water levels would however improve the possibilities to detect the defects.

The samples of the resistivity of the reservoir water at the test site were taken, showing resistivities between 138-184 $\Omega$ m. This is less than a half of what was assumend in the prestudy (400 $\Omega$ m), which will affect the contrast between materials. Water saturated defect zones will thus have less contrast versus surrounding core material than anticipated.

No full laboratory tests of the electrical properties of the soil materials in the defects and in the fill have yet been performed. Only the resistivity of one sample from the core material has been tested, showing challenging transient behaviour. The validity of the assumed input data for the simulations has thus not been able to verify.

Based on the formation curves of the defect material it is probable that the resistivity contrast between the material in the intact core and the defect was smaller in the dam than assumed in the pre-study. This decreased the possibility to detect the defects.

#### **ELFORSK/BC Hydro**

The clay used for sealing on the rock foundation was not anticipated in the Pre-study. This clay is expected to have a very low resistivity and if it was extensively used it would constitute a very conductive layer at the bottom of the dam and thereby create difficulties for the method in handling the very high contrasts in resistivity compared to the rock. This will definitely decrease the resolution of the resistivity measurements in this zone.

In conclusion, the real monitoring situation at the test site seems to have been more difficult than what was assumed in the pre-study, especially for the SP measurements.

#### 4 TEMPERATURE

#### 4.1 Monitoring and evaluation

A number of 23 temperature sensors (PT100) were installed about 5 cm deep in the gravel between the large boulders along the dam toe. Due to the boulders the distance between the sensors varied between 1.2 and 2m, with a mean distance of 1.45m. The temperature of the upstream water was also measured. Data was collected in a logger each five minute. Evaluation was mainly performed by searching significant temperature changes or anomalies.

#### 4.2 Result

The results from the field temperature measurements were summarised by the "monitoring group" in the following table (extracted from the field measurement report, Part 3). Temperature measurements at the dam toe can normally not exactly determine the level of a defect, just the location along the dam. In this case, however, information from the different fillings could be used to estimate also the level. The elevation is therefore set to the inflow level  $\pm 0.5$ m. Four possible leakage outflow zones were found. These zones are indicated in green together with the actual locations marked in red (**figure 5**).

Table 1 Summarised result of temperature measurements

Dam section	Detected	Inflow level	Final width at the dam toe	Seepage flow, q (l/s,m <sup>2</sup> )	Estimated area, A, in the core (width x height)	Leakage flow Q, (=q*A) after filling #3 (l/s)
5.7m	Filling #1 and #2	365.5m	1.5m	0.4	1x1m <sup>2</sup>	0.4
10.2 – 11.6m	Filling #3 or #2	368	2- 3m	0.3	2x1m <sup>2</sup>	0.6
20.7m	May be already at Filling#1, but definitively at filling #3	366	1.5m	0.2	1.5x1m <sup>2</sup>	0.3
26.4 – 28.4m	Filling #1 and #2	365.5m	2 - 3m	>0.6	2x0.5m <sup>2</sup>	>0.6

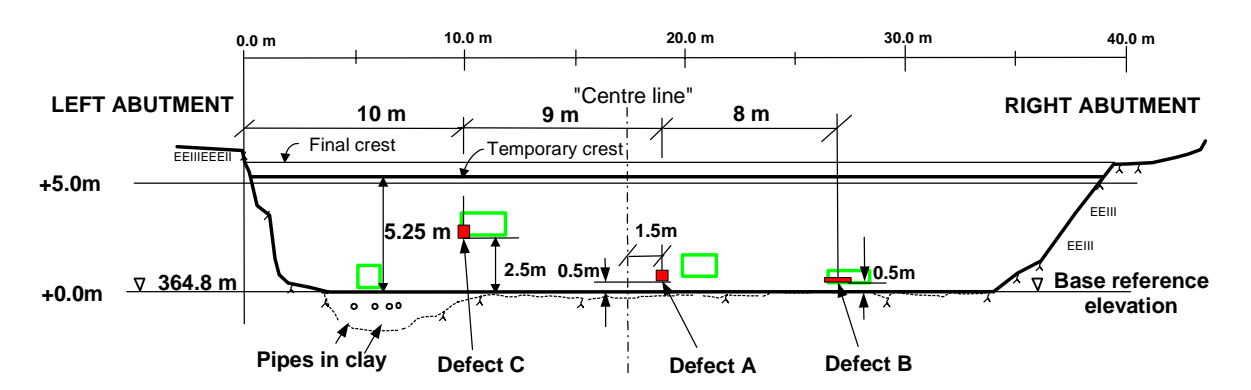


Figure 5 Defect areas from temperature measurements (green) in comparison with actual locations (red).

A good correlation can be seen between the field observations and the actual locations of the built-in defects. The left indicated defect from the field measurements represents observations of leakage along the diversion pipes in the foundation close to the left abutment.

The good quality of the data in combination with the different water levels allowed also the possibility to estimate the seepage flow velocity, as shown in the table above. A first attempt to estimate the total flow was also made based on the information achieved from the dam toe, and a flow of about 2l/s was found. This flow was about 6 times higher than the measured flow (0.35l/s, at Filling #3 when the defects were observed). However, a significant amount of water was leaking under the concrete bar, not only at outflow around the pipes. The real flow was probably about twice the measured flow, according to the visual inspections.

With knowledge of the real defect area (0.16m²) the total seepage flow can be recalculated. Evaluated flow at defect A will then be 0.2\*0.16=0.3l/s, at defect B 0.6\*0.16=0.1l/s, and 0.3\*0.16=0.5l/s at defect C. A total flow in the defects of 0.9l/s is achieved, which agrees better with the estimated total flow. This indicates that the advective heat transport mechanism is well understood. However, the size of the defects will always be larger at the dam toe, and the resolution will depend on the spatial resolution, i.e. the distance between the temperature sensors.

#### 4.3 Discussion

The blind test at Røsvatn confirmed that temperature measurement is a sensitive method to detect seepage outflow. The transient process at the first fillings was however favourable and increased the temperature changes at the test. This situation will not be valid at a normal temperature investigation at a dam. On the other hand, the use of the seasonal temperature variation may give a similar result also at single investigations at full size dams.

The best application of the method is long term monitoring, where slow and small seepage flow changes can be both detected and quantified. Overall experience from temperature measurements shows a sensibility in the order of some  $10^{-5} \text{m}^3/(\text{s,m})$  for dams up to a height of around 30m at measurements in the dam toe. This is about a 10 times smaller flow than what was detected in the test. The measured temperature change was however large at the field tests, and a smaller temperature change should probably have been detected.

The ultimate application of this technology is to monitor the temperature continuously in fibres downstream the core (at new dams) or bury optical fibres in a trench along the dam toe at existing dams. This will provide possibilities to both locate anomalous seepage areas and estimate the small seepage flow changes.

#### 5 RESISTIVITY - FIELD MEASUREMENTS

#### 5.1 Monitoring and evaluation

The resistivity measurements were carried out as two-dimensional (2D) resistivity imaging with 63 electrodes installed on the core crest, with a spacing of 2/3 metre. A modified version of the ABEM Lund Imaging System was used, which allows resistivity and induced polarisation (IP) data to be recorded in seven channels simultaneously. Since the electrodes were installed directly in the dam core the electrode contact resistances were low, and the recorded data stable and of excellent quality.

Measurements were carried out with different electrode arrays. The acquired data was analysed through inverse numerical modelling (inversion). Time-lapse inversion was employed to analyse the data from the repeated measurements for change in resistivity. Evaluation of the resistivity data were made due to: resistivity at each time alone, differences between water levels, and difference between time-steps.

#### 5.2 Result

The results from the field resistivity and IP measurements were summarised by the "monitoring group" in the following table extracted from the field measurement report (Part 3). The size of the defect areas are generally supposed to be smaller in reality than showed by the method, due to smoothing, and secondary disturbance around the defects.

Table 2 Summary of detected defects and possible defects by geoelectrical imaging.

Dam	Observed	Resistivity	Level	Comment
section		evaluation	(m)	
(m)		method		
7 (5-8)	Several	Resistivity at	367-368	Higher resistivity
	levels	each time		Faster/larger decrease in res.
		alone and		Decrease in IP
		difference		
		between levels		
22 (20-24)	All levels	Resistivity at	368-369	Higher resistivity
	and filling	each time		Faster/larger decrease in res.
	#4	alone and		Decrease in IP
		difference		
		between levels		
27 (25-29)	Filling #2	Difference	365-367	Faster/larger decrease in res.
	and	between levels		Decrease in IP
	filling #3	and between		
		time steps		
Possible, bu	ıt less certain re	esult.		
16 (15-17)	After fill-up	Difference	369	Faster/larger decrease in res.
	and drainage	between time-		Decrease in IP
		steps		
27 (26-28)	Several	Resistivity at	369	Higher resistivity
	levels	each time		
		alone		
36 (35-37)	After fill-up	Difference	367-368	Decrease in IP
	and drainage	between time-		
		steps		

Two defect areas (around section 7 and 22m) were detected from initial measurements before filling (i.e. similar to an investigation). Three defect areas, including the two already mentioned, were detected based on several observations (i.e. similar to monitoring). Three other areas were classified as "possible, but less certain", because these anomalies were just observed based on one or two weaker indications. All defect areas are indicated in green together with the actual locations marked in red (figure 6). According to the result in the pre-study none of these defects should be detectable. No attempt to correct for the 3D implication for the depth estimation was made by the monitoring group. The observed defects will therefore appears higher than the real defects.

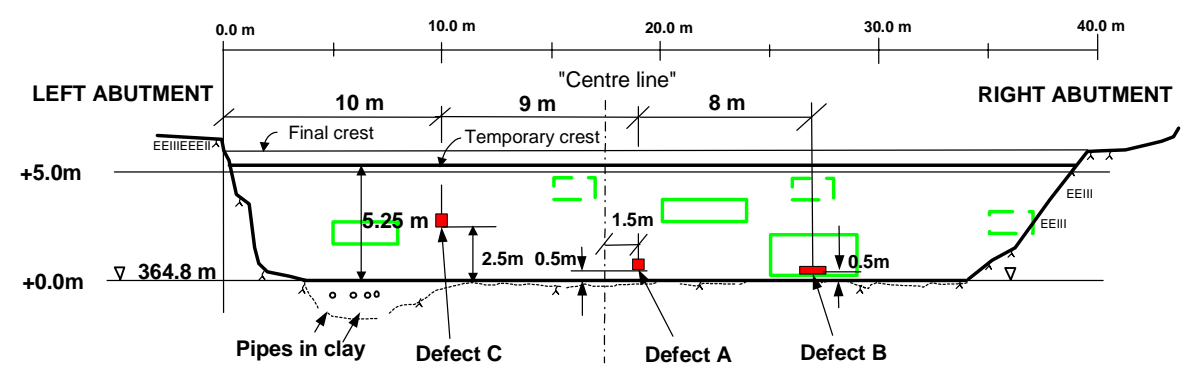


Figure 6 Defect areas from resistivity measurements (green line), "possible but less certain" areas (dotted green lines) in comparison with actual defect locations (red).

The best agreement is found for defect B using the monitoring approach. The second observed defect area is close to Defect A. The horizontal location is about one metre away, while the depth is about 3m higher. The horizontal location is normally easier to determine, but the very small resistivity anomalies in this case may have influenced the interpretation. Defect C was not detected by the measurements. It is also probable that the leakage around the pipes was detected, even though the depth was not correct. This anomaly was observed in the outer part of resistivity image where the result is less certain due to fewer measurements, where it is even more difficult to estimate the depth.

The "possible, but less certain" areas do not match with any of the defects, and may be explained by small variations in the soil properties, way of construction etc. They may also be influenced of the transient resistivity change, which was observed during the test period. Several explanations were discussed such as, slow/different saturation, out wash of fines in rock fill, chemical equilibrium between the water and the soil was not yet obtained.

#### 5.3 Discussion

Ideal installation possibilities gave measurements of excellent data quality, with similar accuracy that is obtained at a full size dam in Sweden in which long term resistivity monitoring are performed. The measurements were in that aspect well performed. However, the real monitoring conditions were less favourable than assumed in the pre-study: the resistivity of the reservoir water was lower than assumed, transient resistivity changes, and probably smaller resistivity contrast between the soil in the defect and in the core.

From the above comparison it is concluded the resistivity measurements detected defect B, despite that it was located 0.5 m above the foundation level. The defect was found by the monitoring approach.

The indication beside Defect A may also agree with the real situation, because of the wide filling of gravel downstream the defects. The defect indicated by the field measurements close to the left abutment was possibly influenced by the leakage along the diversion pipes in the foundation in this area. These two defects were detected by pure resistivity differences alone (i.e. the normal investigation approach), which should not have been possible according to predictions in the pre-study. Both were also confirmed by the relative evaluation methods (i.e. the monitoring approach).

It is notable that Defect C was not detected while Defect A was detected by the monitoring approach. These defects are identical in size, but Defect C is closer to the crest and should be easier to detect. However, according to the pre-study none of these defects should have been detected. Defect A was detected by the monitoring approach, which needs some time and different water levels. May be the less number of measurements and water levels above the level of Defect C, the comparison possibilities are fewer. A defect will then be more difficult to detect.

The monitoring approach (i.e. evaluating changes, seasonal variations etc) increases the detection ability, as clearly shown in the test. Long term measurement will probably be necessary to detect real seepage anomalies in normal dams using resistivity. However, the investigation approach could also be valuable.

#### 6 SP SURVEYS - FIELD MEASUREMENTS

#### 6.1 Monitoring and evaluation

Two types of SP-measurements were performed in the project: time-series measurements using fixed installed electrodes (i.e. similar to long-term monitoring), and repeated one-time measurements (similar to single investigations). The latter measurements were made in three cross-sections and one off-shore section.

For the time-series measurements 49 non-polarizable Cu-CuSO<sub>4</sub>electrodes were installed along the upstream edge of the exposed dam core. The electrode spacing was 0.8m and the profile covers section 0 to 38.4m. The voltage measurements were performed with the same multi-electrode measuring system that was used for the resistivity measurements. The telluric variation, which was also recorded during all measurements, was found to be large, and higher than expected. The pre-study indicated very small SP anomalies, generally less than 10mV. Useful information from raw data was extracted by: telluric correction, spike removal filtering, and finally, and moving median filtering.

Evaluation was basically made assuming that influx areas acquire a negative charge and outflux areas acquire a positive charge, as showed by the calculations in the pre-study. The measured potential generally depends on the pressure gradient, i.e. the water level. However, the resistivity changes (in space and time) must also be accounted for. The monitoring noise, and the transient processes complicates the evaluation. Generally, it was concluded that any area with high SP variation over time should be considered as possible defect location.

#### 6.2 Result

The results from the field SP measurements were summarised by the "monitoring group" in the following table extracted from the field measurement report (Part 3). Due to the weak anomalies it was not possible from the field measurements to surely indicate the depth to the possible defects, although some data depths were discussed in the report. They were however not presented in the final table, due to its uncertainty. The upper level of the defect was set therefore set to the inflow level.

The upper four defects shown in the table were obtained from the time-series measurement while the last one at 30m was detected from an investigation on the shoreline. However, all SP-anomalies are small, and close the monitoring accuracy. No information about defects was obtained from the cross sections at section 10m (where Defect C was located), 21m, and 31m.

Table 3	Summarised	result of SP	measurements

Dam section (m)	Observed at	Comments
2.4-3.2	Filling 1, 3, 4, 6 5 (w)	<368m
12.8-14.4	Filling , 2, 4 1 (w)	<368m
20.0-24.8	Filling 3, 4, 5 (w)	<368.5m
27.2-28.0	Filling 1(w), 2(w), 3(w)	<368m, very tentative result
30	Shoreline profile	367m

The presented defect areas obtained from the SP measurements are presented together with the defects in **figure 7.** These reported areas are indicated in green together with the actual defect locations marked in red. In figure 7 below the areas identified from the field data by the "monitoring group" are indicated down to the foundation elevation.

Only Defect B is detected by SP-measurements. However, the detection is weak, and should not have been reported as defect just based on the information from just SP-measurements. "There are also a number of weaker anomalies that one would not dare interpret as possible defects areas based on SP alone. Section 27.2-28m is one such example." However, resistivity measurements should generally be used to at SP measurements to improve the interpretation.

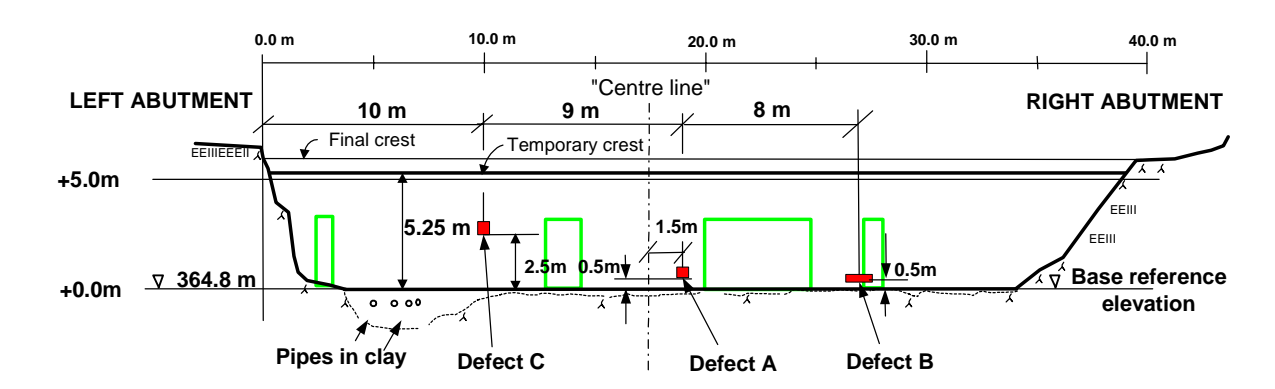


Figure 7 Defect areas from SP Surveys (green) in comparison with actual locations (red).

The conditions for the SP measurements were found to be much more complicated and less favourable than was assumed in the pre-study. The tellurics were large, and the resistivity of the core material and the reservoir water was also lower than expected. This means that any SP anomalies will be attenuated to about the half, compared with the predictions in the pre-study. The cross coupling coefficients are still unknown and could affect the result in any way.

#### 6.3 Discussion

From the above comparison it is concluded that only defect B could be found by the SP measurements and even this indication was a weak one. The result, however, cannot be interpreted as the method not being sensitive enough to detect small seepage/material anomalies, due to the unfavourable monitoring situation at the test site.

According to the predictions in the pre-study, none of these defects should be detectable using SP. This conclusion is verified by these tests. However, laboratory tests of the cross-coupling coefficient of the different materials are needed to confirm the above conclusions.

#### 7 VISUAL OBSERVATIONS—FIELD MEASUREMENTS

#### 7.1 Monitoring and evaluation

Most leakage areas in embankment have been detected by visual inspections of the dam toe. This traditional method was also used here on a more regular base for each filling except for filling #1. The method will only be able to detect the outflow, and will not say anything about which level a defect is located.

#### 7.2 Results

The results from the visual observations in the field were summarised by the "monitoring group" in the following table extracted from the field measurement report (Part 3). Six different areas were observed at the dam toe.

oummariseu i	esuit of visual ob	servations.			
Dam section	Observed at	Outflow level	Inflow level	Extension	Estimated Seepage flow
	-141 //- 4	(m)	(m)		(1/s)
Sec 0-2m	Filling #1 and	Dam toe	367		
	#2	+0.5m			
	(Morning after	(Seepage			
	lowering the	face in			
	reservoir)	silty clay)			
Sec 4-6m	Filling #3	Dam toe	368.5	1-2m wide	
Sec 6- 11.5m	Filling #4	Dam toe	369.5	3-5 m wide	
Sec 8.5m	Filling #3	Dam toe - 1m	368	Around the pipe	0.2
Sec 18,	Filling #3	Dam toe	368	2-3m wide	
21-23m					
Sec 27m	Filling #1 and	Dam toe	366.5	0.5x0.3m	0.1-0.3

Table 4 Summarised result of visual observations.

These areas are indicated in green together (using the inflow level as the upper limit and the outflow level as the lower limit). The real defect locations marked in red (**figure 8**).

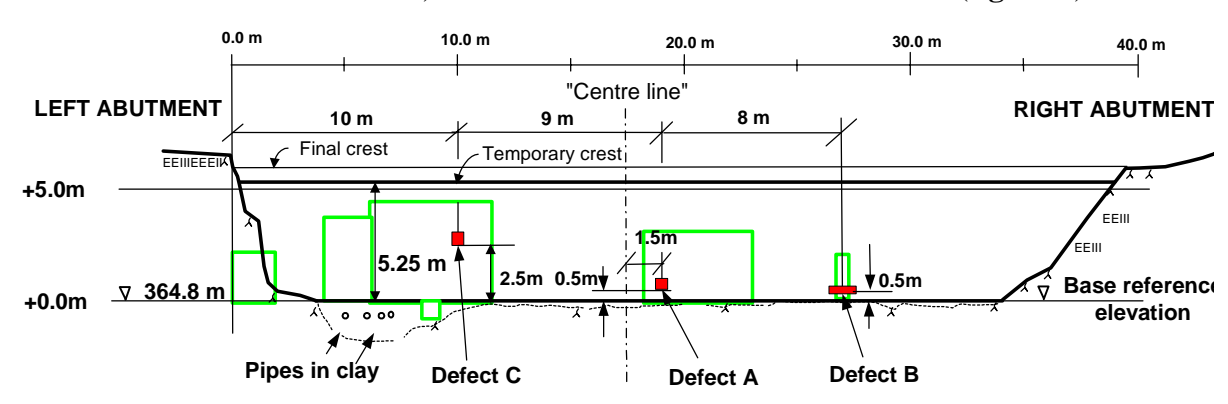


Figure 8 Defect areas from visual observations (green) in comparison with actual locations (red).

Both defect B and C were detected by the visual inspections, as well as the seepage around the pipes in the clay. The width at the dam toe was large at Defect C, while the outflow from Defect B was very concentrated. It is notable that the outflow was about 1m above the level of the defect. This indicates that the bottom of the support fill may have a much lower hydraulic conductivity than expected.

The outflow detected in section 21-23m is probably coming from Defect A, located about 10m upstream. If so, the leakage path would have turned to the right 1-2m during the passage through the rock fill, which is not unlikely in the actual material. Due to the construction of the defects, with gravel of about 2m length perpendicular to the defect, it is also possible that the water will find its way entering anywhere in the gravel, i.e. a deviation of  $\pm 1$ m may be possible. This could also explain the difference of the location of the defect in the core and the outflow in the core. A combination is also possible.

The estimated local outflow at section 8.5m and 27m seems to be in the same order as the measured and calculated values.

#### 7.3 Discussion

The visual observations proved the occurrence of other seepage areas than the constructed defects, and the observation identified leakages both in the foundation and in the abutments. These leakages are assumed to be in the same order of magnitude as the seepage through the built in defects.

Defect B and C were detected, and maybe also Defect A. However, one must consider that measurement at the dam toe will just give an indication of the location outflow. The most reasonable way is to assume that the water will take the shortest way to the toe, but this will not always be true. It may therefore be reasonable to assume that the observed outflow at sec 18m, and 21-23m all comes from Defect A, located at sec 19m.

Visual inspection of the dam toe is a well known and a well established method for dam surveillance, and will probably never be replaced by another method. The performance showed at the test was also successful. However, the inspection possibilities at the site were excellent, most of time, with good accessibility, initially almost dry soil, and no vegetation. During rainy days the sensibility was reduced, because rain water and outflow water was mixed. The ability to detect low seepage flow during rainfall will thus be significantly reduced.

The observed outflow by the "monitoring group" at sec 27m (about 1.5m above the concrete sill or at elevation 366.3m) is surprisingly high. The level has therefore been checked versus photos taken from the tests. According to those photos it was found that the level of the outflow should be corrected to about 365.8m, i.e. 0.5m below the reported level (**figure 9**). This is still a remarkable high outflow level in a rock fill material, and 0.5m above the Defect B.

The outflow was first observed at filling #1 when the water level was +367m, but could have started earlier. The outflow disappeared when the reservoir was emptied. According to

the field notes made by the "monitoring group" at filling #2, there was no outflow at a water level of 365.98m. The outflow was again observed at a water level of 366.34m. These observations are more accurate than the estimated level from filling #1. These observations indicate that the leakage water comes from the reservoir.

The temperature of the leakage water was also measured on the following day to 18.2°C, which was exactly the same temperature as the water in the reservoir. The leakage seems therefore to have a clear correlation with the upstream water. Other possible sources as rain or ground water outflow can also be excluded due to nice sunny weather, to high temperature of the leakage water, and not constant flow as expected from ground water outflow. This indicates that the water must come from the reservoir.



Figure 9 Observed outflow at sec 27m, about 1m above the concrete sill. The high amount of fines in the support fill can also be seen.

The most probable reason for the high outflow is the large amount of fines could be seen in the lowest part of the rockfill. These fines have probably fallen between the boulders when constructing the support fill, causing a reduced hydraulic conductivity (maybe to  $10^{-4}$ m/s, and probably lower than the materials used in the defect). The seepage face was also high, typically about 0.5m, according to observations made by the "monitoring group". Even higher seepage face was also observed locally.

To ensure drainage in the downstream shoulder uniform rock fill 300-400mm was instructed to be placed in a zone downstream of the defects. In addition a filter fabric was to be placed at top of the uniform rock layer about 0.5-1.0m above reference level, in order to reduce the risk of fines falling down into the uniform rock layer. The only sign of such a fabric is seen some dm above the leakage outflow, i.e. about 1.2m above the reference level. However, the placing of uniform rock has not been confirmed, and the observation of

the exit point for the leakage indicates that some amount of fines that can be seen on the downstream face also can be found below the filter fabric.

It is reasonable to assume that the concentrated leakage outflow at sec 27m was connected to defect B. A reasonable explanation may be that the crushed rock downstream, in combination with the low permeable layer with fines between the boulders, could create a leakage path "in the upper part of the fines", entering at a high level at the downstream toe (**figure 10**). Due to the low hydraulic conductivity, the infiltrated amount of water will be reduced. However, some water will also enter the dam toe, which was seen by the temperature measurements.

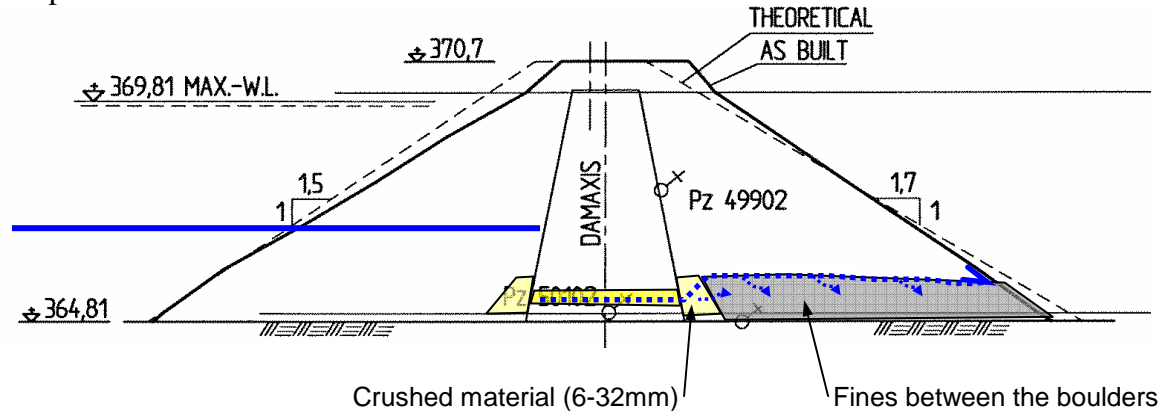


Figure 10 Possible explanation of the observed leakage at the dam toe at sec 27m.

The hypothesis above has been tested by analysing the seepage through the section using different permeability in the lower portion of the rockfill in the downstream shell. A high seepage exit point of +365.8m can be obtained by assuming that the lower part of the downstream supporting fill does not exceed  $10^{-4}$  m/s. Should the permeability be higher than  $10^{-4}$  m/s it generates a lower exit point of seepage (**figure 11** and **12**).

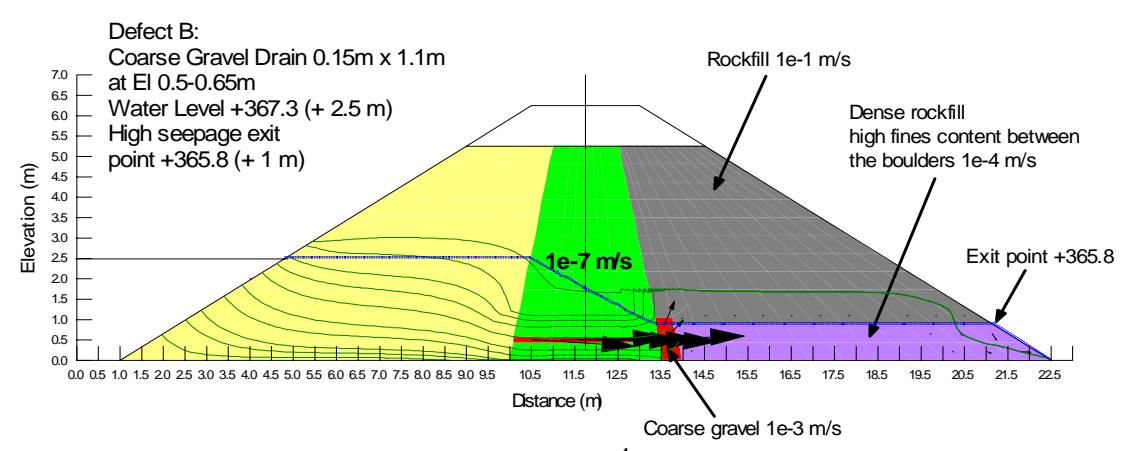


Figure 11 Phreatic line assuming a permeability of 10<sup>-4</sup>m/s in the lower portion of the downstream shell.

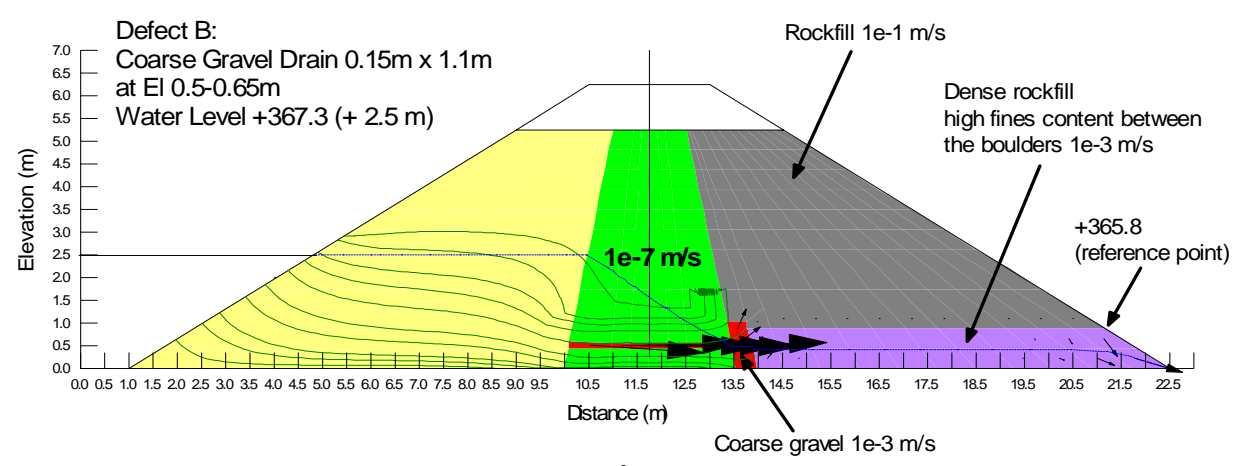


Figure 12 Phreatic line assuming a permeability of 10<sup>-3</sup>m/s in the lower portion of the downstream shell.

#### 8 INTEGRATION OF MEASUREMENTS RESULTS

In the measurement report (PART 3) discussions were made concerning the measurements. The best agreement was found between visual inspections and temperature measurements. If the same weight of the assumed for all methods, three main defect areas were found:

"The most significant defect is found around section 22m, which is shown by all methods. The elevation is more uncertain varying from elevation 365 to 368m.

A second significant defect is observed at section 27m at elevation 365-367m. The SP anomaly is however weak and interpreted only as possible defect.

A third area is probably somewhere around 5 m, and at any level between 365 and 369m. This defect is probably more diffuse and also located closer to the abutment where the detection and resolution capability of the methods are reduced."

The above observations from the measurement report are indicated in green together with the real locations marked in red in **figure 13**.

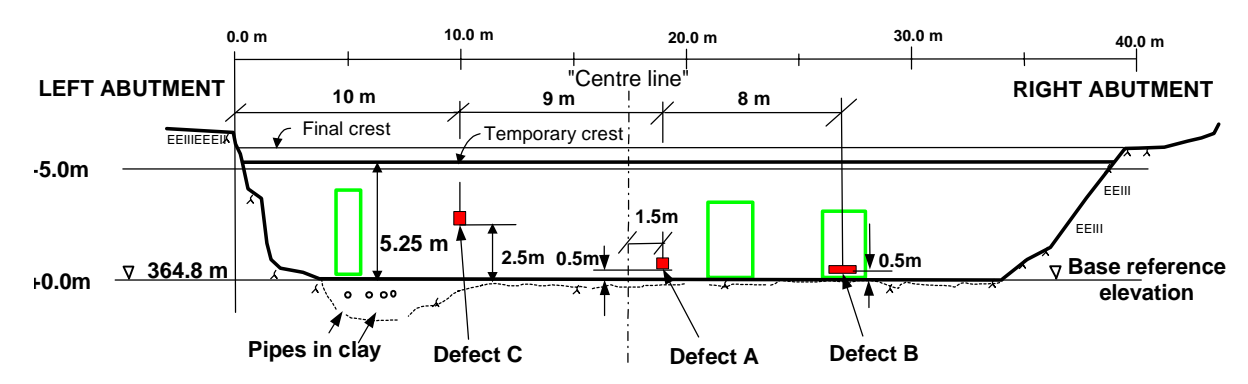


Figure 13 Defect areas according to the collected final information from all methods (green) in comparison with actual locations (red)  $\frac{1}{2}$ 

Defect B is detected using the summarized information from all methods, as well as the outflow around the pipes. Defect C was not found to be a main defect area although it was indicated by some of the methods.

It is interesting that all methods, including the visual inspections, indicate a defect at section 22m, i.e. some metres right of Defect A. This deviation can be accepted for the dam toe methods (temperature and visual inspections) but is larger than the expected accuracy for the electrical methods. However, if the construction of the defects may have caused a concentration of the flow to the right, just at the exit of the defect from the core, this may affect the electrical methods. Such a deviation might be possible, according the findings above about the high level of the outflow from Defect B.

Integration of several methods should be made, but they should not have the same influence of the result. In this case, the result from SP-measurements should have had a lower weight due to the difficult monitoring conditions.

#### 9 CONCLUSIONS AND RECOMMENDATIONS

All defects built in the dam were small, and none should have been detected according to the predictions made in the Pre-Study. However, the pre-study assumed an investigation approach where anomalies due to material differences should be able to detect. Due to the different water levels in the reservoir a monitoring approach could be adopted that increased the detection level of the methods.

Three defects (Called A, B and C) were constructed carefully, but an undesired leakage area occurred around the drainage pipes (called Defect D), with a similar leakage flow as the other three defects. Hence, four defects exist in the dam. The location of the original defects is well known. However, it should be pointed out that all methods used indicate a defect area about 2 meters to the right of Defect A. Due to the material heterogeneity in the lower part in the downstream fill, a deviation from the basic water flow direction (upstream – downstream) cannot be excluded.

All the four defects in the core were detected by temperature measurements and by visual inspections at the dam toe, if we allow a deviation of 2 meters. Both these methods are performed from the downstream toe, and cannot exactly locate the defects in the core, neither along the dam nor at the level. The conditions at the site were however favorable for both these methods compared to normal conditions at a typical embankment dam. Nevertheless, both these method are reliable and easy to understand.

The section for Defect D was probably detected by resistivity measurements based on the investigation approach alone. If a two meter deviation can be accepted also the section for Defect A was found by the same approach. These defects were confirmed using the monitoring approach, by which also Defect B was detected. However, the depth for both Defect D and A was by the investigations indicated at a higher elevation than the real defects. Defect C was not detected. In total, this result is well above the expectations given in the pre-study, although defect C should have been detected.

The conditions for the SP-measurements were much more complicated than indicated in the pre-study, and none of the defects should be detected by the method. However, using the monitoring approach defect B was indicated as a weak anomaly, close to the monitoring accuracy. Another indication of a defect was given 2 meters to the right of Defect A. The other defects were not detected, while two other areas were pointed out.

No final conclusion about the general application of resistivity and SP can be made until the electrical properties of the soil material have been determined. The experience from these tests indicates that resistivity and SP seems less sensitive than temperature and visual inspections, but the conditions at the test were in some aspects favorable to the latter methods. Both resistivity and SP will give information in the core, in opposite to the other methods that just give information at the dam toe. The information given by the resistivity measurements was in this test more informative than the SP measurements.

The test show that temperature, resistivity, and may be SP can be used at investigations, but result from single or short time investigations are complicated to evaluate, and less accurate than result from long time monitoring. However, the methods use different approaches for

#### **ELFORSK/BC Hydro**

seepage detections and it therefore recommended combining several methods. Moreover, it is important to understand the fundamentals for the processes when applying the methods. The actual monitoring situation at a real dam may also be difficult to predict, as shown in this study.

The result from several geophysical measurements should not be integrated in a "blind way". Each method has its optimum performance, and uncertainties which must be considered when combining all result. The weight of each method will thus vary between different dams, and monitoring conditions.

Temperature, resistivity, and SP are expected to be more suitable methods for long time monitoring. This was indicated in the pre-study, and proved in the field test where monitoring approaches (based on differences in time and space, relative differences etc) were used in order to detect the defect areas. The result from these tests verifies also the experience gained from the ongoing long term monitoring tests in Sweden.

# Internal Erosion Detection at the Røsvatn Test Site

# Part B Design and construction of the dam and the defects

Åke Nilsson SwedPower AB Steve Garner BC Hydro

# Design and construction of the dam and its defects

# **Table of Contents**

1	В	BACKGROUND	1
2	D	DESIGN OF THE DEFECTS	2
	2.1	GENERAL	2
	2.2	DAM GEOMETRY	
		RESERVOIR OPERATING AND THEORETICAL LEAKAGES	
	2.4	DESCRIPTION OF TEST SITE AND INSTRUMENTATION	8
3	C	CONSTRUCTION MATERIALS	10
4	C	CONSTRUCTION	12
5	P	PIEZOMETER READINGS AND LEAKAGES DURING TESTING	17
6	R	REFERENCES	20

### 1 Background

The field test to study geo-electrical techniques used a test embankment which was constructed in July 2003 as part of the research programme Stability and Breaching of Embankment Dams. As discussed in the Memorandum of Understanding between EBL and Elforsk/BC Hydro the test embankment was modified to allow testing of the capabilities of geo-electrical techniques. The modifications included the installation of several defects through the core of the dam. The defects were constructed in order to test the expected ranges of capabilities of the geo-electrical techniques. The geophysical tests were planned to take place prior to an overtopping of the rock-fill dam.

The defects were designed with varying configurations at different locations and elevations within the core. In order to properly identify the characteristics of each of the defects, various flow conditions were planned and implemented. This was done by operating the reservoir at 4 different operating levels for a period of 1 day per level. In order to allow the geophysical instruments to maximize their capabilities, the dam was constructed temporarily only to the top of core during the testing period.

As a base for the construction of the embankment the design of the defects was presented to the 'reference group' in "Design of defects for investigation by geo-electrical techniques: Self Potential and Resistivity" by Steve Garner, BC Hydro and Åke Nilsson, SwedPower, dated 29 May 2003. Since the test was arranged to be a blind test the design was not presented for the 'monitoring group'.

# 2 Design of the defects

#### 2.1 General

The defects were designed to the lines, grades and dimensions as shown on the sketches, **Figures 1 - 4**. The figures show the geometry of the embankment when it was raised to the top of the core.

After the geo-electrical tests were completed the embankment was completed to its final crest elevation. An as-built drawing of the embankment when it was completed is shown in **Figure 5**.

### 2.2 Dam geometry

The as-built geometry shown in **Figure 5** deviated some from the designed geometry, but it can be summarised as follows:

Embankment height: 5.25m during testing (5.9m final height) above base reference

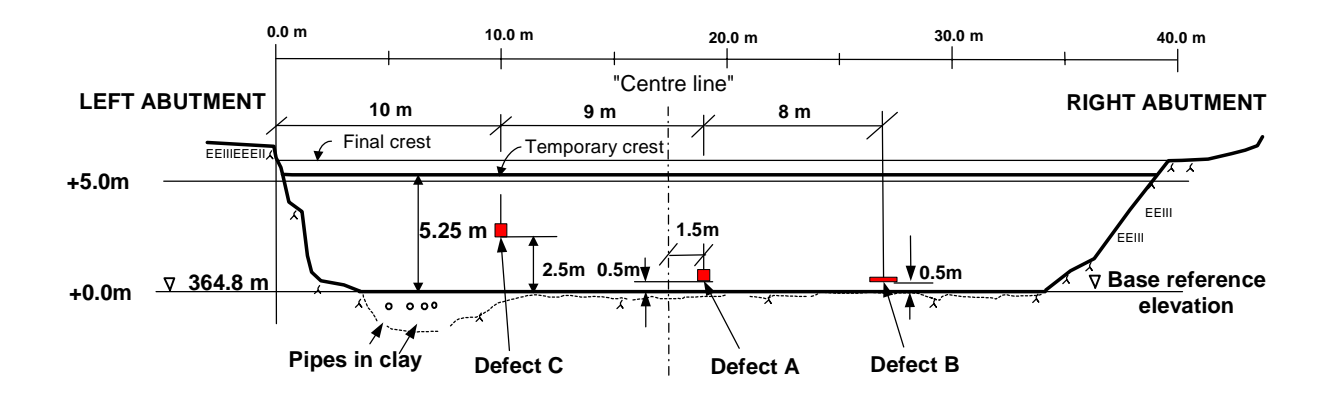
elevation

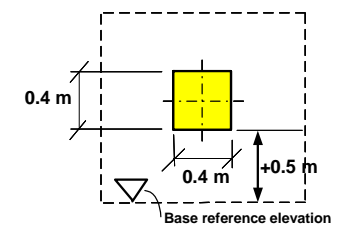
Crest length: Approximately 37m

Slope downstream: 1V:1.45H (designed 1V:1.7H)
Slope upstream: 1V:1.55H (designed 1V:1.5H)
Crest width: 4.5m (of which 1.5m was moraine)

Central core: Width 1.50m at the crest and sloping 5V:1H

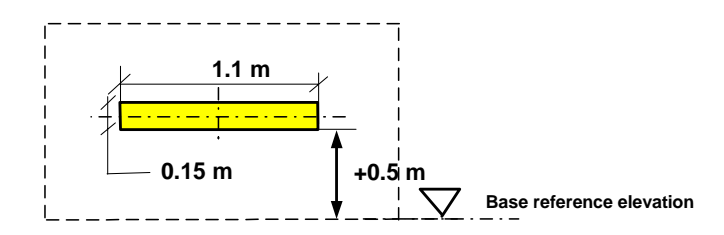
The exact width of the core was never measured during construction. From the as-built drawing, which also shows the surveyed piezometer locations, it can be concluded that the width of the core was constructed somewhat wider than designed. Piezometer "Pz 49902" was according to the instruction to be installed in the moraine 0.5 m from the downstream side. However, according to the surveyed coordinates for the piezometer (which can be assumed to be correct) the location is outside the theoretical downstream side of the core.





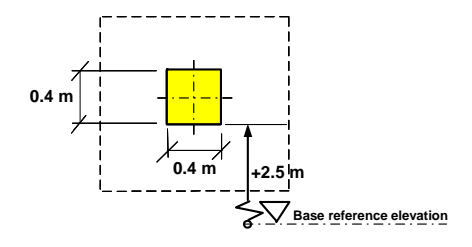
### Defect A

Square  $0.4 \text{ m} * 0.4 \text{ m} = 0.16 \text{ m}^2$ Located at chainage 19 m and 0.5 m above reference elevation



### Defect B

Rectangular 0.15 m \* 1.1 m = 0.16 m<sup>2</sup> Located at chainage 27 m, and 0.5 m above reference elevation



### Defect C

Square  $0.4 \text{ m} * 0.4 \text{ m} = 0.16 \text{ m}^2$ Located at chainage 10 m, and 2.5 m above reference elevation

Figure 1 Location and sizes of defects

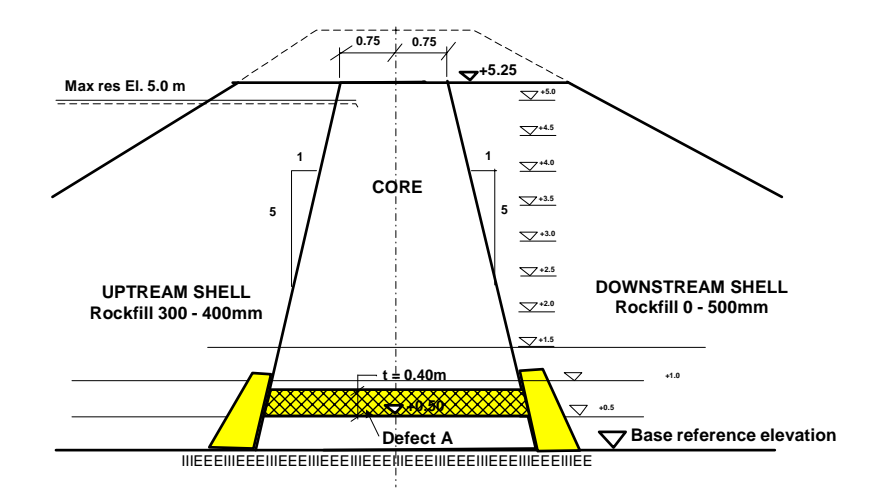


Figure 2 Defect A

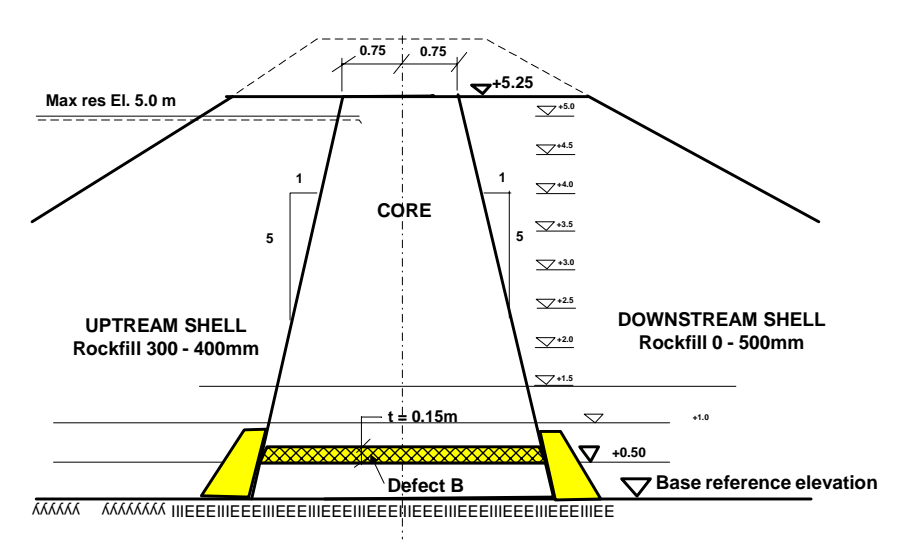


Figure 3 Defect B

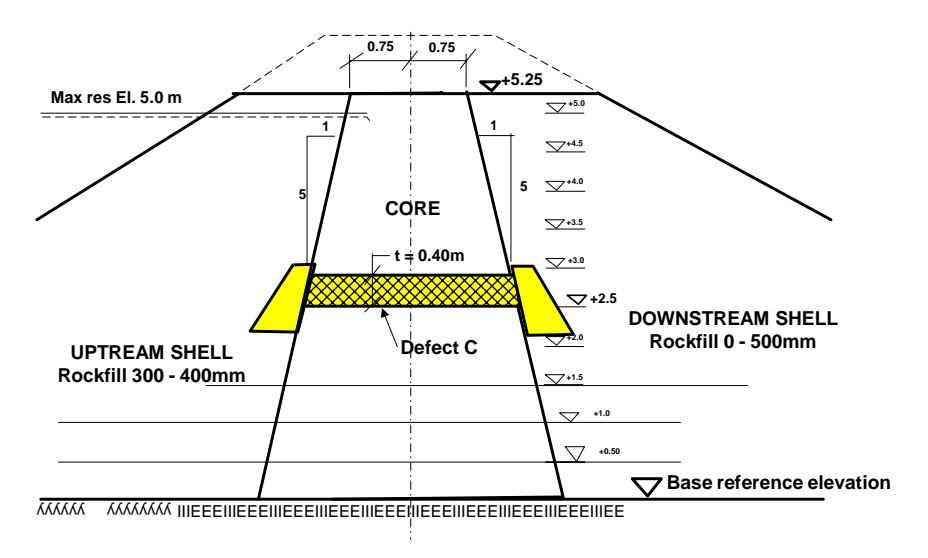


Figure 4 Defect C

### 2.3 Reservoir operating and theoretical leakages

The reservoir was operated at 4 different operating levels for a period of 1 day per level as follows:

**Table 1 Reservoir operation levels** 

Filling, date	Operating Level
	(Above reference elevation)
#1, July 30	3.4
#2, July 31	2.4
#3, Aug 1	3.7
#4, Aug 2	4.9
#5, Aug 4	4.9-3.4
#6, Aug 5	3.4

As shown in Part D "Field measurements" the reservoir was regulated in filling level #1 to #6 according to **table 2**. The reservoir levels are also shown in figure 26 in chapter 5 below.

Table 2 Summary of field test activities

Date	Activity	
July, 30	All installations OK. Filling #1 started a 1.10pm	
One emergency packer came out, and all water was release		
July, 31	Filling #2 was successful, as well as the measurements.	
Aug, 1	Filling #3 was successful, as well as the measurements.	
Aug,2	Filling #4 started at 9am. After completing all measurements in the evening, the valves were opened to lower the reservoir.	
Aug,4	Filling #5: Valves closed at the same water level as for filling #3.	
Aug,5	Filling #6: Repeated measurements with empty reservoir.	

Results of theoretical calculations of the seepage through the defects are shown in **figures** 5-7. The figures show one water level for each defect as typical examples of the calculation that were carried out. The leakages through the defects A, B and C at different operation levels are listed in the following table.

The hydraulic conductivity for the specified material for the defects has been assessed to be 0.001 m/s based on grain size distributions. This assumption shows leakages in the same order of magnitude as measured in the field, see section 6 below.

**Table 3 Theoretical leakages** 

Water level, m	Leakages, l/s (K=0.001 m/s)				
	Defect A	Defect B	Defect C	Total	
2.5	0.12	0.10	-	0.22	
3.7	0.19	0.15	0.07	0.41	
4.8	0.24	0.19	0.14	0.57	

Coarse Gravel Drain 0.4m x 0.4m At El 0.5-0.9m Water Level 2.5 m

Coarse Gravel Drain 0.15m x 1.1m

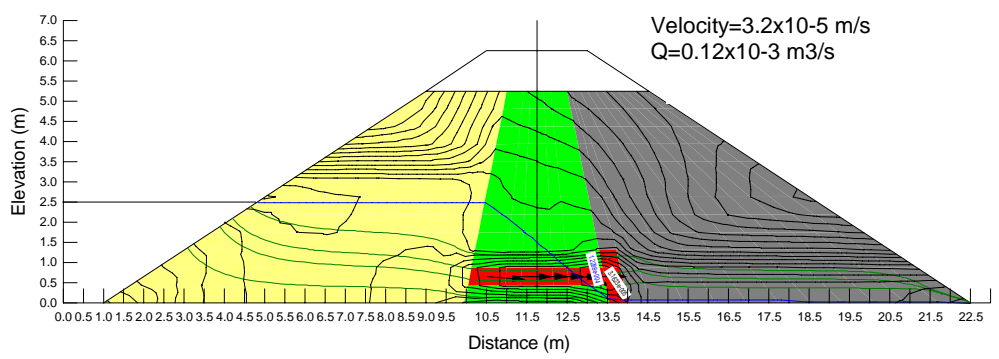


Figure 5 Defect A, Gravel Drain 0.4m x 0.4m, At El 0.5-0.9m, water level 2.5m

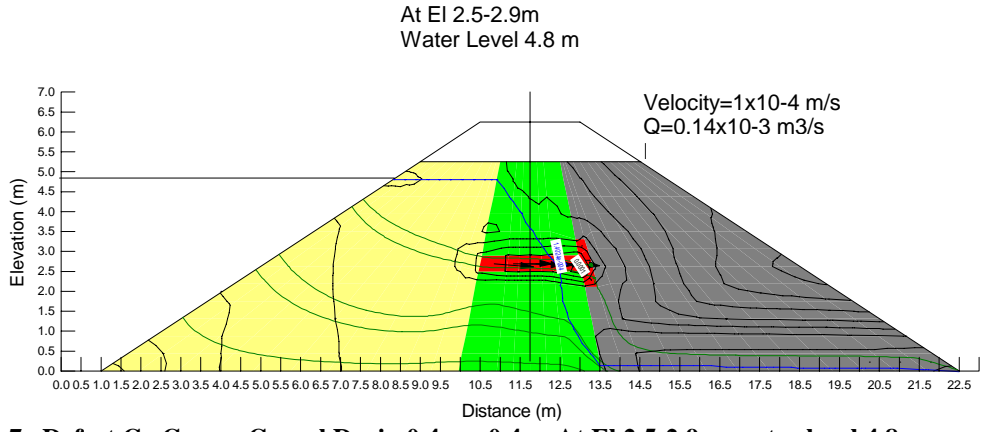
At El 0.5-0.65m Water Level 4.8 m

Velocity=1x10-4 m/s
Q=0.19x10-3 m3/s

Output

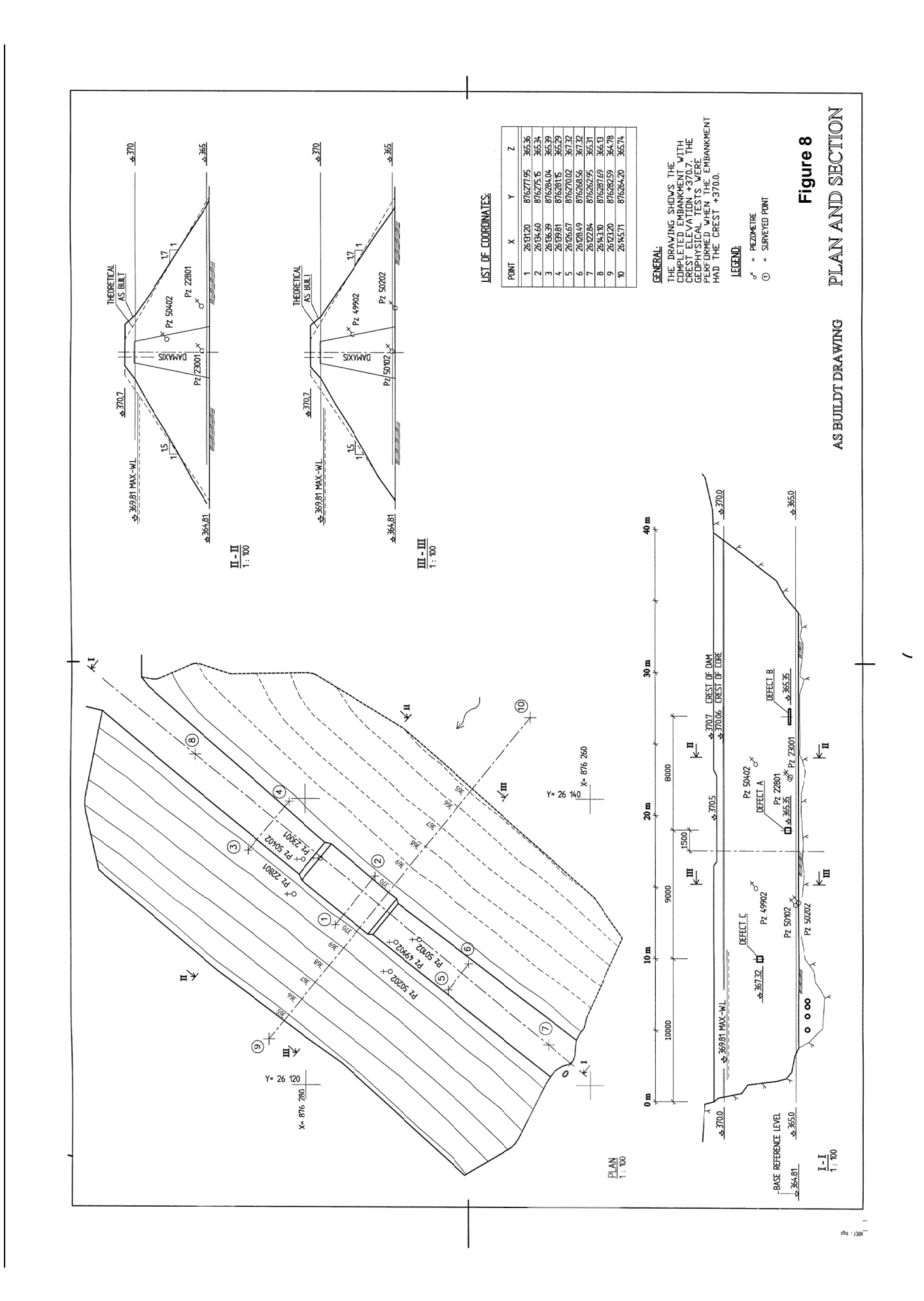
Outp

Figure 6 Defect B, Coarse Gravel Drain 0.1m x 1.6m, At El 0.5-0.9m, water level 4.8 m



Gravel Drain 0.4m x 0.4m

Figure 7 Defect C, Coarse Gravel Drain 0.4m x 0.4m, At El 2.5-2.9m, water level 4.8 m



### 2.4 Description of test site and instrumentation

The test site is located about 600 m downstream of the Rössvatn Dam. The test dam creates a small reservoir of about 70 000 m<sup>3</sup> extending all the way up to the Rössvatn Dam. The three Rössvatn Dam spillway gates with a total capacity of 450 m<sup>3</sup>/s feed directly into the test reservoir and make it possible to maintain a constant reservoir level.

A concrete sill at elevation +364.81m just downstream of the test dam, defines the level of the foundation. The foundation of the dam is outcropping rock at approximately the sill elevation from approximately chainage 9m to 34m close to the right abutment. Also the left abutment (Ch 0 - appr. 3m) is in rock. The right abutment (Appr. Ch 34 - 39m) is in rock partly covered by a gravely moraine. Close to the left abutment (Appr. Ch 3 – 9m) the rock elevation is deeper and the depth to the rock unknown. In year 2001 the material (partly gravel and stones) above the rock was removed and replaced by clay up to the sill elevation in order to uniform the foundation and to stop potential leakage through and along the foundation surface.

In the area of chainage 3 - 9m diverson pipes were installed and backfilled with clay, see **Figure 9**.



### Figure 9 Diversion arrangements in the foundation close to the left abutment

Just downstream of the dam a concrete sill was constructed and a Thomson weir was installed, see **figure 10**. The concrete sill was intended to catch all the leakage through the dam. There was later found to be some leakages through the downstream sill in the area for the diversion pipes close to the left abutment.

By measuring the water height in the weir the leakage was measured. The weir was made of a 3 mm iron plate. The opening is 90 degrees and the capacity is given by:

$$q = 0.0137 \cdot (H \cdot 0.1)^{2.5}$$

Where H is in mm and q is in 1/s



Figure 10 Weir where the seepage flow during the test was measured manually.

### 3 Construction materials

The core was constructed of moraine with a low content of boulders. The gradation for material less than 19 mm is shown in **Figure 11**.

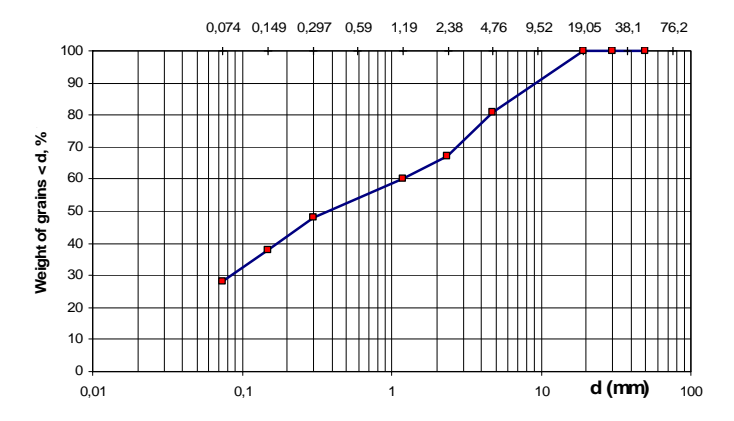


Figure 11 Grain size distributions for the moraine in the core

The downstream shoulder was well-graded rock fill from tunnel spoil 0-500mm, and in the upstream shoulder uniform rock fill 300-400mm. The gradations are shown in **Figure 12**.

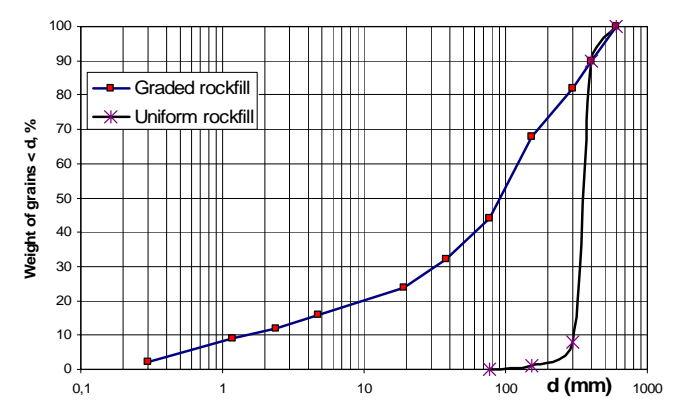


Figure 12 Grain size distributions for the rock fill in the shoulders Well-graded rock-fill downstream and uniform rock-fill in the upstream shoulder.

The material in the defects was taken from an alluvial deposit used in year 2002 for the test 2A-C-02, see grain size distribution *Figure 13*.

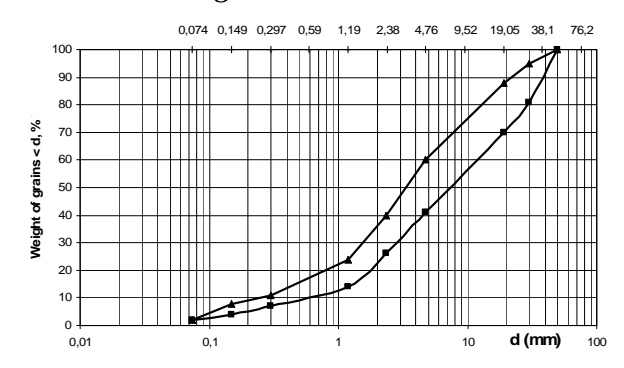


Figure 13 Grain size distributions for alluvial deposit used in year 2003 for test 2A-C

The material having a particle size less than approximately 2 mm was removed by sieving and washing. After processing the grain size distribution for the remaining material was determined to have the grain size distribution shown in **Figure 14**.

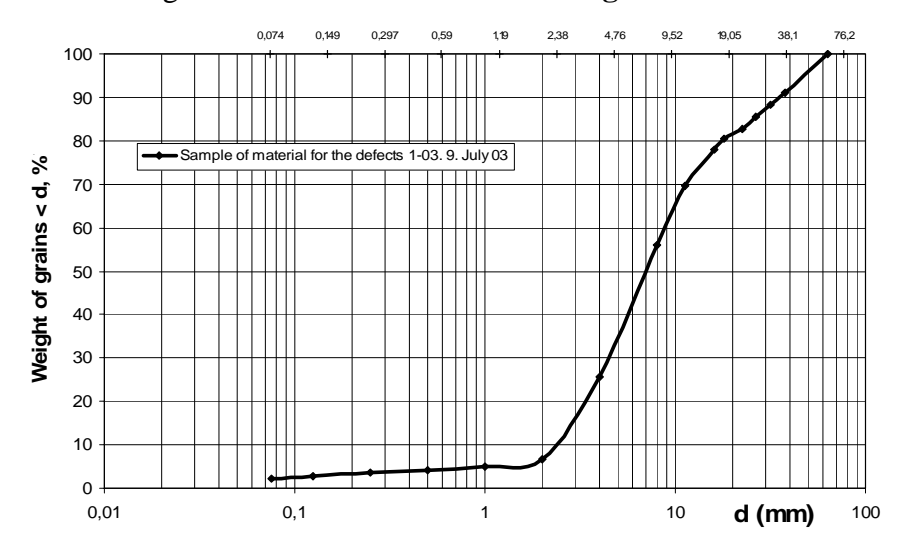


Figure 14 Grain size distributions for material used in the defects

A filter fabric protected the material in the defects in order to not be contaminated by the moraine in the core. Filters were also constructed around the upstream and downstream ends of the defects to ensure that moraine from the core did not influence upon the contact between the material in the defect and the material in the shoulders.

The material used for filter downstream of the defects was crushed rock (macadam 6-32mm) with gradation according to **Figure 15**.

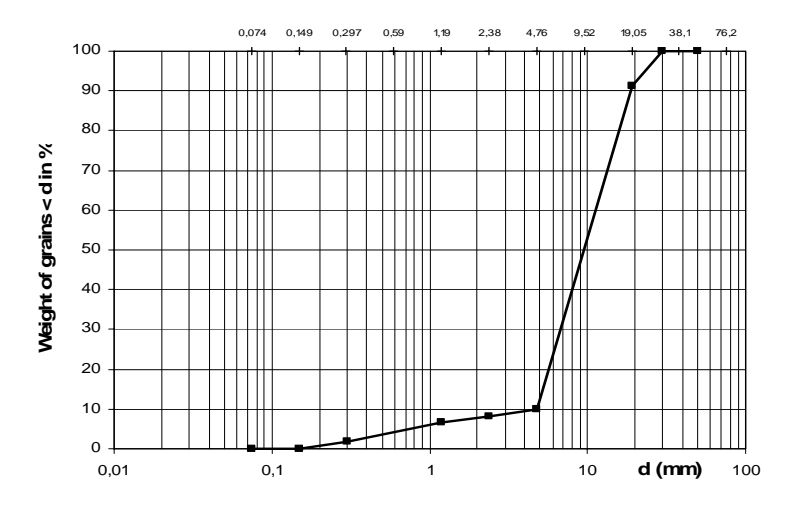


Figure 15 Grain size distributions for material used as filter between material in the defects and the upstream and downstream shoulders

To ensure drainage uniform rock-fill (300-400mm) was specified to be placed in a zone through the downstream shoulder and in contact with the filter downstream of the defects. In addition a filter fabric was to be placed at top of the uniform rock layer, in order to reduce the risk of fines penetrating into the uniform rock layer.

## 4 Construction

Moraine, which was used for the core, was spread by a backhoe and compacted in 0.7 m layer thickness by a vibrator attached to the backhoe arm. The well-graded rock fill from tunnel spoil 0-500mm and the uniform rock-fill 300-400mm was compacted with a toed vibratory roller compaction in 1 m layer thickness.

The moraine normally had a moisture content of approximately 6%, which is approximately the optimum moisture content for heavy compaction. The porosity was found to be approximately 0.244, (Ref. 1). However, it was very sunny weather during construction and part of the core was compacted dry of optimum.

The construction of the defects is illustrated below in **Figure 16-25**.



Figure 16 View from downstream at the time when the construction of the defects started



Figure 17 View from the upstream side.

Defect A can be seen to the left and defect B to the right in the photo



Figure 18

Excavation for defect A



Figure 19 Defect A, filter fabric is arranged before the placing the gravel into the excavation



Figure 20 Defect A, the gravel in the defect is surrounded of filter fabric before the placing of the moraine continued



Figure 21 Defect B, excavation



Figure 22 Defect B, the gravel in the defect is placed and surrounded by filter fabric



Figure 23 Defect C, filter fabric surrounds the gravel and filter has been placed to connect the material in the defect to the rock fill in the shoulders of the embankment.



Figure 24 The zero point at the left abutment

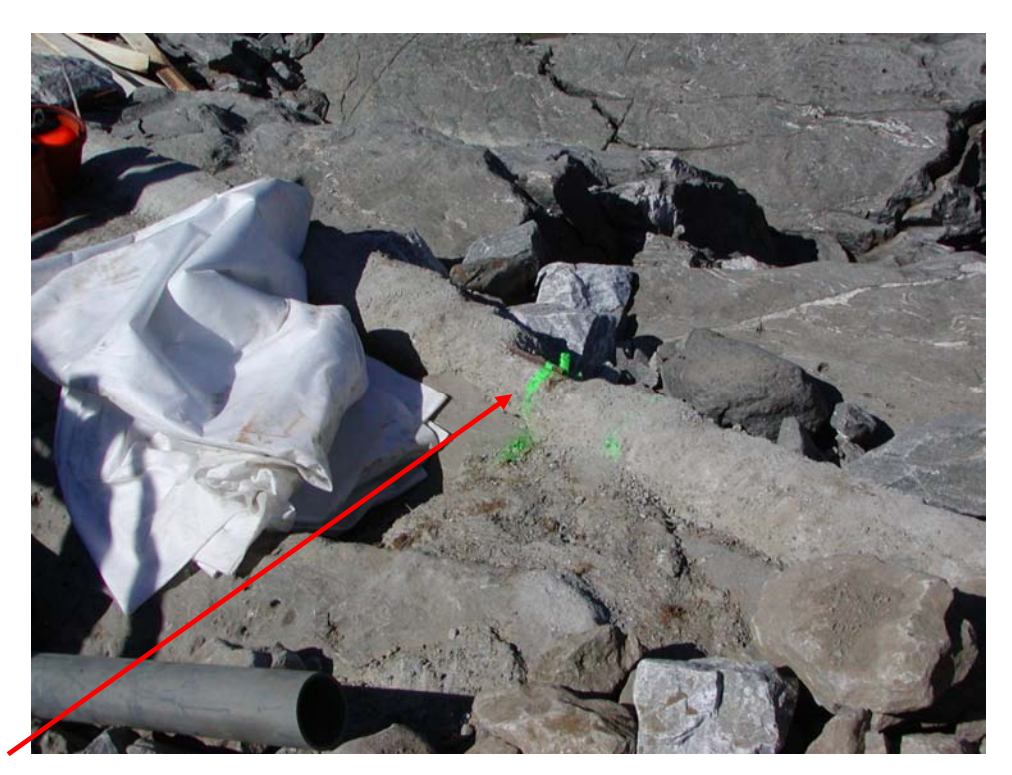


Figure 25 The "centerline" for the embankment marked at the concrete sill downstream of the embankment.

# 5 Piezometer readings and leakages during testing

During the construction six piezometers were placed inside the dam body for monitoring of pore pressures. The instruments were installed in Section II between Defect A and B and in Section III located between Defect A and C. The pore pressures were measured manually by the "monitoring group" during the testing period. The results of the measurements of are shown in **Figures 26-27** together with the reservoir elevations.

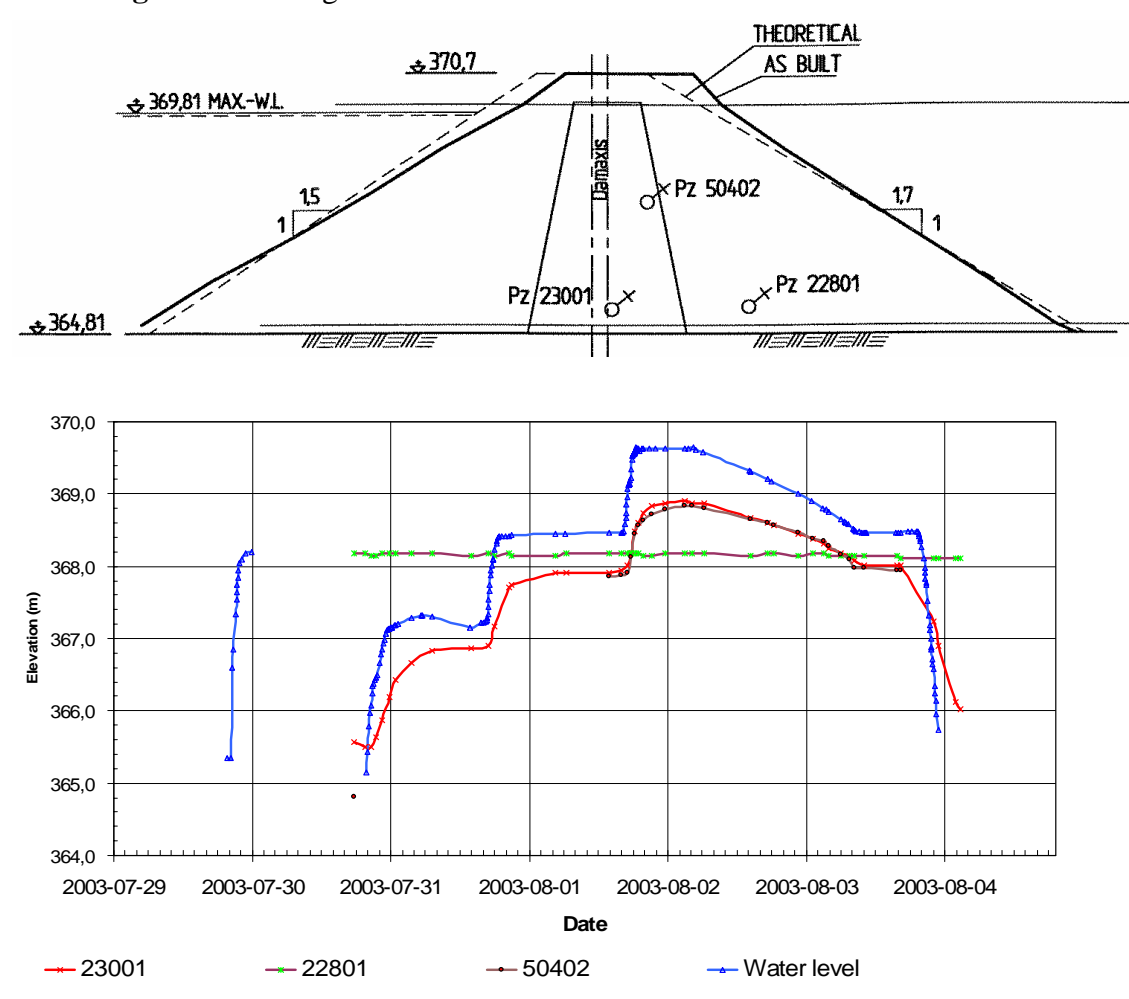


Figure 26 Location of piezometers in Section II and measurements during the period of the geo-electric measurements

The pore pressure response is surprisingly quick and the piezometer (Pz 23001) in the centre of the core and close to the foundation follows the reservoir pressure with a 2-3 hour time lag. At full storage level the pore pressure in the centre of the core is some 0.5m lower than the reservoir water level.

The piezometer (Pz 50402) at the downstream side of the impervious core and 3m above the foundation shows similar response with a measured level approximately 0.5m lower than the upstream water level. This piezometer was specified to be installed approximately 0.5m from the downstream side of the core.

The piezometer (Pz 22801) installed in the downstream shoulder close to the foundation elevation shows no response to the upstream reservoir level. This piezometer is either out of order or it is incorrectly calibrated.

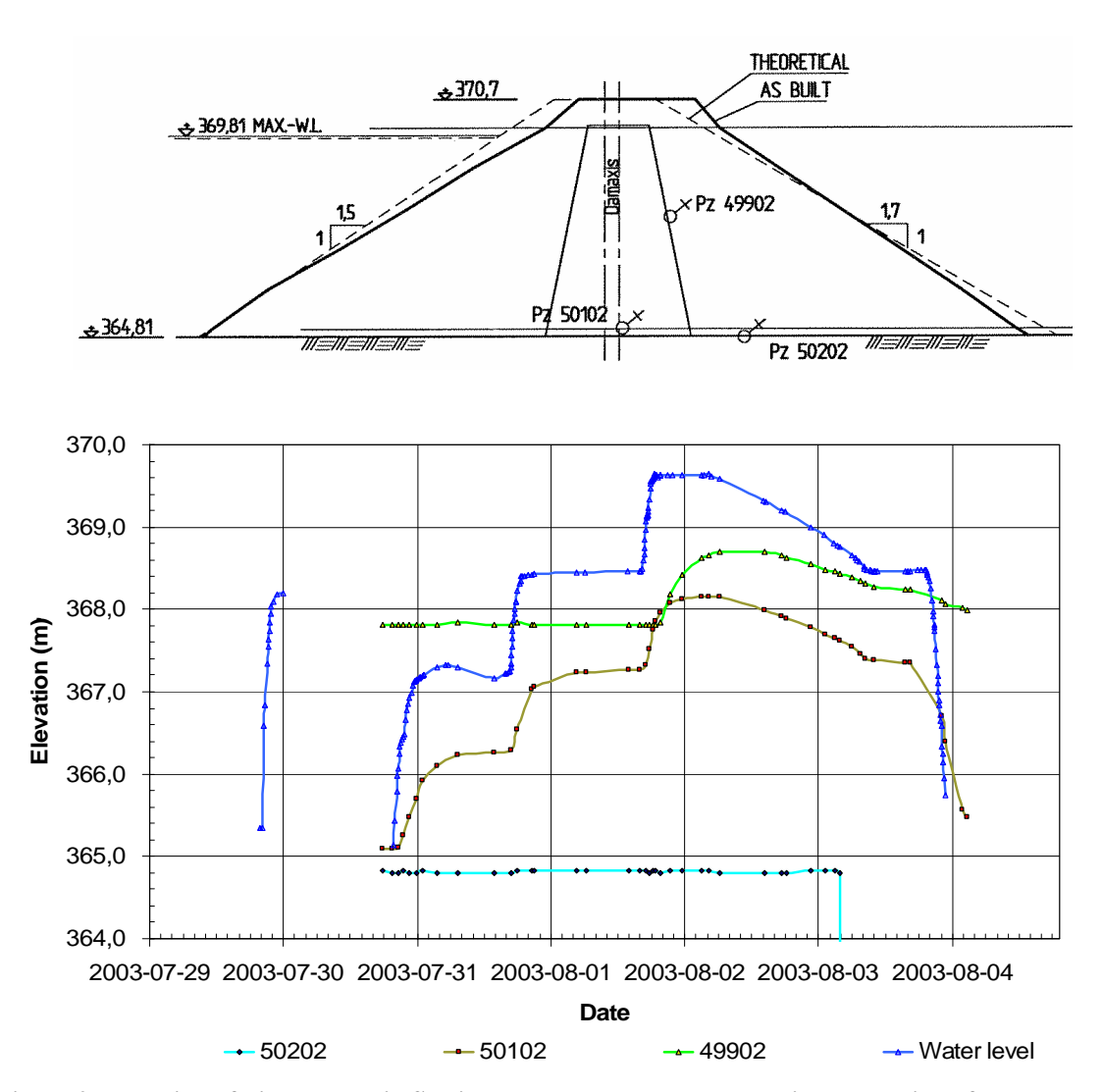


Figure 27 Location of piezometers in Section III and measurements during the period of the geo-electric measurements

The piezometers in section III show similar trend as the piezometers in section II. The pore pressure response is surprisingly quick and the piezometer (Pz 50102) in the centre of the core and close to the foundation follows the reservoir pressure with a 2-3 hour time lag. At full storage level the pore pressure in the centre of the core is some 1.1m lower than the reservoir water level.

The piezometer (Pz 49902) at the downstream side of the impervious core and 3m above the foundation shows similar response but measured levels are approximately 0.5m lower than the upstream water level. This piezometer was specified to be installed approximately 0.5m from the downstream side of the core.

The piezometer (Pz 50202) installed in the downstream shoulder close to the foundation elevation shows as expected no response to the upstream reservoir level.

The fast response e.g. for piezometer 50102 (located at the foundation level in the centre of the core) when the reservoir was raised 2.5 to 3.7m above the referense elevation indicates that the permeability of the morain is fairly high. The high permeability can be a result from the compaction of the moraine dry of optimum moisture content. Analyses of the transient flow by SEEP/w using different permeability for the moraine indicate that the permeability can be in the order of 10<sup>-5</sup> m/s.

**Figure 28** shows the transient flow for a permeability of 10<sup>-5</sup> m/s (in all directions) in the moraine, indicating that the time lag will be a couple of hours to reach a flow fairly close to steady state seepage. The shape of the theoretical phreatic line (compared to the response of Pz 49902 when the reservoir was raised at higher water levels) also indicates that the permeability in the field is higher in hizontal direction compared to the vertical direction. This is as expected and assumed be caused by the spreading and compaction of the morain in layers.

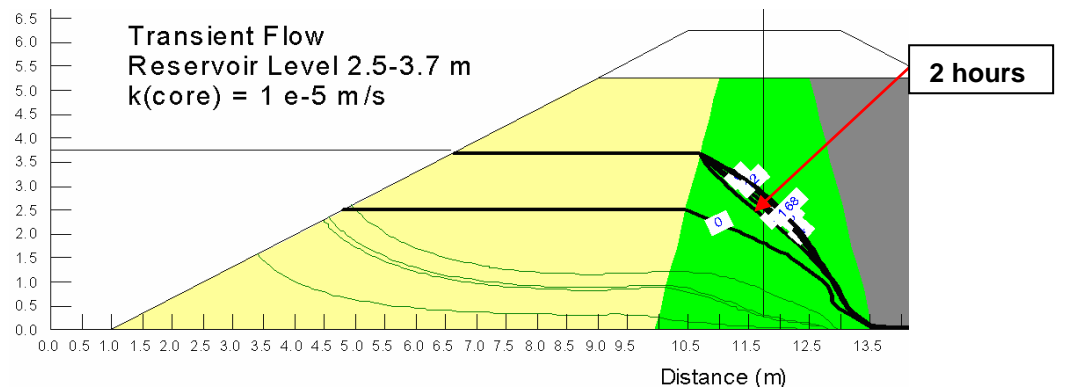


Figure 28 Transient seepage flow, permeability 10-5 m/s in the moraine, each time increment equals 1h

The leakages were measured manually by the "monitoring group" during the testing period. The results of the measurements of leakages are shown in **Figure 29** together with the reservoir elevations. The measured leakages indicate, as shown in section 2.3 above, a permeability in the order of  $10^{-3}$  m/s for the gravel in the defects.

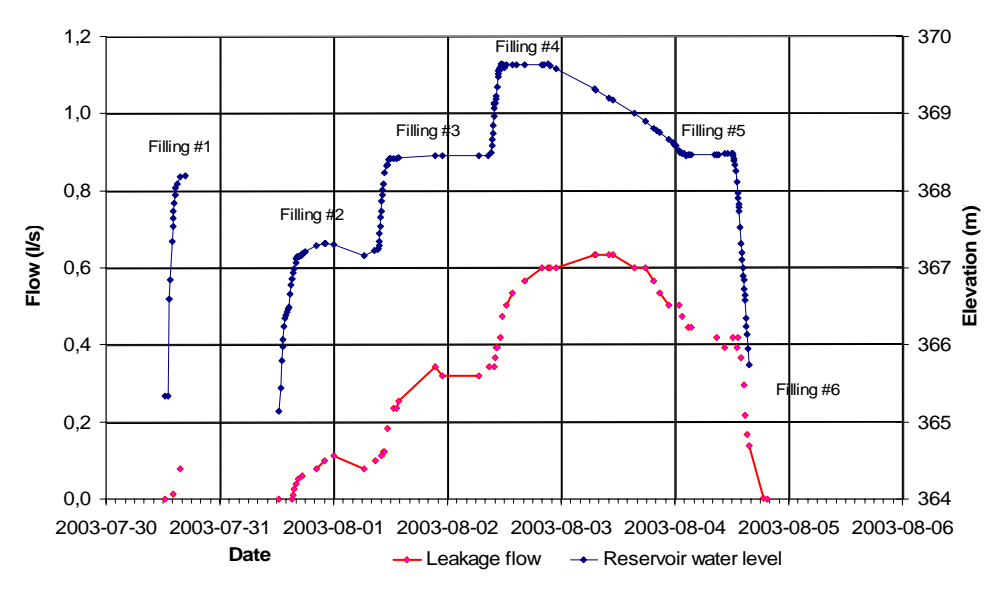


Figure 29 Reservoir level and leakages during the period of the measurements

# 6 References

[1] A LÖVOLL, "Breach formation in embankment dams. Results from Norwegian field tests". International Seminar, Breaching of Embankment Dams, Oslo, Norway, 21-22 October 2004.

# Internal Erosion Detection at the Røsvatn Test Site

PART C
Pre-Study and Field
Measurements using
Resistivity, Self Potential,
and Temperature

**October 3, 2003** 

Sam Johansson and Johan Friborg HydroResearch Sam Johansson AB Torleif Dahlin and Pontus Sjödahl Lund University

### **Summary**

Resistivity, Self Potential, and Temperature are three indirect methods for leakage monitoring in embankment dams The performance of these methods was tested in a blind test at the unique test dam at Røsvatn in Norway within a project, jointly funded by BCHydro, Elforsk AB and EBL represented by Statkraft Grøner. The dam is a small rockfill dam designed and constructed with zones of relatively high permeability located in the low permeability core material.

The project team was separated into a "defect design group" which did not participate in the monitoring, and a "monitoring group" which had no knowledge of the locations and sizes of the zones of high seepage. This report is written by the "monitoring group" before any information was given about the defects. A pre-study (Part 1 of this report) in order to guide the defect design group was delivered as a draft to the design group in early June 2003. Field measurements were made in August 2003. The results are presented in Part 2 of this report.

### Part 1 - Pre-Study

The dam used in the pre-modelling is 40m long and 6m high. The abutments consist of rock and are steep. Data about soil properties for this application are rare, especially for the cross-coupling coefficient. The values are assumed based on literature data, and experience from dam monitoring in Sweden. The variation for all these parameters may be large and laboratory test should be done after the monitoring.

In order to estimate some defects that can be detected, sensitivity analysis has been made due to: depth from the core crest, size, and flow change. The size of the defect as well as the geometry has been tested for several types. Six defect types were defined but calculations were only made for the four types with areas between  $0.25 \, \mathrm{m}^2$  and  $1.0 \, \mathrm{m}^2$ . The simulations showed that surely detectably defects for both resistivity and SP must be in the order of one  $\, \mathrm{m}^2$  if the defect is located in the middle of the dam. Defects in the lower part will be difficult to detect. Defects should not be placed close to the abutments due to boundary influence. The sensitivity for one-time investigation is significantly lower than the sensitivity for long-term monitoring. The result of this study will therefore not be valid for long-term monitoring.

The soil properties are important to verify and several laboratory tests should be done. Drainage of excess water from construction and from precipitation may also affect the result. The variation in compaction during construction may in this case be seen as resistivity variations caused by temperature changes between the soil and the water in the reservoir. A detected resistivity anomaly will thus have two unknowns (resistivity of the soil and temperature). Temperatures should be measured of the soil during construction and at the dam toe during the field tests.

#### Part 2 - Field measurements

Measurements were made with empty reservoir at three occasions and at five filling levels. The original methods (Resistivity, Self Potential and Temperature) were used together with IP (Induced Polarization) and Visual Inspection at the dam toe.

In total 61 electrodes for resistivity measurements were installed along the exposed dam core with a spacing of 0.67m. Excellent data quality was achieved due to good electrode contact and short electrode separations. For the time-series SP measurements 49 non-polarizable Cu-CuSO<sub>4</sub> electrodes were installed with a separation of 0.8m. SP was also measured manually in three cross-sections, and along the shore-line. Temperature measurements were carried out along the dam toe, using 23 temperature sensors with a separation of about 1.5m.

Transient thermal impact due to short time temperature changes and temporal resistivity changes in the core material were found to be more complicated than what was foreseen in the Pre-Study. The resistivity of the reservoir water was also lower than assumed, which will reduce the contrast between materials. The resistivity of the unwashed downstream support fill was probably lower than expected. Moreover, the clay used for sealing on the rock foundation was not anticipated, which will decrease the resolution of the method in this zone. The conditions for the SP measurements were found to be more complicated than assumed in the pre-study. Furthermore, the resistivity of the core material and the reservoir water was lower than expected, causing lower SP anomalies than predicted in the pre-study.

The collected final information from all methods shows three main defect areas. The most significant defect is found around section 22m, which is shown by all methods. The elevation is more uncertain varying from elevation 365 to 368m. A second significant defect is observed at section 27m at elevation 365-367m. The SP anomaly is however weak and interpreted only as possible defect. A third area is probably somewhere around section 5m, and at any level between 365 and 369m. This defect is probably more diffuse and also located closer to the abutment where the detection and resolution capabilities of the methods are reduced.

There is a good agreement between the results of the methods tested, and they support each other in the composite evaluation. Geophysical methods should as far as possible be used together in order to improve the quality and reliability of the evaluation. IP-measurements agree with resistivity measurements and IP should be further tested for seepage detection in embankment dams. Repeated measuring (or better, regular monitoring) is recommended. Temperature measurement at the dam toe may be a good complement to visual inspections for seepage outflow detection at the dam toe. The sensors should be buried close to the seepage face or deeper so that short-time temperature variation can be avoided.

The results from the field test can be further evaluated and should be compared with the known defects before taking any further steps. Finally, these conclusions are drawn without any knowledge of the real location of the defect and some of the conclusions may therefore be changed after revealing the defects.

# Content

### SUMMARY

1	INTRODUCTION	
P	RT 1 - PRE-STUDY	
2	MODEL DAM       3         2.1 DESIGN       3         2.2 MATERIAL PROPERTIES       3         2.3 DESIGN OF POTENTIAL DEFECTS       4         2.4 SENSITIVITY       5	
3	ESTIMATION OF TEMPERATURE CHANGES         6           3.1 TEMPERATURES IN SOIL AND WATER         6           3.2 THERMAL PROCESSES         7	
4	RESISTIVITY - MEASUREMENT METHODOLOGY AND PARAMETER CHANGE 9 1.1 MEASUREMENT LAYOUT AND ESTIMATED MONITORING ACCURACY 9 1.2 BASIC MODELLING PRINCIPLES 9 1.3 RESULT	
5	SELF POTENTIAL - MEASUREMENT METHODOLOGY AND PARAMETER CHANGE 10 5.1 MEASUREMENT LAYOUT AND ESTIMATED ACCURACY	6
6	CONCLUSIONS23	
P	RT 2 - FIELD MEASUREMENTS	
7	THE DAM AND GENERAL MEASUREMENTS       25         7.1 DAM DESIGN       25         7.2 WATER LEVELS       25         7.3 SEEPAGE MONITORING       26         7.4 MONITORING PROGRAM       27         7.5 LABORATORY MEASUREMENTS       28	
8	TEMPERATURE – FIELD MEASUREMENTS       31         3.1 INSTALLATION AND MONITORING METHOD       31         3.2 ESTIMATED INITIAL TEMPERATURE IN THE CORE       32         3.3 RESULTS       32         3.4 EVALUATION       36         3.5 DETECTED DEFECTS       38	

### ELFORSK/BC Hydro

9	RI	ESISTIVITY – FIELD MEASUREMENTS	40
	9.1	INSTALLATION	
	9.2	RESULTS EXTENDED LINE	41
	9.3	RESISTIVITY MEASURING RESULTS	42
	9.4	RELATIVE DIFFERENCE VERSUS WATER LEVEL	
	9.5	RELATIVE DIFFERENCE VERSUS TIME	
	9.6	INDUCED POLARISATION RESULTS	
	9.7	DETECTED DEFECTS	51
1(	) SE	P - FIELD MEASUREMENTS	52
•		TIME-SERIES MEASUREMENTS	
		RESISTIVITY EFFECTS.	
	10.3	ONE-TIME MEASUREMENTS	59
	10.4	CONCLUSIONS	63
	10.5	DETECTED DEFECTS	64
1-	ı VI	SUAL OBSERVATIONS	65
•		GENERAL	
		DAM TOE OBSERVATIONS AT FILLING #1	
		DAM TOE OBSERVATIONS AT FILLING #2	
		DAM TOE OBSERVATIONS AT FILLING #3	
		DAM TOE OBSERVATIONS AT FILLING #4	
	11.6	DETECTED LEAKAGES	66
12	2 FI	ELD MEASUREMENT – DISCUSSION	68
		REAL CONDITIONS VERSUS ASSUMPTIONS IN THE PRE-STUDY	
	12.2	RESULTS	69
	12.3	FIELD SCALE VERSUS OTHER SCALES	71
13	B PF	ROPOSED NEXT STEPS	73
•		FIRST STEP - COLLECTION OF EXPERIENCE.	
		SECOND STEP – TRANSFERRING RESULT TO OTHER SCALES	
	13.3	THIRD STEP – REPEATED OR NEW TESTS IN DIFFERENT SCALES	74
14	ı cı	ONCLUSIONS	75
1	5 A(	CKNOWLEDGEMENT	76
46	e Di	EEEDENCES	77

### 1 Introduction

Resistivity, Self Potential, and Temperature are three indirect methods for leakage monitoring in embankment dams. The methods have been used in several embankment dams for investigation and monitoring at research applications and practical use. The interpretation of the result is however sometimes uncertain, and furthermore often difficult to verify with other methods. BCHydro (Canada), Elforsk AB (Sweden) and EBL represented by Statkraft Grøner (Norway) jointly conducted a research project in order to test the performance of those methods at the unique test dam at Røsvatn in Norway. The dam is a small rockfill dam designed and constructed with zones of relatively high permeability located in the low permeability core material.

The project team was separated into a "defect design group" which did not participate in the monitoring, and a "monitoring group" which had no knowledge of the locations and sizes of the zones of high seepage. This arrangement allowed making the monitoring project as a blind test of the capability of these methods performed. This report is written by the "monitoring group" before any information was given about the defects.

The staff and their responsibilities in the project are shown below.

Defect design group	Monitoring group	
Steve Garner, BCHydro	Torleif Dahlin. LTH Resistivity	
Åke Nilsson, Swedpower AB	Johan Friborg, SP	
	HydroResearch	
	Sam Johansson, Project leader, temper	
	HydroResearch	visual inspection,
	Pontus Sjödahl, LTH	Resistivity, visual inspection

A reference group was also created for the project including: Des Hartford (BCHydro), Lars Hammar (Elforsk AB), Aslak Lövoll (EBL), Einar Ødemark (Statkraft-Grøner), Tina Fridolf (Svenska Kraftnät), and Malte Cederström (Vattenfall Vattenkraft).

This study and the field monitoring is similar to a one time geophysical dam investigation, i.e. not long term monitoring that is the objective of our ongoing research project (funded by Elforsk AB, Svenska Kraftnät, and Dam Safety Interest Group). The ability and sensitivity to detect seepage will thus not be similar. Some experiences will however be relevant also for long term monitoring.

A pre-study was made by the monitoring group in order to guide the defect design group. The result is found part 1 of this report (chapter 2-6), and was delivered as a draft to the design group in early June. The dam including the defects was constructed in June-July. Measurements were made in August. The results are presented in Part 2 (chapter 7-11) followed by discussions and conclusions.

Part 1 - Pre-Study June 03, 2003

### 2 Model dam

### 2.1 Design

The dam used in the pre-modelling is 40m long and 6m high. The abutments consist of rock and are steep. During the measurements the crest of the dam will not be covered by rock fill, i.e. a direct access to the core will be allowed during measurements.

In the following calculations we have used the size of the proposed dam as shown in Figure 2-1. The core of the real dam may be steeper (10:1 instead of 4:1). The proposed core material (moraine) may also be replaced by a silty sand (grain size 25-40% finer than  $0.075 \, \text{mm}$ ,  $d_{\text{max}} < 0.8 \, \text{mm}$ ).

Central moraine core (fines > 25%;  $d_{max}$ <60mm) constructed in 1m layer with a 4 ton vibratory roller.

- A: Downstream rock fill support (0-500mm, d<sub>10</sub>>10mm
- B: Upstream rock fill support (300-400mm)

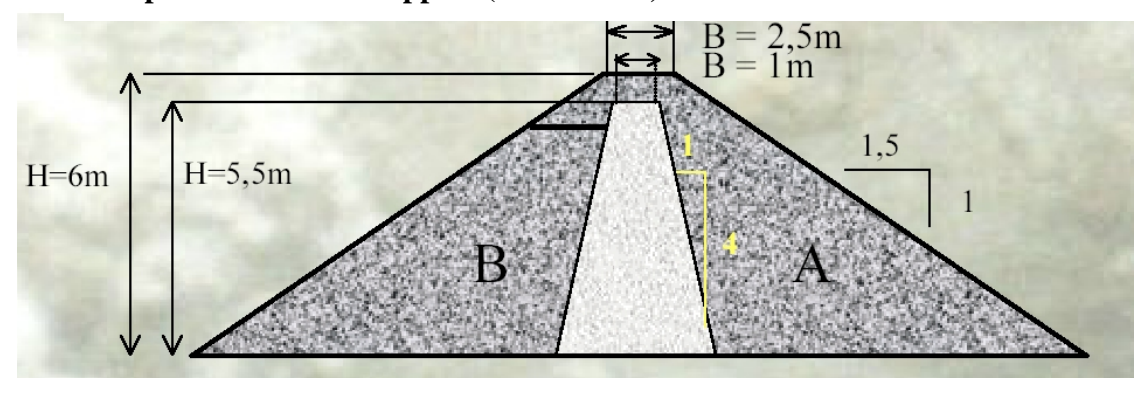


Figure 2-1 Cross section of the planned dam.

#### 2.2 Material properties

Data about soil properties for this application are rare, especially for the cross-coupling coefficient, L. The values used in this study (see Table 2-1), are assumed based on several literature data (Archie 1942, Bergström 1998, Schön 1996) and experience from dam monitoring in Sweden. The variation for all these parameters may be large and laboratory test should be done after the monitoring.

Table 2-1	Assumed material data for the calculations.
rame 4-r	Assumed material data for the calculations.

	Porosity	Resistivity	K	L
		(Qm)	(m/s)	(A/m)
Moraine	0.18	500	1.0E-06	3.0E-05
Fine sand	0.25	2800	1.0E-04	5.0E-05
Coarse sand	0.28	2400	1.0E-03	6.0E-05
Gravel	0.31	2100	1.0E-02	7.0E-05
Rockfill A	0.35	20000	1.0E-01	
Rockfill B	0.35	1700	1.0E-01	
Water		400		

### 2.3 Design of potential defects

The location, size and material used in the defect areas zone are unknown. In order to estimate some defects that can be detected, sensitivity analysis has been made due to:

- Depth from the core crest
- Size
- Flow change (K, H)

Calculations are made for three depths (1m, 3m and 5m), but only for one reservoir level (0.5m below the crest). The size of the defect as well as the geometry has been tested for several types. The largest reasonable size of the defect is about the maximum construction layer thickness, i.e. 1m and the smallest will probably be about one decimetre high. The extension along the dam can be up to some meters. Six defect types were thus defined but calculations were only made for the four types in the middle:

- SS: Small square  $(0.25*0.25=0.08m^2)$
- MS: Medium square (0.5m\*0.5m=0.25m<sup>2</sup>)
- MW: Medium wide (0.25\*1.0=0.25m<sup>2</sup>)
- LS: Large square (1\*1=1.0m<sup>2</sup>)
- LW: Large wide (0.4\*2=0.8m<sup>2</sup>)
- XLW: Extra large wide  $(0.4*4=1.6m^2)$

Table 2-2 Estimated flow using Darcy's law, and I=0.5, assuming final water level in the reservoir. (Other flow rates due to eventual step wise filling will not be studied.)

Defect type		Geometry:			Flow (m <sup>3</sup> /s)		
	Height (m) Width (m) Area (m2)		Fine sand	Coarse sand	Gravel		
SS	0.25	0.25	0.06	3.1E-06	3.1E-05	3.1E-04	
MS	0.50	0.50	0.25	1.3E-05	1.3E-04	1.3E-03	
MW	0.25	1.00	0.25	1.3E-05	1.3E-04	1.3E-03	
LS	1.00	1.00	1.00	5.0E-05	5.0E-04	5.0E-03	
LW	0.50	2.00	1.00	5.0E-05	5.0E-04	5.0E-03	
XLS	2.00	2.00	4.00	2.0E-04	2.0E-03	2.0E-02	
XLW	1.00	4.00	4.00	2.0E-04	2.0E-03	2.0E-02	

### 2.4 Sensitivity

A defect in the dam can be detected if the change is larger than the monitoring accuracy. A detection index, DI, has been defined to present and compare the result for each of the methods. The index is defined as the "Estimated Change" (which is the result from the prestudy calculations) divided with the "Monitoring and Evaluation Accuracy" (which is estimated as the possible accuracy for the situation on the test dam). There are several other secondary factors however, which may affect the sensitivity such as variation of soil characteristics and temperature. The detection index grades have been chosen as follows:

• Undetectable: DI < 1 (Estimated change < Monitoring and Evaluation Accuracy)
• Detectable?: DI  $\approx$  1 (Estimated change  $\approx$  Monitoring and Evaluation Accuracy)
• Surely detectable: DI > 1 (Estimated change > Monitoring and Evaluation Accuracy)

### 3 Estimation of temperature changes

### 3.1 Temperatures in soil and water

The seasonal temperature variation that is used for seepage detection using resistivity cannot be used in this case as done in the long term monitoring project. The temperature will however affect the measurements due to temperature differences between the construction material and the water. At this stage there are many uncertainties about those temperatures, and it's therefore suggested that those temperatures are measured during the test to allow corrections later. No detailed calculations are needed, just a first estimation of reasonable temperature in soil and water.

No meteorological data is available for the test site so data has been taken from Sädva dam, one of the test sites for geophysical long term monitoring in Sweden. Sädva dam is located around 130 km from the site and at similar elevation, and available temperature data from Sädva (Figure 3-1) are used in the following to estimate the temperature in the dam.

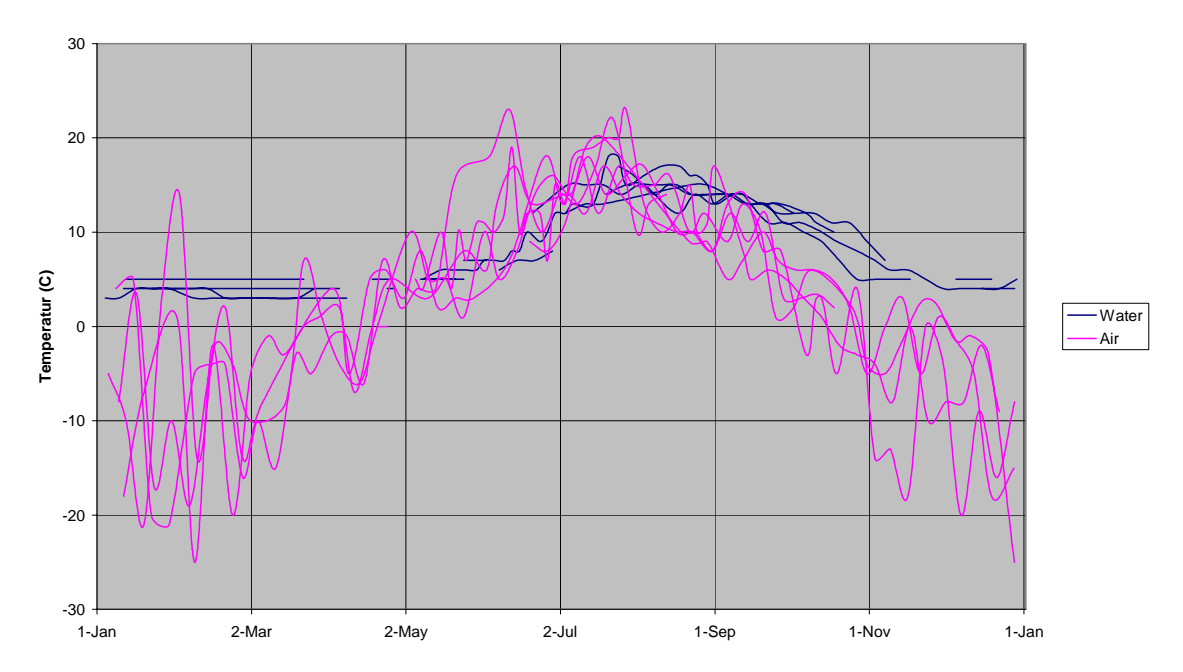


Figure 3-1 Water and air temperature for five different years at Sädva (1997 -2002). The water temperature is taken at a bottom inlet that explains the high temperature in the winter (about  $4^{\circ}$ C).

If we assume that the construction of the dam will start in June, the soil material will have a low temperature, probably just a few °C. This is lower than the air temperature in the summer and the soil will slowly be warmed up during construction. The soil temperature will probably not exceed 10°C, because the size of the dam gives a long time (some months) to achieve thermal equilibrium. The temperature in the dam will thus vary several degrees.

The temperature within the dam will be similar to or lower than the mean water temperature during the construction time. A temperature difference of 5°C seems reasonable if the reservoir upstream the test dam is filled in August. The difference may be smaller and depends on the water level in the reservoir that gives the depth to the gate openings. A warm summer may on the other hand give a larger temperature difference but 10°C is probably a maximum. The largest variation will occur at high seepage.

#### 3.2 Thermal processes

The main heat transport process in embankment dams is the convective flow, given by the seepage. At very low seepage flow as in low-permeable till heat conduction may be of the same order. We can thus assume that the heat transport in the proposed material in the defect (fine sand, coarse sand, and gravel) will be given by the convective flow.

The thermal velocity,  $v_T$  caused by the advective flow by the seepage (Johansson and Dahlin, 1996 or Johansson, 1997) can be used to estimate the travel time for the temperature front to reach the end of the core (neglecting heat losses), see Table 3-1 This approximate approach is reasonable since the input temperatures are just estimations at this stage. The result shows that a temperature anomaly can be expected for all defect depths and at all materials, within a monitoring time of about one day. An almost direct temperature effect should thus be considered, especially at coarse sand gravel. At fine sand changes could be expected during the measurements.

Table 3-1	Calculated travel	times for different	depths and materials.

	Hydraulic Conductivity, K	Volumetric Heat capacity	Flow q=K*I	Thermal velocity		(h) to end	of core
	(m/s)	$(MJ/(m^3,K))$	(m/s)	(m/d)	Depth 1m	Depth 3m	Depth 5m
Moraine	0.000001	2.1	5E-07	0.09	833	1389	2222
Fine sand	0.0001	2.5	0.00005	7.3	10	17	26
Coarse sand	0.001	2.5	0.0005	73	1.0	1.7	2.6
Gravel	0.01	2.4	0.005	756	0.1	0.2	0.3

The temperature dependence on the resistivity is shown in Figure 3-2. The assumed resistivities in Table 2-1 decrease with about 20% between 5 and 10°C. Several important observations can be made, especially:

- The resistivity contrast between the moraine and the sand/gravel will decrease during the measurements, i.e. the sensitivity will decrease slightly due to different travel time.
- Resistivity variation in the non-damaged part of the dam will thus be sign of heterogeneous material, compaction and construction.

• We can not distinguish between a temperature change or a change of material properties. Note that coarse sand at 10°C have the same resistivity as fine sand at 15°C or gravel at 6°C.

The chosen material and their resistivity values will thus affect the resistivity in the same order as the temperature, assuming 5-10°C difference between the soil and water during the summer.

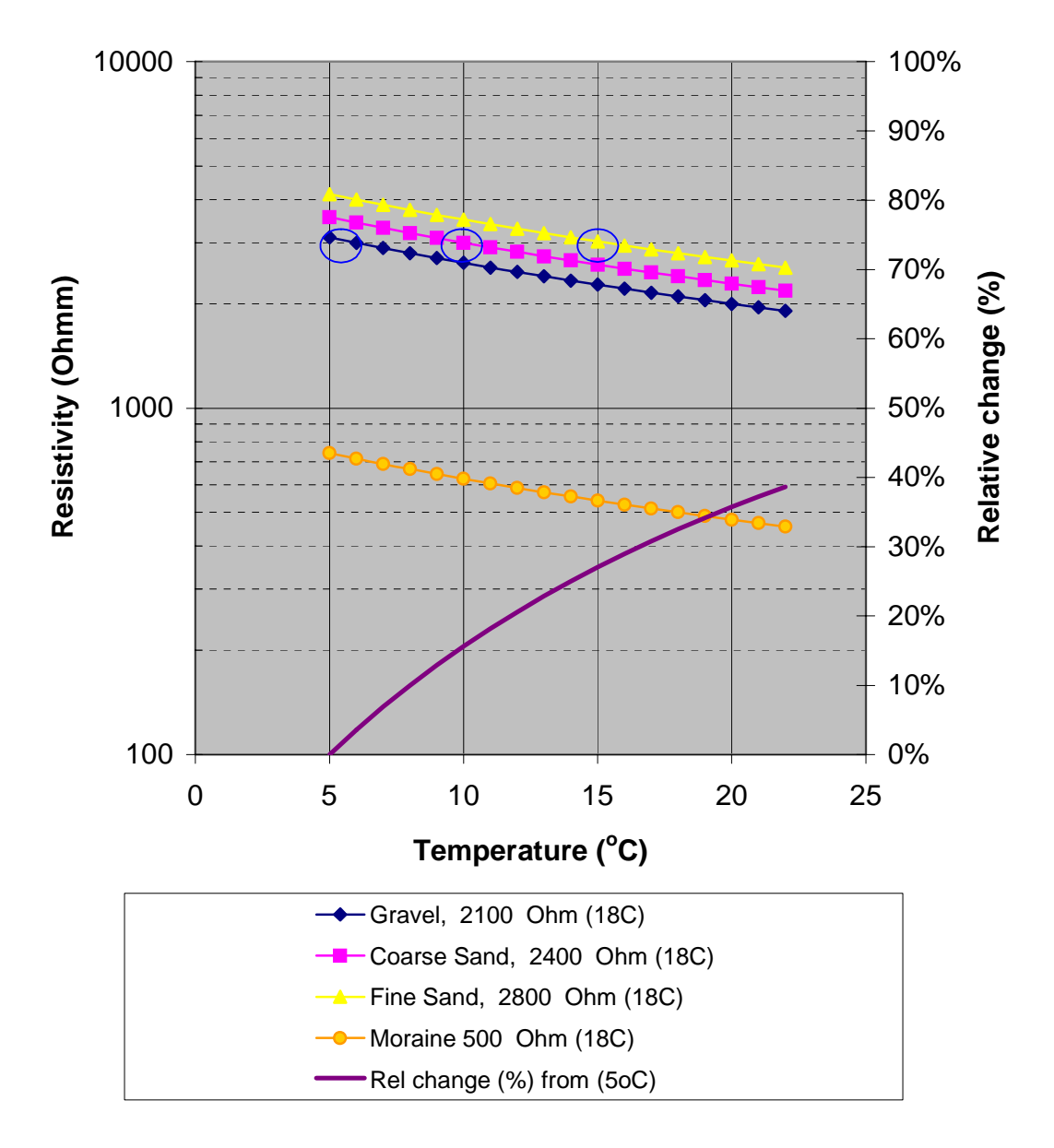


Figure 3-2 Resistivity of the soil as function of temperature showed in logaritmic scale. Relative changes shown on the left axis. Note that the relative change is the same for all materials due to the linear resistivity change with temperature.

# 4 Resistivity - Measurement methodology and parameter change

#### 4.1 Measurement layout and estimated monitoring accuracy

The resistivity modelling was designed to be as relevant as possible for the actual field experiments, in terms of material properties and geometry. Measuring was to be carried out as two-dimensional (2D) resistivity imaging with electrodes installed along the crest of the dam. This is the most convenient way to arrange the electrodes, and the most relevant since it is often the only practical option for monitoring installation in existing dams.

For the field measurements a layout of 63 electrodes along the crest of the dam with a spacing of 2/3 metre was planned. Since the electrodes will be installed directly in the dam core we expect to get low electrode contact resistances. Under such conditions we expect to get very high data quality, which in combination with the short electrode separations is believed to result in average measurement errors below 1%.

Test measurements will be carried out with different electrode arrays, and namely gradient, pole-dipole and dipole-dipole arrays. Measurements will also, at least for some of the time steps, be carried out as combined resistivity and induced polarisation (IP) surveying.

The modelled data was analysed through inverse numerical modelling (inversion) using the commercial software Res2dinv (Loke et al. 2001), using the same approach as intended for the acquired field data. Time-lapse inversion was employed to analyse the data from the repeated measurements for change in resistivity, which has the advantage of focusing the results on actual change and suppressing artefacts due to data noise (Loke 2001).

#### 4.2 Basic modelling principles

In order to assess the resolution capability of the measurement concept outlined above, three-dimensional (3D) forward numerical modelling of resistivity measurements was carried out. The 3D modelling was done using the resistivity modelling software *Res3D*, developed by Dr. Bing Zhou at University of Adelaide, Australia. It can be used to calculate three-dimensional potential field or apparent resistivity values for a complicated geological model. It handles arbitrary electrode configurations. An efficient finite element method has been applied to the modelling (Zhou and Greenhalgh 2001).

A geometrical model over the planned dam design was created, and the measurement configurations were simulated. By comparing output results from the forward models of the healthy dam and the dam with different built-in defect the detection level of the defects scenarios could be estimated.

The results presented here only include modelling involving the gradient array. The three-dimensional model of the planned embankment construction was built using cell dimensions of (x, y, z) = (0.25, 0.50, 0.25) meters, resulting in a full model of (82, 82, 23)

cells not including the boundary zones. Design parameters and assumed resistivities are presented elsewhere in this report. Boundary conditions are assumed to be regular rock (20000  $\Omega$ m) at the foundation and abutments and air elsewhere.

The simulated measurements in the modelling study involve 518 individual measurements, using the gradient array, with a layout along the top of the dam core with the electrodes placed into the top of the core. Previous studies have shown that the gradient array demonstrates reliable results (Dahlin and Zhou 2001; Dahlin and Zhou 2002). Moreover, it is suitable for field measurements as it can be used with multi-channel equipment making it very efficient. A minimum electrode spacing of 1 metre is assumed here. In practical measurements, depending on the conditions at the site, it might be possible to reduce the minimum spacing down to 2/3 of a metre thereby increasing the resolution slightly.

Apparent resistivity values from the measurements simulated in the three-dimensional modelling were collected both for a healthy dam model and for a modelled dam with the assumed defects. Anomaly pseudosections were plotted to get a rough estimate of the size of the anomaly. Subsequent to that the data sets were inverted using the L1-norm optimisation method to estimate true ground resistivities. These resistivities were compared and the anomaly effect, defined by the change in resistivity due to the simulated defect, was estimated and presented. All defects were located at the midpoint of the section.

#### 4.3 Result

#### 4.3.1 Healthy dam

Simulations were made for the healthy dam using the gradient array. Two-dimensional inversion was carried out on the forward model output data. This is the only feasible way to invert apparent resistivity data from embankment geometries available today, even though it needs to be done with attention as the geometrical rules for two-dimensional inversion is clearly violated. As can be seen from the 2D inverted dam model resistivities are increasing with depth even though the core is assumed to have a constant resistivity with depth (Figure 4-1). This is explained by the fact that at larger depths a larger earth volume is involved for the current flow, and in that case the effect from the embankment slopes and the high-resistive downstream fill will increase.

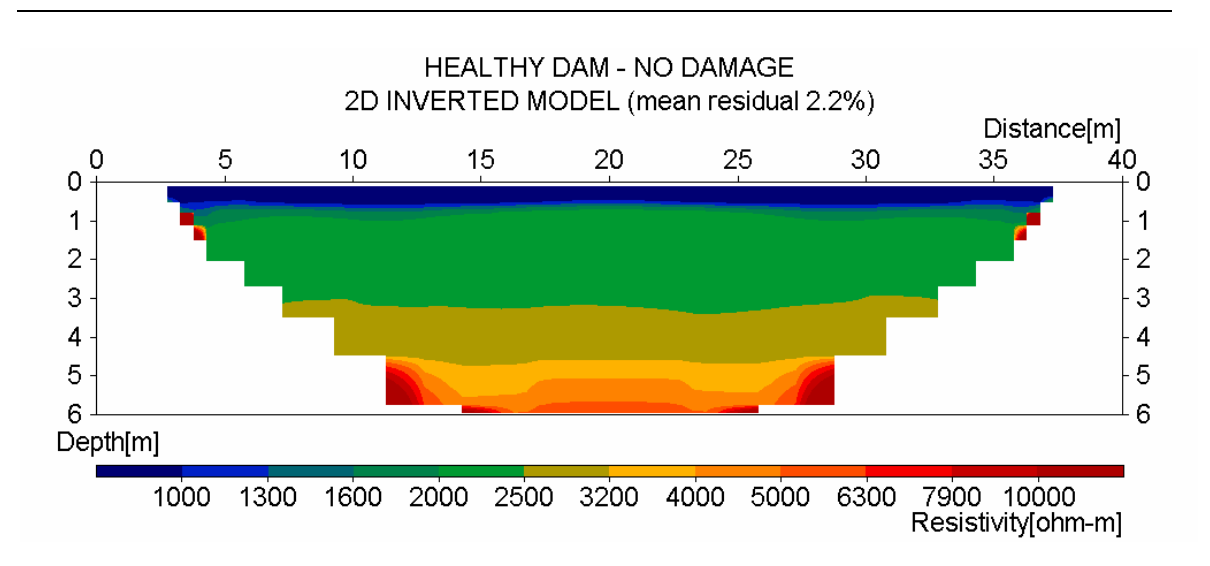


Figure 4-1 Inverted resistivity of a healthy dam.

## 4.3.2 Defect - medium

Simulations were done for all three depths for fine sand, coarse sand and gravel. For the medium square defects the shallowest one is obviously detectable (Figure 4-2), whereas no effect at all is seen from the two deeper locations. The same goes for the medium wide defects.

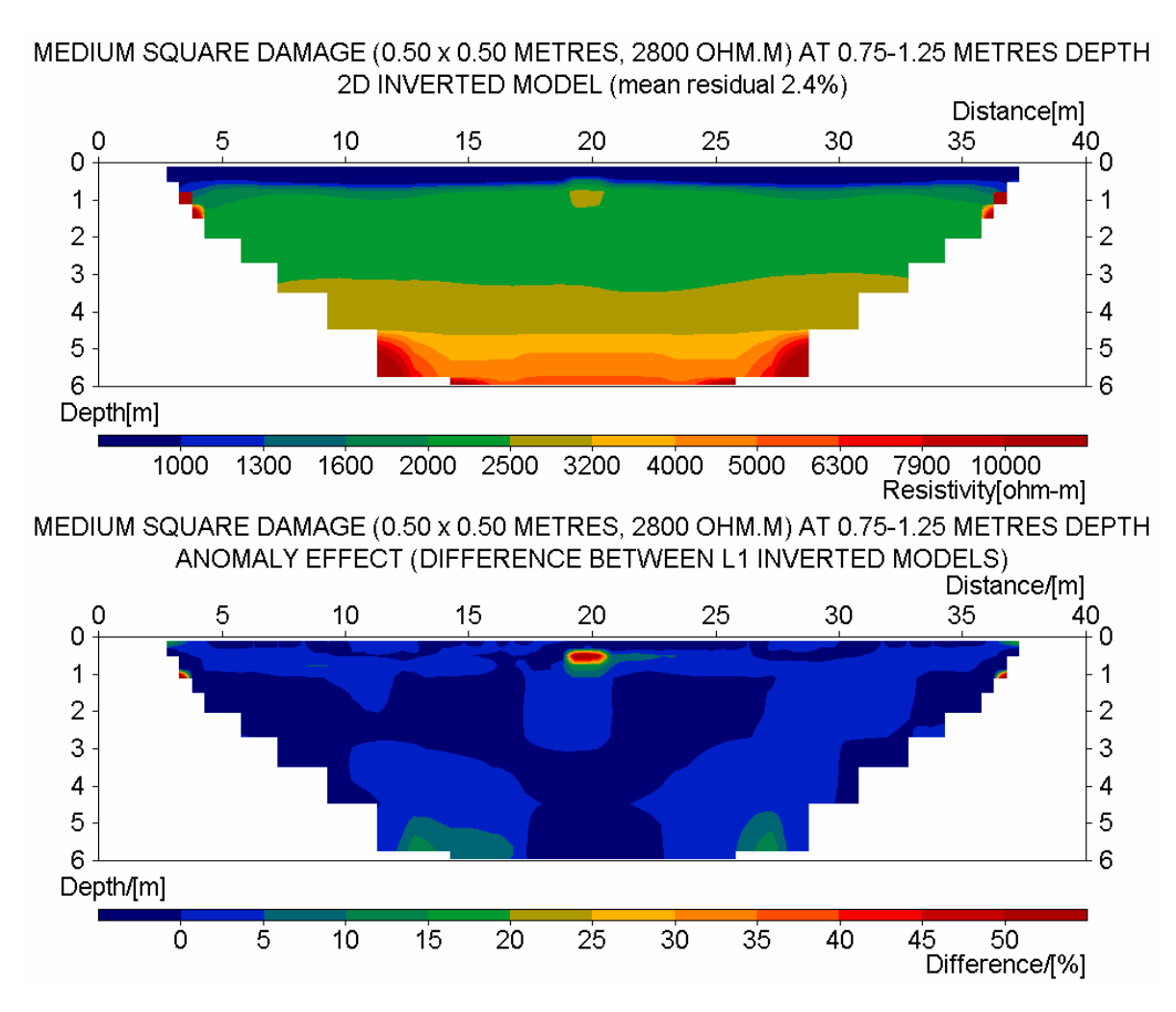


Figure 4-2 Inverted models (above) and difference model (below) for he medium square defect of fine sand located at 1 m depth.

## 4.3.3 Defect - large

Simulations were done for all three depths for fine sand, coarse sand and gravel. In this case both the large square (Figure 4-3) and the large wide defects are detectable for all depths, but harder to locate the deeper they are positioned. For the largest depth there is a tendency that the defect area is smeared out and due to this it seems very difficult to confidently identify the exact location. Moreover, the depth seems to be somewhat distorted for the medium depth, where the impression is that the defect area is placed more shallow than is the real case. This distortion of lateral location is something we have seen from prior studies of dam geometries (Sjödahl et al. 2002) and is something that we need to accept as long as 3D inversion schemes are not available and practically usable.

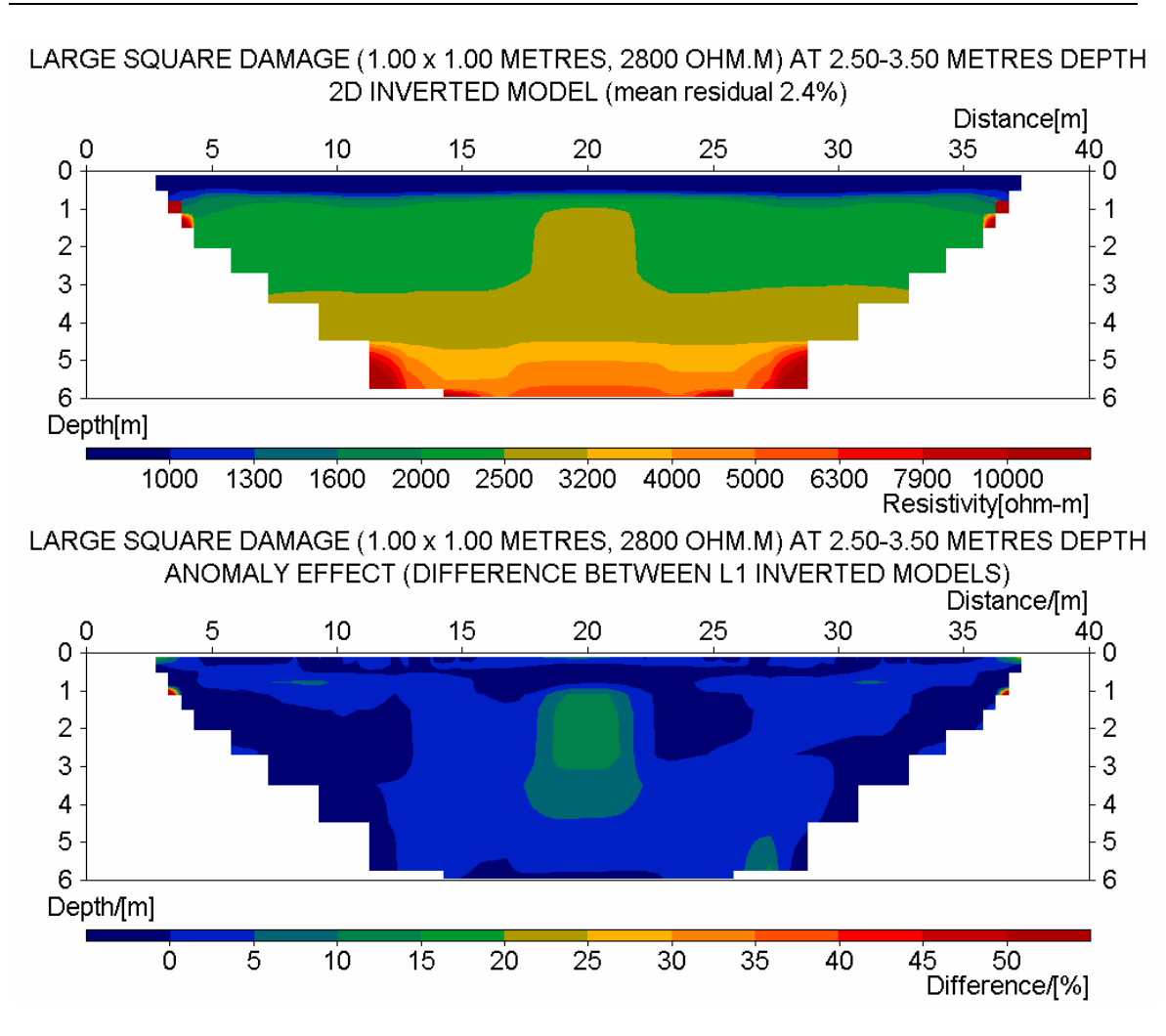


Figure 4-3 Inverted models (above) and difference model (below) for the large square defect of fine sand located at 3 m depth.

#### 4.4 Discussion

The size of the anomaly effect is affected by location, extension and resistivity contrast of the defect. At this moment the resistivity contrast is kept unchanged but it is important to keep in mind the importance of the material parameters assumptions. The size of the anomaly is varied and the medium square size might need a smaller electrode spacing to improve resolution. The depth is important; high depths are naturally both more difficult to detect and has a tendency to be smeared out in space.

Evaluating the in-field detectability of the defects from these theoretical values of anomaly effects needs some kind of error estimation. Measurement errors should be less than 1 % assuming good electrode grounding conditions and moderate ambient noise levels, but with high contact resistances average measurement errors can easily amount to several percent. Error in the calculations, both the 3D forward model and the inversion, are estimated to be less than 5 %. With these assumptions, anomaly effects of 10% or more will be surely

detectable, and as defined in chapter 2.4 the detection index is defined as the detectable anomaly divided by this number. The detection index for 1m depth are well over 1, i.e. all defect level decreases rapidly with depth, as seen in Figure 4-4.

Table 4-1 Detection index DI for depth 1, 3 and 5m.

Defect	Fine sand	Coarse sand	Gravel	
Medium (Area= 0.25m²) Medium square	DI <sub>1m</sub> =9, Surely Detectable DI <sub>3m</sub> <1, Undetectable DI <sub>5m</sub> <1, Undetectable	ectable DI <sub>3m</sub> <1,Undetectable DI <sub>3m</sub> <1, Undetectable		
Medium wide	DI <sub>1m</sub> =9, Surely Detectable DI <sub>3m</sub> <1, Undetectable DI <sub>5m</sub> <1, Undetectable	DI <sub>1m</sub> =10 Surely Detectable DI <sub>3m</sub> <1,Undetectable DI <sub>5m</sub> <1, Undetectable	DI <sub>1m</sub> =8 Surely Detectable DI <sub>3m</sub> <1, Undetectable DI <sub>5m</sub> <1, Undetectable	
Large (Area= 1m²) Large square	DI <sub>1m</sub> =32,Surely Detectable DI <sub>3m</sub> ≈1, Detectable DI <sub>5m</sub> <1, Undetectable	DI <sub>1m</sub> =30, Surely Detectable DI <sub>3m</sub> ≈1, Detectable DI <sub>5m</sub> <1, Undetectable	DI <sub>1m</sub> =27, Surely detectable DI <sub>3m</sub> ≈1, Detectable DI <sub>5m</sub> <1, Undetectable	
Large wide	DI <sub>1m</sub> =42 Surely Detectable DI <sub>3m</sub> ≈1, Detectable DI <sub>5m</sub> <1, Undetectable	DI <sub>1m</sub> =38, Surely Detectable DI <sub>3m</sub> ≈1, Detectable DI <sub>5m</sub> <1, Undetectable	DI <sub>1m</sub> =33 Surely detectable DI <sub>3m</sub> ≈1, Detectable DI <sub>5m</sub> <1, Undetectable	

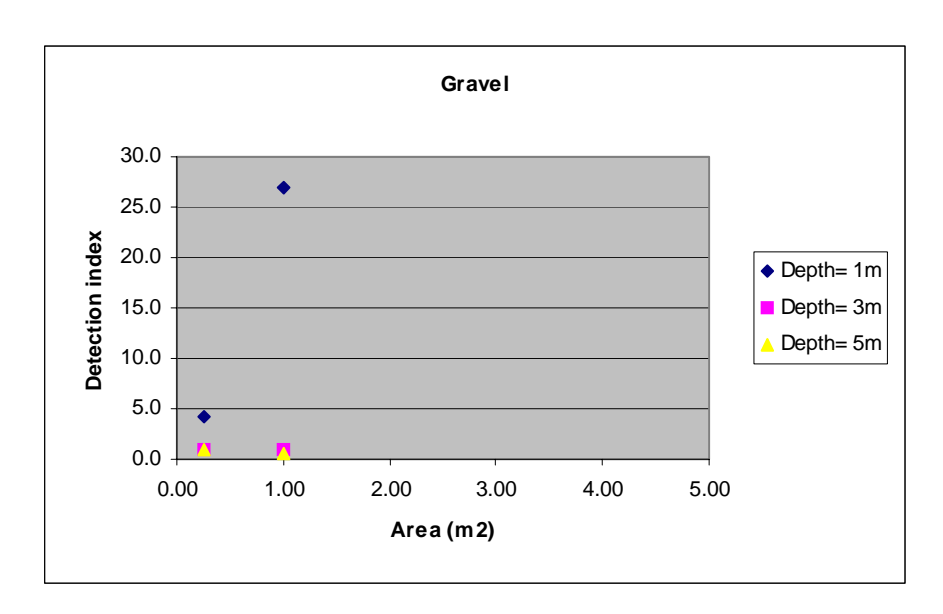


Figure 4-4 Detection index as a function of area for different depth to the defect.

It is important to realize that the modelling results are dependent on the assumptions made concerning material properties. Little data on the resistivity of soil materials used for dam construction was found before carrying out the modelling, and it is important to verify that the assumptions are valid through laboratory analysis of soil samples and in-situ

measurements at representative sites. It is probably well motivated to repeat modelling for other material properties when such data becomes available.

It should also be pointed out that the modelling only accounts for changes in material properties, without any consideration of temperature induced variation in resistivity. As shown in Figure 3-2 the resistivity of the soil material varies significantly with temperature, and the resistivities used here can in fact coincide to some extent if the temperature variation is not in phase. This fact, together with the rather small to small changes caused by the anomalous zones, adds to difficulties of detecting zones of anomalous leakage with measurements carried out at a single point in time. On the other hand, a temperature variation will add temporal variation to the resistivities, which is not restricted to the defect area itself but will also affect a volume around the anomalous zone. This should strongly increase the possibility to detect zones of anomalous leakage. The effect of temperature was considered by Johansson et al (in the well known but still unpublished parameter study), but at that time 3D modelling was not available so the results cannot be directly compared. It would be valuable to carry out modelling that takes the temperature-induced variation into account using the same software and modelling parameters as presented here.

# 5 Self potential - Measurement methodology and parameter change

#### 5.1 Measurement layout and estimated accuracy

Johansson et al (2001) estimate the detection limit in a monitoring installation to be between 10 and 20 mV. For the present investigation we need not worry about any seasonal variation. An estimated detection limit of 10 mV will be used in the following discussion.

### 5.2 Basic modelling principles

Friborg (1997) describes the basis of the modelling procedure. The main idea is that, when integrated over the whole space, the conduction current must equal the streaming current generated by the fluid flow. This means that where there are discontinuities in the streaming current there must exist conduction current sources with strength equal to the value of the discontinuity. For the present study there will only be a streaming current in the core since the cross-coupling coefficient is assumed to be zero in the rock fill surrounding the core. Within the core the streaming current density,  $J_{\text{stream}}$ , is equal to:

$$J_{\text{stream}} = L \text{grad}(h), \tag{5.1}$$

where L is the cross-coupling coefficient and grad(h) is the hydraulic gradient.

Since discontinuities in streaming current occur only at the boundaries of the core this is where the conduction current sources are located.

When the conduction current sources are known the coupled hydraulic and electric problems have been transformed into a purely electrical one. Equation 5.1 gives the magnitude of the current sources to input to the modelling procedure. To solve the electric problem we have used Res3D, a 3D resistivity modelling software (Zhou and Greenhalgh, 2001).

The modelling of the streaming potential will use the following simplifying assumptions:

- Only the streaming potentials generated by the defect area will be calculated. This will be the deviation from the background streaming potential.
- The increased hydraulic conductivity in the defect area should not affect the overall hydraulic situation.
- Flow across the boundary between the core and the defect area will be neglected.
- The conduction current density at the ends of the defect area will be approximated by current point sources with equivalent total current.

#### 5.3 Results

Some selected results of the numerical modelling are shown in Figure 5-1, Figure 5-2 and Figure 5-3. Each panel shows the SP values at one profile perpendicular to the dam crest and one profile parallel with the crest. The perpendicular profile crosses the dam right above the defect area. The parallel profile runs at a position 1 m. downstream of the centre of the crest. This is the planned location for the field measurements.

#### 5.3.1 Defect - medium

The medium defect has a cross section of  $0.25m^2$ . Figure 5-1 and Figure 5-2 show the results of the modelling. For this defect the amplitudes of the anomalies are less than 3mV, and consequently not detectable with the assumptions made for the purpose of the present modelling. There are also only very small differences between the square and the wide defect.

#### 5.3.2 Defect - large

The large defect has a cross section of 1.0m<sup>2</sup>. The results of the modelling are shown in Figure 5-3 and Figure 5-4. For this defect the anomalies are less than 15mV, which should be detectable. There are only very small differences between the square and the wide defect.

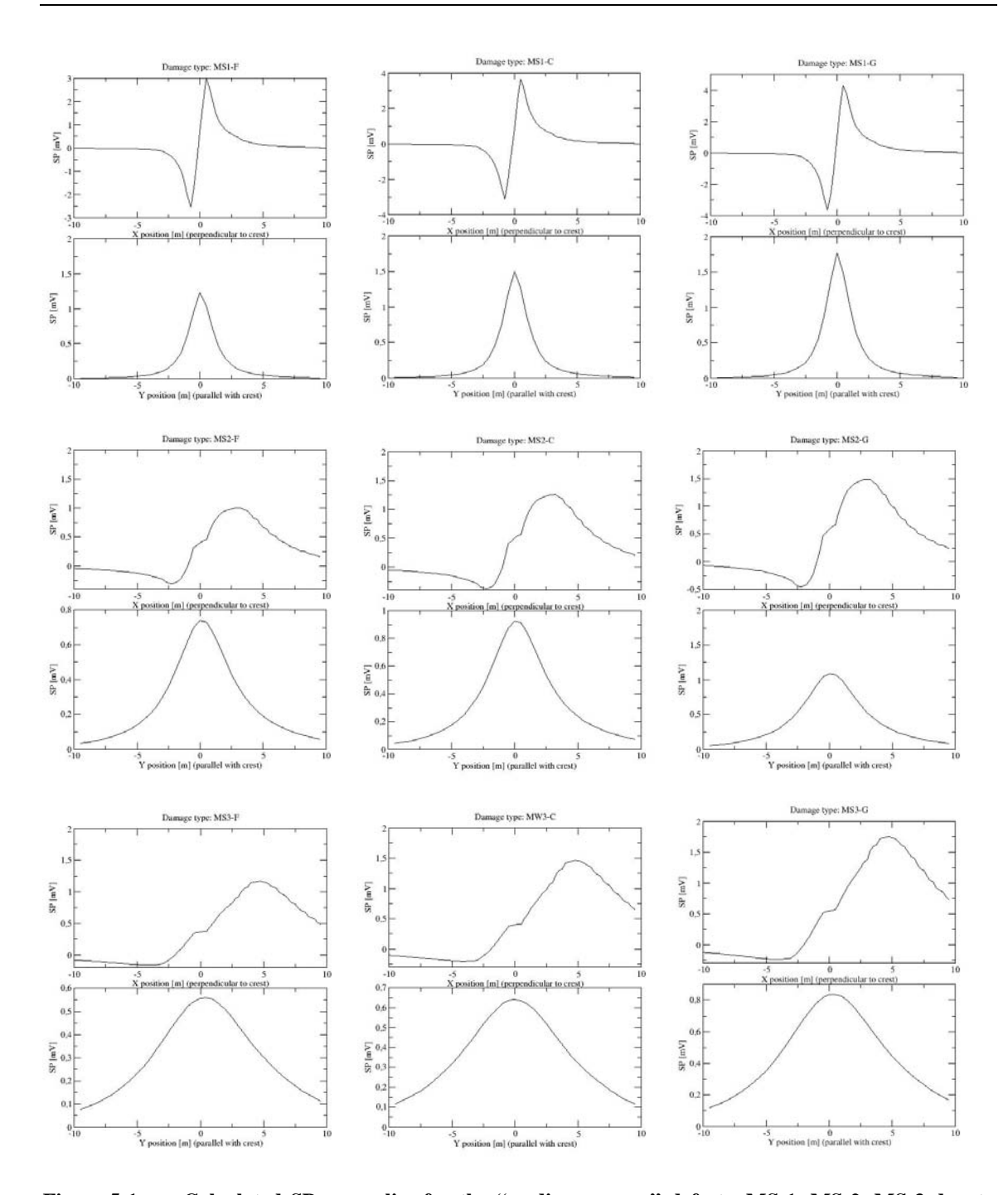


Figure 5-1 Calculated SP anomalies for the "medium square" defects. MS-1, MS-2, MS-3 denote defects at 1, 3 and 5 metres, respectively. The letters F, C and G indicate the type of material in the defect area (F=fine sand, C =coarse sand, G=gravel).

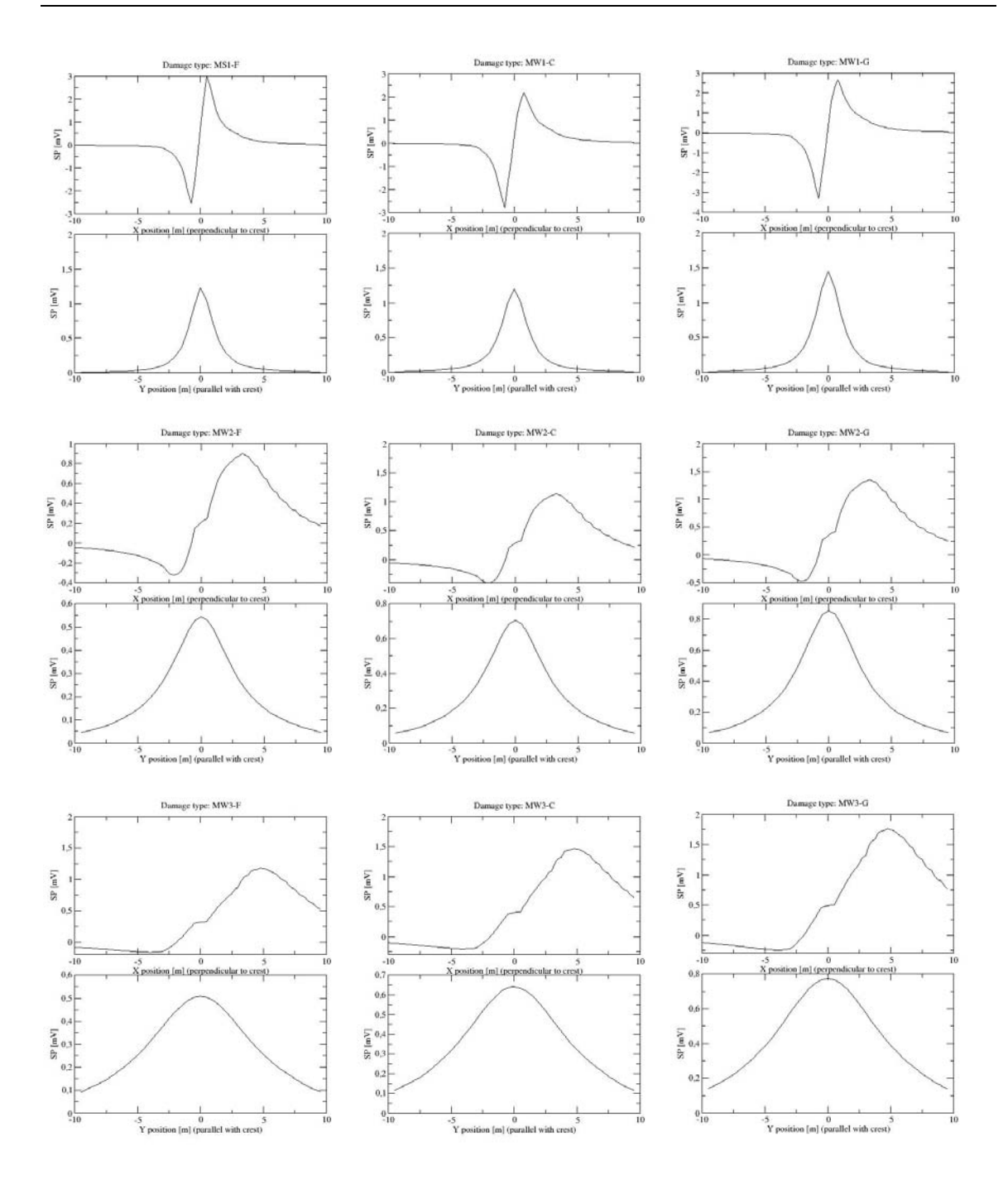


Figure 5-2 Calculated SP anomalies for the "medium wide" defect. MW-1, MW-2, MW-3 denote defects at 1, 3 and 5 metres, respectively. The letters F, C and G indicate the type of material in the defect area (F=fine sand, C=coarse sand, G=gravel).

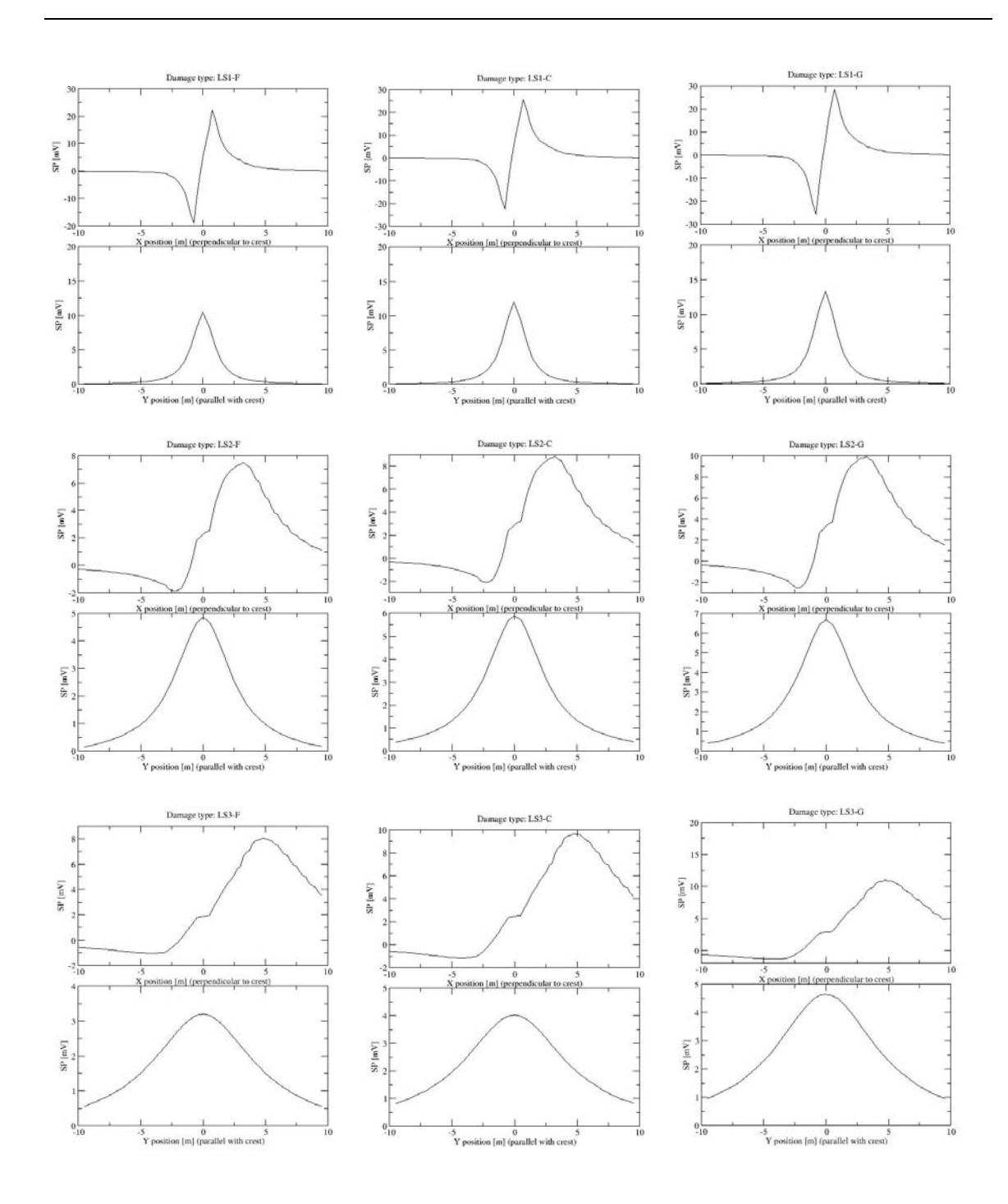


Figure 5-3 Calculated SP anomalies for the "large square" defect. LS-1, LS-2, LS-3 denote defects at 1, 3 and 5 meters, respectively. The letters F, C and G indicate the type of material in the defect area (F=fine sand, C=coarse sand, G=gravel).

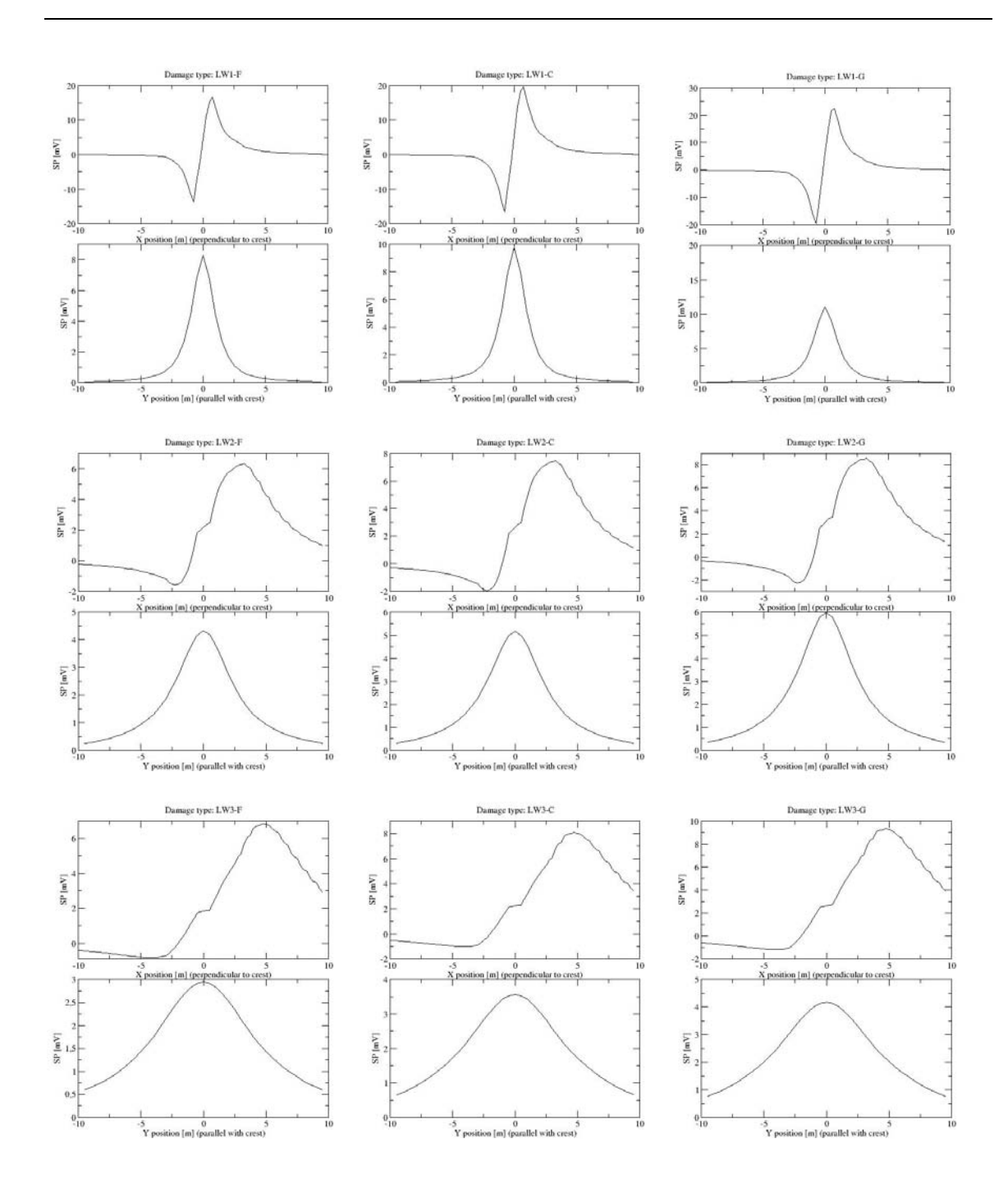


Figure 5-4 Calculated SP anomalies for the "large wide" defect. LW-1, LW-2, LW-3 denote defects at 1, 3 and 5 meters, respectively. The letters F, C and G indicate the type of material in the defect area (F=fine sand, C =coarse sand, G=gravel).

#### 5.4 Discussion

Table 5-1 summarizes the results of the numerical modelling experiments, by way of a detection index (DI). The DI is simply the amplitude of the anomaly at the profile parallel with the dam divided by an estimated smallest observable anomaly amplitude. The smallest detectable anomaly has been estimated to be 10 mV. The results indicate that in order to be detectable the defect must be quite large and located at shallow depth.

The location of the electrode line is also important to achieve maximum signal-to-noise ratio. The optimum position of the line varies with defect depth; the deeper the defect the further downstream should the electrodes be placed. It appears that a decent compromise would be to place the electrodes between 1 and 2 meters downstream of the dam centre. This does, however, not agree with the practice recommended in the CEA SP-manual (CEATI report No T992700-0205), which states that the upstream edge of the dam should generally be the primary location. We will consequently defer the final choice of electrode location until we have inspected the dam site.

The accuracy of the predictions one can make based on these numerical results is limited by the lack of knowledge of realistic in-situ values of the streaming potential cross-coupling coefficient. In this work we have opted to use values based on results found in the literature. Based on our previous experience with SP measurements on embankment dams we must express some doubts about the applicability of these values. Field measurements have on several occasions shown the existence of anomalies much larger than those predicted by the present numerical modelling.

Table 5-1 Detection index DI for depths 1, 3 and 5m.

Defect	Fine sand	Coarse sand	Gravel
Medium (Area= 0.25 m <sup>2</sup> )  Medium square	DI <sub>1m</sub> < 1, Undetectable DI <sub>3m</sub> < 1, Undetectable DI <sub>5m</sub> < 1, Undetectable	$DI_{1m} < 1$ , Undetectable $DI_{3m} < 1$ , Undetectable $DI_{5m} < 1$ , Undetectable	$DI_{1m}$ < 1, Undetectable $DI_{3m}$ < 1, Undetectable $DI_{5m}$ < 1, Undetectable
Medium wide	$DI_{1m}$ < 1, Undetectable $DI_{3m}$ < 1, Undetectable $DI_{5m}$ < 1, Undetectable	$DI_{1m}$ < 1, Undetectable $DI_{3m}$ < 1, Undetectable $DI_{5m}$ < 1, Undetectable	$DI_{1m}$ < 1, Undetectable $DI_{3m}$ < 1, Undetectable $DI_{5m}$ < 1, Undetectable
Large (Area= 1.0 m <sup>2</sup> ) Large square  Large wide	$DI_{1m} \approx 1$ , Detectable? $DI_{3m} < 1$ , Undetectable $DI_{5m} < 1$ , Undetectable $DI_{1m} \approx 1$ , Detectable? $DI_{3m} < 1$ , Undetectable	$DI_{1m} \approx 1$ , Detectable? $DI_{3m} < 1$ , Undetectable $DI_{5m} < 1$ , Undetectable $DI_{1m} \approx 1$ , Detectable? $DI_{3m} < 1$ , Undetectable	$DI_{1m} = 2$ , Detectable $DI_{3m} \approx 1$ , Detectable? $DI_{5m} < 1$ , Undetectable $DI_{1m} > 1$ , Detectable $DI_{3m} < 1$ , Undetectable
Large wide	,	, , ,	, ,

## 6 Conclusions

Surely detectably defects for both resistivity and SP must be in the order of one m<sup>2</sup> if the defect is located in the middle of the dam. Defects in the lower part will be difficult to detect. Defects should not be placed close to the abutments due to boundary influence. Avoid the area closer than 5-10m from the abutments (1-2H) especially for deep located defects (this is valid both for resistivity and SP).

The soil properties are important to verify by laboratory tests, and several should be done. Drainage of excess water from construction and from precipitation may also affect the result in some extent.

The variation in compaction during construction may in this case be seen as resistivity variations caused by temperature changes between the soil and the water in the reservoir. A detected resistivity anomaly will thus have two unknowns (resistivity of the soil and temperature). Perhaps the combined use of resistivity and SP will give some additional interpretation aspect.

Temperatures should be measured of the soil during construction, and if possible also after construction. Measurements should also be carried out at the dam toe during the field measurements.

A core of moraine is assumed for all simulations. If the moraine were be replaced by a silty-sandy material the resistivity contrast would be lower, as well as the detection ability. If the resistivity is lower than assumed, it will reduce the possibility for direct detection by resistivity measurements at one occasion. Lower water resistivity will also reduce the SP signals and thus the detection ability.

It must be observed that the sensitivity for one-time investigation is significantly lower than the sensitivity for long-term monitoring. The result of this study will therefore not be valid for long-term monitoring.

## **Part 2 – Field Measurements**

## 7 The dam and general measurements

### 7.1 Dam design

The detail design of the dam was not known during the measurements or at the evaluation, and evaluation has to be done without for example exact knowledge concerning variation in depth to bedrock and similar information. It is, however, known that a rather thick clay layer was put in place around the drainage pipes at the foundation of the dam, which will certainly affect the electrical measurements. Furthermore, the support fill on the upstream side was washed to remove fine particles, which was not done for the downstream side support fill. The latter means that the high resistivity assumed in the pre-study modelling is probably not relevant.

The reservoir can be drained using four outlet pipes (one Ø150mm, and three Ø200mm). Two pipes are operated by valves while the other are equipped with inflatable rubber packers. The outflow capacity is about 0.05-0.1m<sup>3</sup>/s for each pipe at high pool.

#### 7.2 Water levels

Water level in the reservoir was observed regularly towards a level gauge, located about 20 metre upstream the dam crest. The water level in the reservoir was measured regularly (Figure 7-1). The lowest levels are more uncertain since they were below the gauge and are estimated.

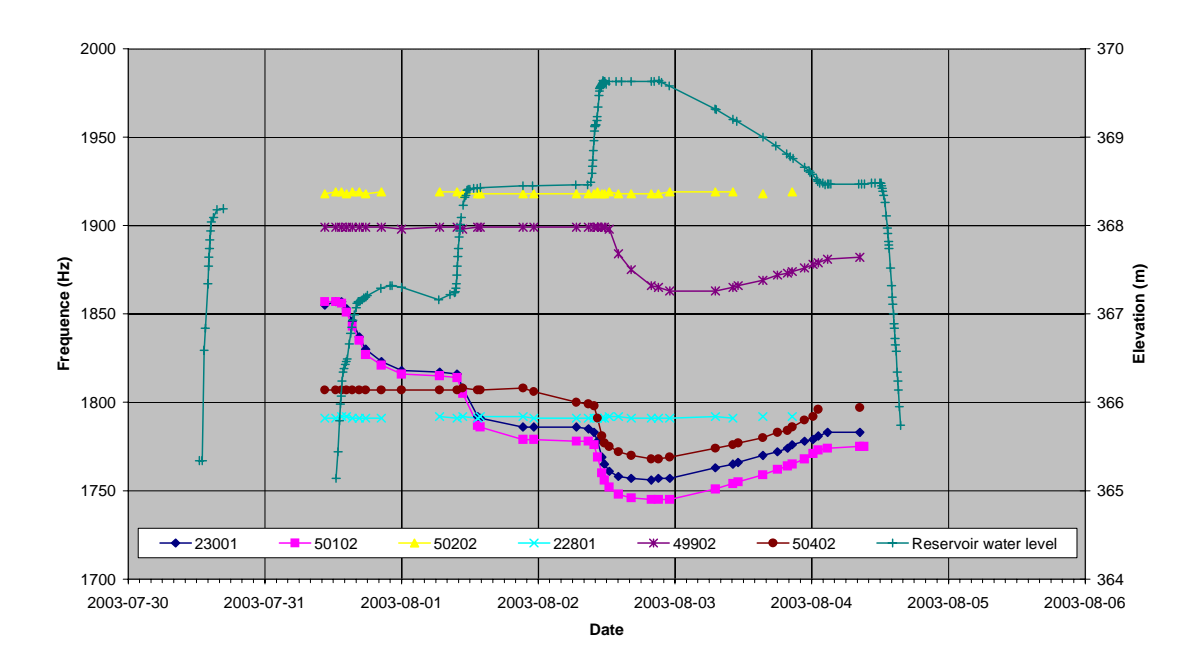


Figure 7-1 Reservoir water level and pore pressures in the piezometers (just measured frequencies, the location of the piezometers are unknown).

Six vibrating wire pressure sensors were also installed in the dam. Their locations and levels are unknown. Frequency readings were taken manually during the tests (Figure 7-1), but the result has not been converted to pressure, as decided by the reference group. The vibrating wire piezometers were also measured regularly. Their levels and locations are still unknown, but the result gives some indication if the condition is transient or stationary.

## 7.3 Seepage monitoring

All leakage water is intended to be caught in a weir at the left abutment. The weir was built in into the concrete bar located downstream the dam toe. Measurements were made regularly during the tests. The visual inspections showed however that some water was passing under the bar around section 5-6m. This outflow will probably collect water from the left part of the dam, maybe up to section 10-12m. The total leakage will thus be higher than measured, and only valid for the right and the middle parts of the dam.



Figure 7-2 Seepage flow weir downstream the dam.

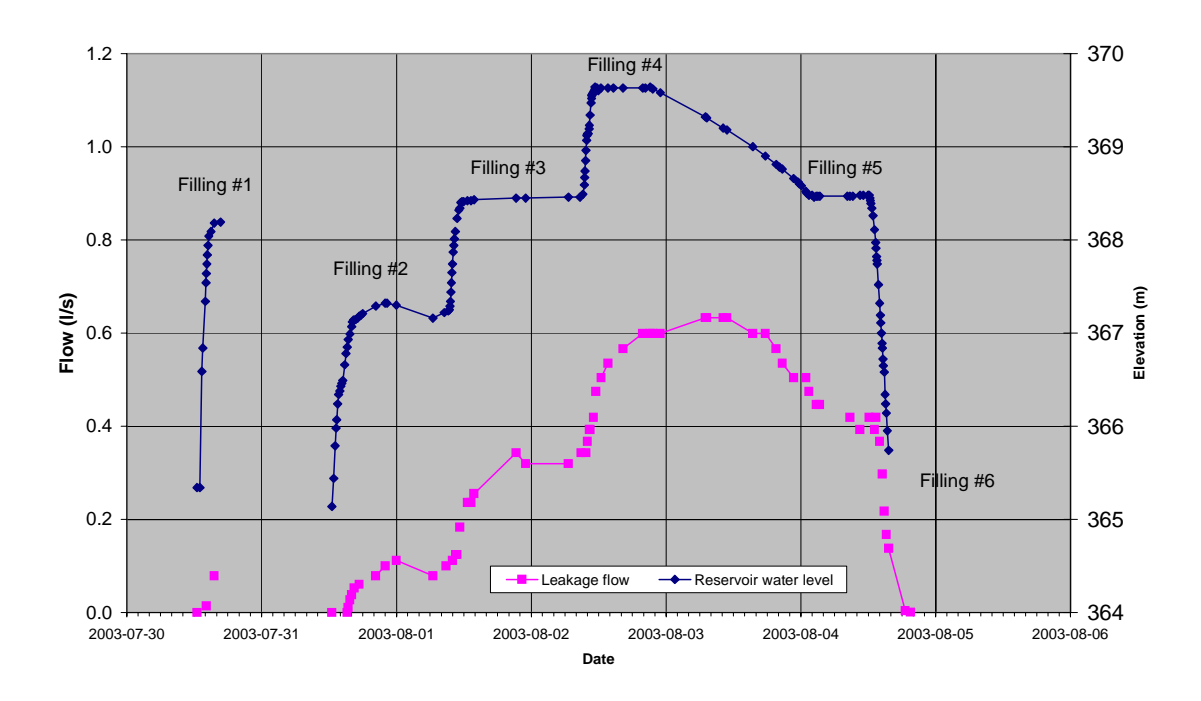


Figure 7-3 Seepage flow (l/s) in the weir.

## 7.4 Monitoring program

A summary of the activities and a general monitoring description is found below. Details of the monitoring are presented in the following chapters for each method.

Table 7-1. Summary of field test activities.

Date	Activity
July, 28	Travels, and unpacking and start of the installation
July, 29	Installation of electrodes completed, and installation of temperature
	sensors started. Initial measurements were taken.
July, 30	All installations OK. Filling #1 started a 1.10pm
	One emergency packer came out, and all water was released.
July, 31	Filling #2 was successful, as well as the measurements.
Aug, 1	Filling #3 was successful, as well as the measurements.
Aug,2	Filling #4 started at 9am. After completing all measurements in the
	evening, the valves were opened to lower the reservoir.
Aug,3	Continuous SP-measurements during the water level decrease
Aug,4	Filling #5: Valves closed at the same water level as for filling #3.
	Some measurements were repeated, before the final release started.
Aug,5	Filling #6: Repeated measurements with empty reservoir. Packing
	and travelling back

## 7.5 Laboratory measurements

Samples were taken from the dam site in order to estimate approximate material resistivities through laboratory tests. Reservoir water samples were collected at two locations; one was taken right on the upstream side of the dam and another some 50 metres upstream. Samples of the moraine core, the fill (unwashed) and the clay used for sealing fractures in the bedrock foundation were also collected.

All test results are preliminary. The equipment is new and verifications with other equipment is desirable but not carried out so far. The repeatability of all tests are however satisfying. The sample holder used consists of a 200mm cylindrical plexiglass tube with an inner diameter of 50mm (Figure 7-4). At both ends stainless steel plates work as current electrodes creating a homogeneous current flow in the tube. Potential electrodes are put into small holes at known distances along the walls of the tube.



Figure 7-4 Sample holder for laboratory resistivity measurements.

The reservoir water has lower resistivities than expected (Table 7-2). The sample taken close to the dam is noticeably more conductive than the one taken further upstream. This is explained by the fact that the water close to the dam was observed to be slightly muddy probably due to dissolved fine grains from the dam construction leading to a decrease in resistivity.

Table 7-2 Electrical properties of reservoir water and moraine dam core from preliminary laboratory tests. The tests were carried out at 23°C. The formula  $\rho_t = \rho_{18} / (1 + \alpha(T-18))$  was used for temperature adjustment of the water.

Sample	Description	Meas. resistivity	Calc. resistivity
		(23°C) [Ωm]	$(18^{\circ}\text{C})[\Omega\text{m}]$
Water1	Right on upstream side of test dam (2003-08-04 14:00)	122	138
Water2	In small stream 50m upstream test dam (2003-08-04 19:00)	163	184
Core1 (wetted)	Material piles across road from test dam, moraine core (2003-08-05 09:00)	320	•
Core1	Material piles across road from test dam, moraine core (2003-08-05 09:00)	220-400	-

Measured resistivities on the core material were ranging from approximately 220-400  $\Omega$ m (Table 7-2). The measurements were made with and without adding water. Fractions larger than 8mm were removed. Water saturation and degree of compaction is affecting the results significantly but at this stage compaction was carried out by hand trying to resemble conditions at the dam site.

One sample was saturated with water collected at the site, and for this sample only a few measurements were taken. The sample with no water added was kept for measurements over a long time (measurements are still running after 13 days). An unexpected clear resistivity decrease (more than 40%) with time was identified. The resistivity decrease was more rapid at the start, but still had not completely levelled out after 13 days (Figure 7-5).

The cause of the decrease in resistivity of the core sample is not clear. Since the cylinder is sealed with o-rings the moisture content should not have changed. Unfortunately, the temperature variation was not recorded during the experiment, but the outdoor temperatures have been decreasing during the measurement period which means that the indoor temperature in the laboratory have deceased rather than increased. Hence, if there were any significant temperature effect it would increase rather than decrease the resistivity.

A tentative explanation might be that the mineral grains settle gradually over a period after the compaction in the cylinder, and that this process increases the contact between the grains and thereby enhance the surface conduction. Furthermore, anisotropy can be expected in the material after the compaction. Possibly this has some significance in a process where the mineral grains of the core material re-orient themselves gradually after the compaction is completed. Similar processes can be expected for the core material in the dam. If this is the case it should be noted that the compaction direction, and thereby the plane of anisotropy, is perpendicular to the electrode layout direction in the laboratory case, whereas in the field experiment the plane of anisotropy is parallel to the electrode layout. Hence, the change with time might be different in the field case if anisotropy is part of the explanation.

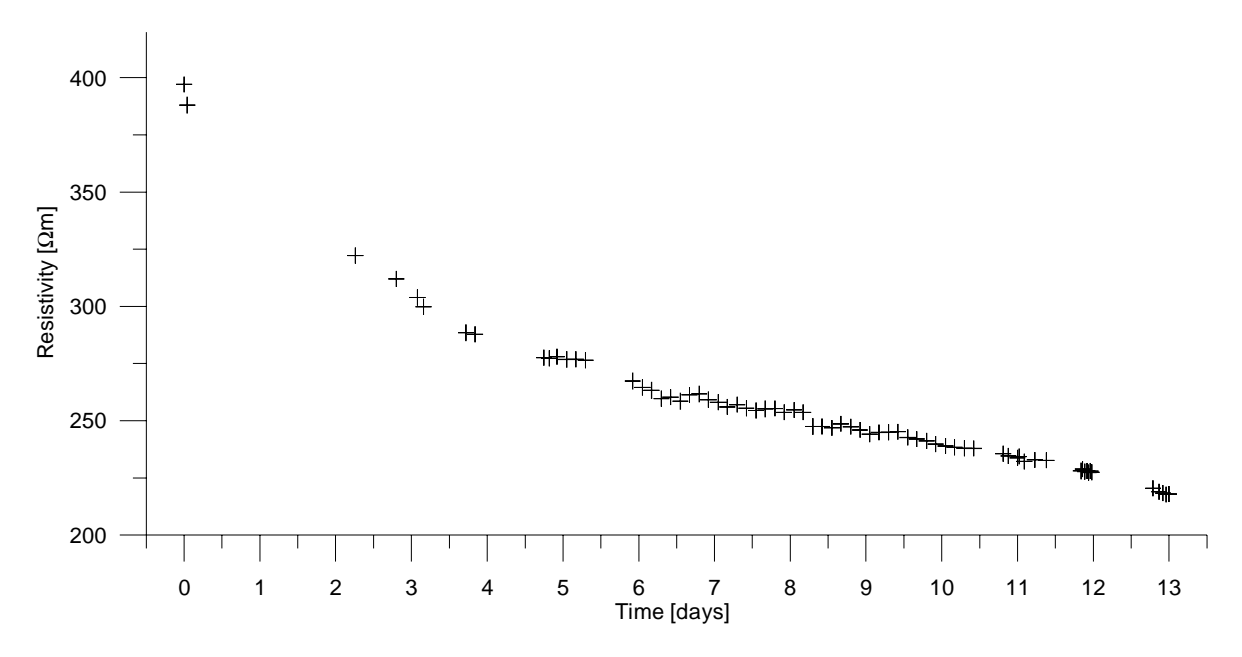


Figure 7-5 Resistivity over time for sample of moraine core from Røsvatn dam.

## 8 Temperature – field measurements

## 8.1 Installation and monitoring method

Temperature measurements were carried out along the dam toe using 23 temperature sensors. The installation was made in order to estimate the temperature change within the dam, and to detect seepage outflow at the dam toe. For measuring the temperature within the dam sensors placed in the core should have been preferred.

The sensors (Greisinger PT100) were installed with a separation of about 1.5m, starting at section 1.1m and ending at section 34.3m at 5cm depth. Some sensors were exposed to sunshine while other was placed in the shadow between large boulders, depending on the installation possibilities. The conditions were also changed during the filling, and some sensors were finally covered by water. The relative accuracy has been estimated to better than 0.1°C, while the absolute accuracy is about 0.2°C.

The water temperature in the reservoir was also measured in a small outflow from the reservoir. All measurements were made each 10s, and mean values were stored for each 5 min in a logger (INTAB PC-100). Manual measurements were also made in the water and manually at certain spots.



Figure 8-1 Temperature sensor before installation in the soil.

The sensors were installed late on July 30, when also seven of the sensors were connected to the logger. The remaining sensors were connected to the logger at 2003-07-30:11.00, before the first filling. Results are available from this time until 2003-08-05:19.00. Result during the night between July 30 and 31 was unfortunately lost due to low battery power.

#### 8.2 Estimated initial temperature in the core

The temperature in the defect areas seems to finally achieve a temperature similar to the water temperature (16-18°C). Some temperature delay is observed both at filling and outflow of water. The temperature in the healthy core will be lower. Temperature measured directly at the leakage at the left abutment was about 10°C during filling #3 and #4. This was due to seepage mainly through the abutment, but also through the core. (This temperature was not affected by sunshine etc). Due to the warming up of the seepage the natural temperature of the rock must thus be <10°C. The core might have a higher temperature since it was constructed during the summer, probably 10-12°C based on the measurements at the dam toe. The temperature difference between the dam material and the water may thus be about 5°C, which is similar to what was estimated in the pre-study.

#### 8.3 Results

Temperatures measured at the dam toe are neither able to determine exactly where a leakage will be located in the core, nor able to define the extent of the leakage. There are several aspects that must be considered:

- A single leak through the dam may give several outflows at the toe.
- A large concentrated leakage flow may be wider at the toe while a smaller leakage will have a more constant width, and
- The distance between the sensors (1.5m) will be the smallest resolution.

The several fillings in this case will give some indications of the elevation of the leakage, while the extent and location at the dam toe may not be similar to the location in the core. Indications may be shown as:

- How quick the temperature response will be at a change filling level
- The length of the transient pulse, and
- The temperature difference between the reservoir water and the outflow water.

The results from the measurements are divided in four parts along the dam in the presentation below. The first part (see Figure 8-2) contains the result from section 1.1m to section 8.6m, and the temperature in the reservoir.

The temperature in the reservoir was about 18.5°C until noon on July 31 when it started to decrease slowly to 16°C on August 5. The daily variations can be ignored for the first days during the filling. As the daily variation at some sensors at the dam toe is large, it can be concluded that those sensors are less sensitive to the seepage flow.

Measurements before and after the first filling is not complete but the result from the sensors at section 1.1m, 2.6m, and 4.2m shows no indication of seepage. A significant change is found at section 5.7m, where an immediate temperature response is seen due to the water level increase. The delayed temperature increase at section 7.2-8.6m is probably not caused by seepage because they are similar to the temperatures during the following sunny days, and also larger than in the reservoir.

The second filling confirms the result from the first filling with immediate temperature response at section 5.7m. Some daily temperature effects can still be seen, which are reduced after the third filling especially at section 4.2m. The outflow width is also increased after the third filling with temperature change also in the adjacent sensors at section 4.2m and 7.2m.

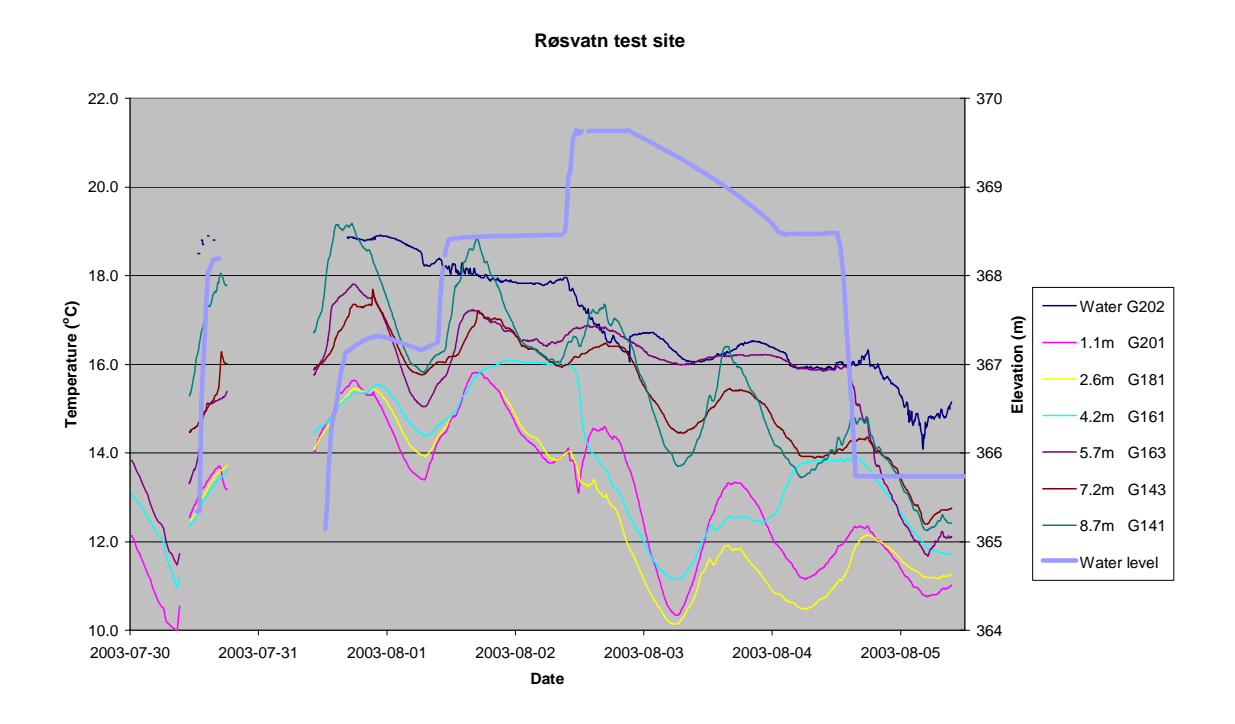


Figure 8-2 Temperature measurements from section 1.1m to section 8.7m (left axis) and water level (right axis).

The measurements from the first and second filling indicate no clear seepage increased temperature change between section 10.2m and 17.6m (Figure 8-3). A temperature anomaly is however seen at section 10.2m and 11.6m after the third filling. The influence of the daily variation can still be seen, indicating a lower seepage than at section 4.7m. A short

temperature dip is also found at section 10.2m that may be caused by a similar temperature change in the reservoir.

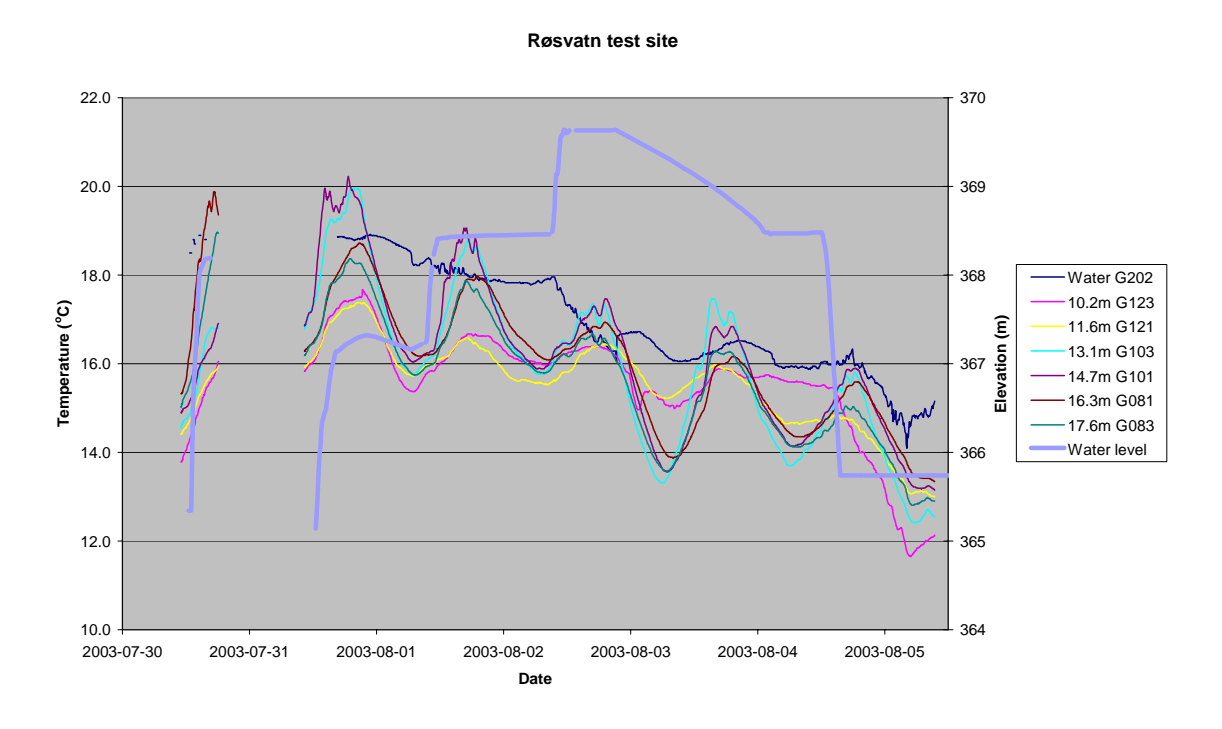


Figure 8-3 Temperature measurements from section 10.2m to section 17.6m (left axis) and water level (right axis).

The part of the dam between section 19.2m and 26.6m exhibits daily temperature variations around section 19.2m and between section 23.8m and 25.1m, (Figure 8-4). Seepage induced temperature variations are seen after the third filling at sec 20.7m, also widening towards section 22.3m probably due to the flow along the dam toe to the weir. There is also a small thermal impact from the sun until the third filling, after which the temperature is much more stable. This part of the dam is close to the seepage weir and with some cm deep water collected between the weir and the dam toe. Some sensors were covered with water at high reservoir levels.

Some remaining sensors towards section 34.3m were also continuously inundated. Significant seepage induced temperature is seen for section 26.4m and 28.4m at the first filling (Figure 8-5). The large variation of temperature at section 34.3m after the third filling was caused by a dislocated sensor. It was immediately put back in place when detected. The effect of the sunshine impact of the shallow water, where the sensors were located can clearly be seen.

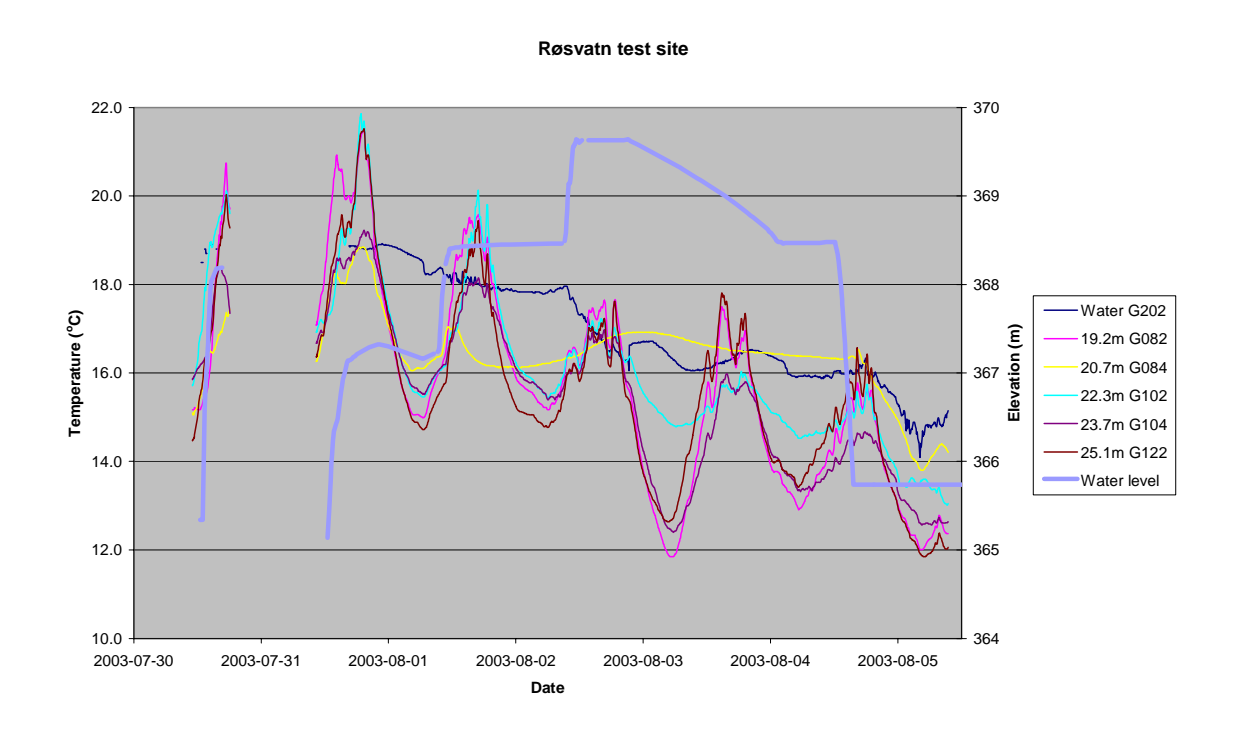


Figure 8-4 Temperature measurements from section 19.2m to section 26.4m (left axis) and water level (right axis).

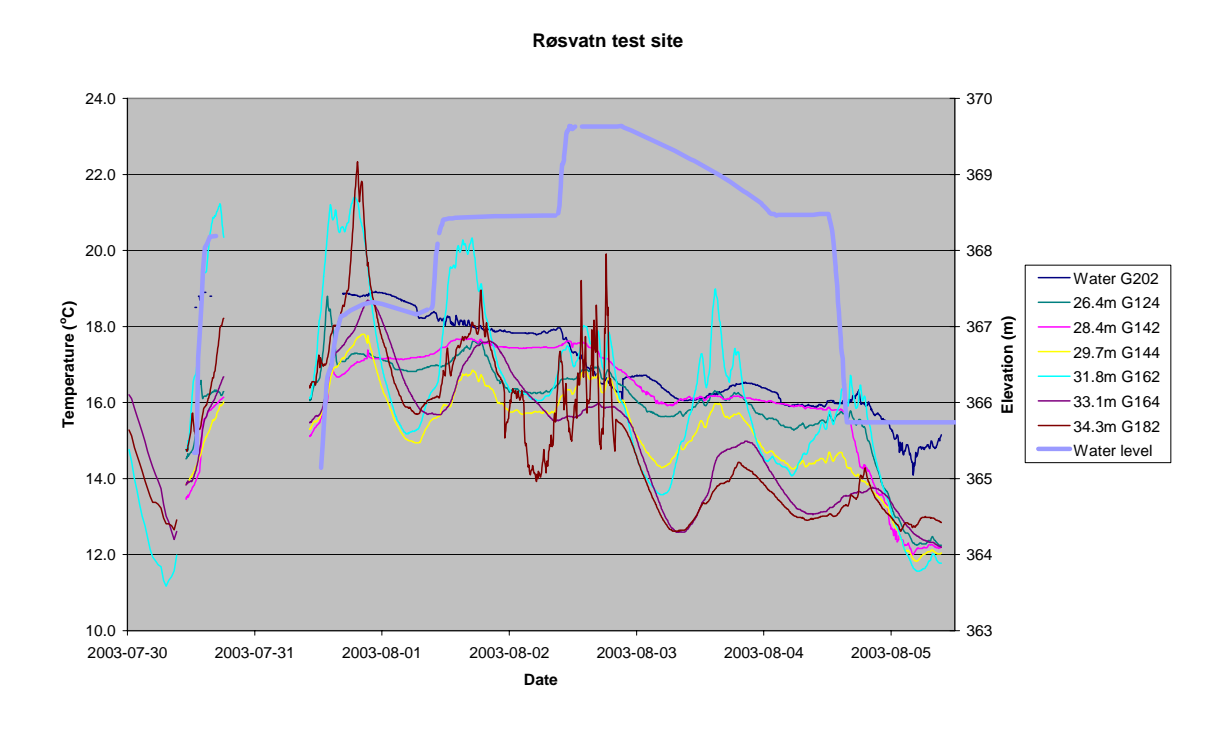


Figure 8-5 Temperature measurements from section 28.4m to section 34.3m(left axis) and water level (right axis).

#### 8.4 Evaluation

Temperature measurements are normally first evaluated based on qualitative analyses. Seepage flow estimations are then made based on time lag and attenuation of the temperature pulse. Those methods are unfortunately not directly applicable in this case due to the transient conditions. Some estimation of the seepage flow can however be made based on the time lag obtained from the fourth filling, when the conditions became less transient.

First, some comments from all fillings (Figure 8-6 to Figure 8-8) may be of interest to show the thermal response at the dam toe in the outflow areas that were described above. Before the real filling started the reservoir was filled by the natural inflow to the reservoir, which explains the quick temperature rise in section 26.4m before the first filling started. Significant response can also be seen for section 5.7m and 28.4m. The slow temperature increase in the remaining points is probably caused by the sunshine. The temperature dip in section 26.4m may be caused by a small movement of the sensor. Similar result was also obtained from filling #2 that was made up to almost the same level as the first filling.

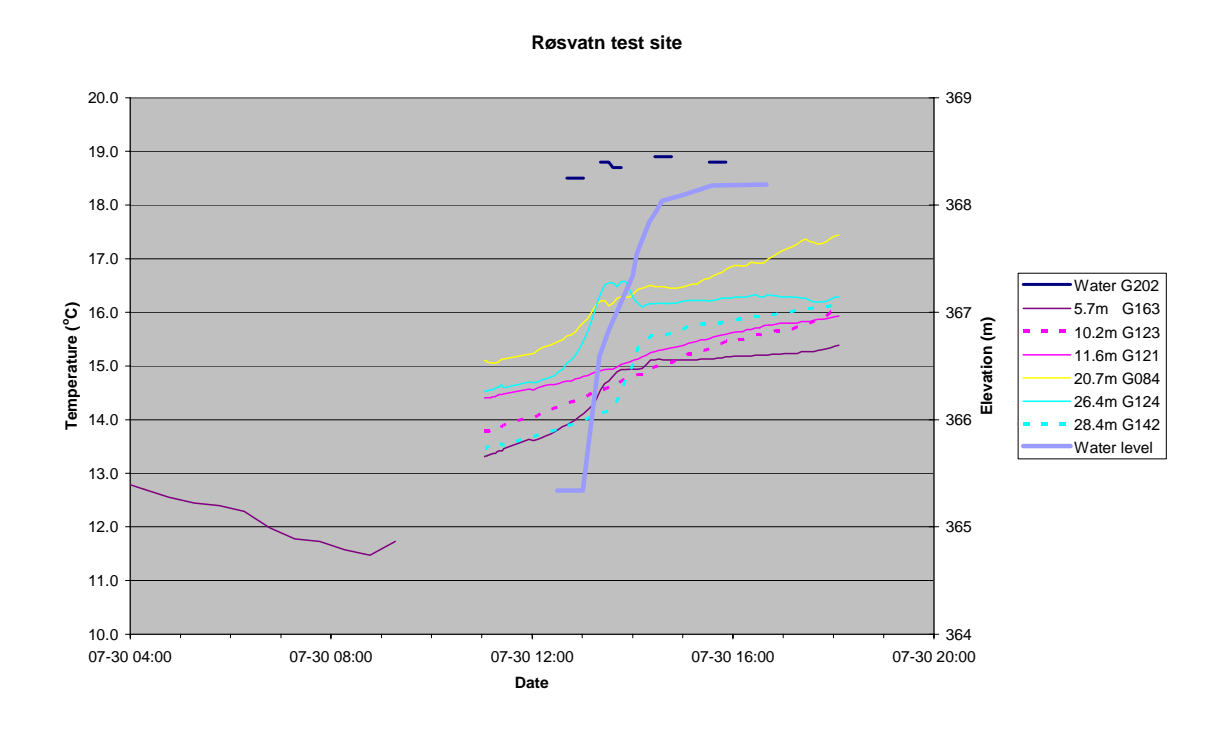


Figure 8-6 Measured temperature at filling #1 (left axis) and water level (right axis).

The first response at the filling #3 (Figure 8-7) is seen in section 20.7m, probably due to the transient flow, as the slower one at section 10.2 and 11.6m. The response at section 5.7m and 26.4/28.4m can also be seen.

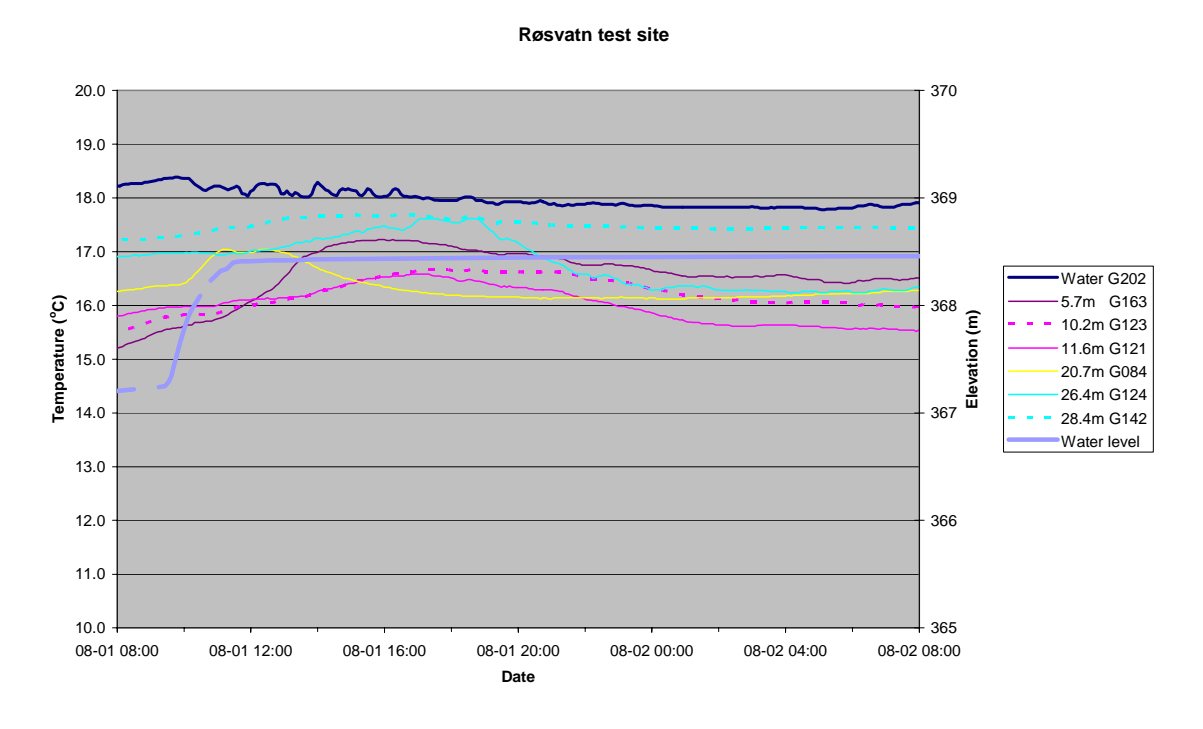


Figure 8-7 Measured temperature at filling #3 (left axis) and water level (right axis).

The water temperature at filling#4 was slowly decreasing, and the temperature contrast between the water and the core was thus smaller. The condition started to become less transient. Time lags for the maximum temperature can then be evaluated from the data summarized in Table 8-1, as well as the seepage flow rates for the different leakages.

Table 8-1 Calculated seepage flow from estimated lengths and observed time lag.

Dam Section (m)	Leakage lenth (m)	Time lag (s)	Seepage flow, q (l/s,m²)
5.7	18	22000	0.41
10.2	12	19000	0.32
11.6	12	24000	0.25
20.7	12	32000	0.19
26.4	18	17000	0.53
28.4	18	12000	0.75

The highest seepage flow rate is about 0.6l/s,m<sup>2</sup> at the leakage at section 26.4/28.4m. (The real value would have been ever higher if the measurements have been made directly in the out-flowing water that was seen on the downstream face). The lowest seepage flow is about 0.2l/s,m<sup>2</sup> at section 20.7m. The leakage flow at section 5.7m is about 0.4l/s,m<sup>2</sup>, and about

0.31/s,m<sup>2</sup> at section10.2/11.6m. The total flow in those leakages is however unknown, unless the leakage area can be estimated. Temperature measurements at the dam toe alone will not give enough information. Some estimation is however presented in the next section, based on the width of the thermal disturbance at the dam toe, and the response at different water levels.

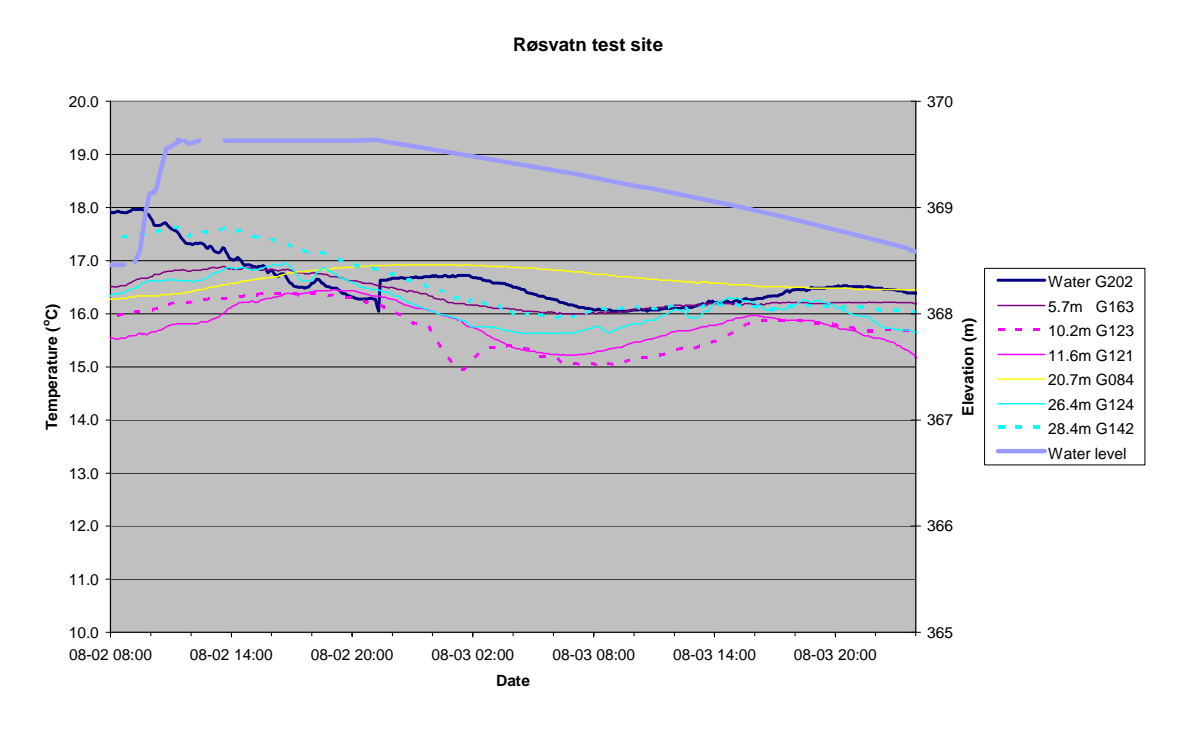


Figure 8-8 Measured temperature at filling #4.

#### 8.5 Detected defects

In conclusion, four leakage paths have been detected as summarised in Table 8-2. The locations at the dam toe may not correspond to the location in the core, but will probably be close. Information about the level and area are interpreted data based on the information from the different fillings. Only the inflow level can be used to estimate the level of the defect. The thermal response is clear at large flows, but at small flow the response may be delayed. It may then be seen after further fillings, which could be misleading. As a consequence, the vertical extension of the defect is not possible to verify, and a height of 1m is therefore assumed.

Seepage flow calculations are based on time lag and estimated areas. The size of the areas is more or less reasonable assumptions. All assumptions to finally obtain the leakage reduce the accuracy, but the final values are probable of the right order of magnitude. The result will not be the same as the leakage flow measured in the weir. No corrections have been made for information given by visual inspections that at large flows confirmed both the width and location of the seepage outflow.

 Table 8-2
 Summarised result from temperature measurements.

Dam section	Detected	Inflow level	Final width at the dam toe	Seepage flow, q (l/s,m <sup>2</sup> )	Estimated area, A, in the core (width x height)	Leakage flow Q, (=q*A) after filling #3 (1/s)
5.7m	Filling #1 and #2	365.5m	1.5m	0.4	1x1m <sup>2</sup>	0.4
10.2 – 11.6m	Filling #3 or #2	368	2- 3m	0.3	2x1m <sup>2</sup>	0.6
20.7m	May be already at Filling#1, but definitively at filling #3	366	1.5m	0.2	1.5x1m <sup>2</sup>	0.3
26.4 – 28.4m	Filling #1 and #2	365.5m	2 - 3m	>0.6	$2x0.5m^2$	>0.6

## 9 Resistivity – field measurements

#### 9.1 Installation

The resistivity measurements were carried out as two-dimensional (2D) resistivity imaging with electrodes installed along the crest of the dam. This is the most convenient way to arrange the electrodes, and the most relevant since it is often the only practical option for monitoring installation in existing dams.



Figure 9-1 Electrode layout along the dam crest at the Røsvatn test embankment dam, with non-polarising Cu-CuSo4 electrodes (for SP) to the left and stainless steel electrodes (for resistivity-IP) to the right.

For the field measurements a modified version of the ABEM Lund Imaging System was used, where the instrument part consists of a Terraohm RIP924 receiver-control unit, an Electrode Selector ES10-64 and a Booster SAS2000 that are controlled by a field PC. This set-up allows resistivity and induced polarisation (IP) data to be recorded in seven channels simultaneously, leading to fast and efficient data acquisition. Three electrode cables with 21 take-outs each were used to connect 63 electrodes along the crest of the dam to the ES10-64 with a spacing of 2/3 metre, of which the last 2 electrodes were outside the dam.

Since the electrodes were installed directly in the dam core the electrode contact resistances were low, and the recorded data stable and of good quality. Initially measurements were

repeated for each data point, but since it was hardly ever needed to repeat beyond the second value, stacking of data was skipped in order to allow time to try different electrode arrays. Measurements were carried out with different electrode arrays, namely gradient, pole-dipole, dipole-dipole and Wenner arrays, but the latter only at a few of the time steps measured with the others. Measurements were mostly carried out as combined resistivity and IP surveying, but were done as resistivity measurements only in one case to save time.

The acquired data was analysed through inverse numerical modelling (inversion), using the software Res2dinv version 3.52 (Loke et al. 2001). Time-lapse inversion was employed to analyse the data from the repeated measurements for change in resistivity, which has the advantage of focusing the results on actual change and suppressing artefacts due to data noise (Loke 2001).

In addition to the series of measurements done on the electrode layout on the dam crest, a 80 metres long line with 2-metre electrode separation was measured that extended on each side of the dam.

#### 9.2 Results extended line

The extended resistivity line was measured with the reservoir empty. The corresponding inverted resistivity sections exhibit large contrasts, and where the bottom of the dam stands out as a high-resistive (several thousand  $\Omega$ m) bottom layer (Figure 9-2). The dam itself exhibits resistivities in the range a few hundred to a couple of thousand  $\Omega$ m. The general shape of the bedrock agrees well with the preliminary drawings of the dam, with a steep slope to the left and a more gradual to the right.

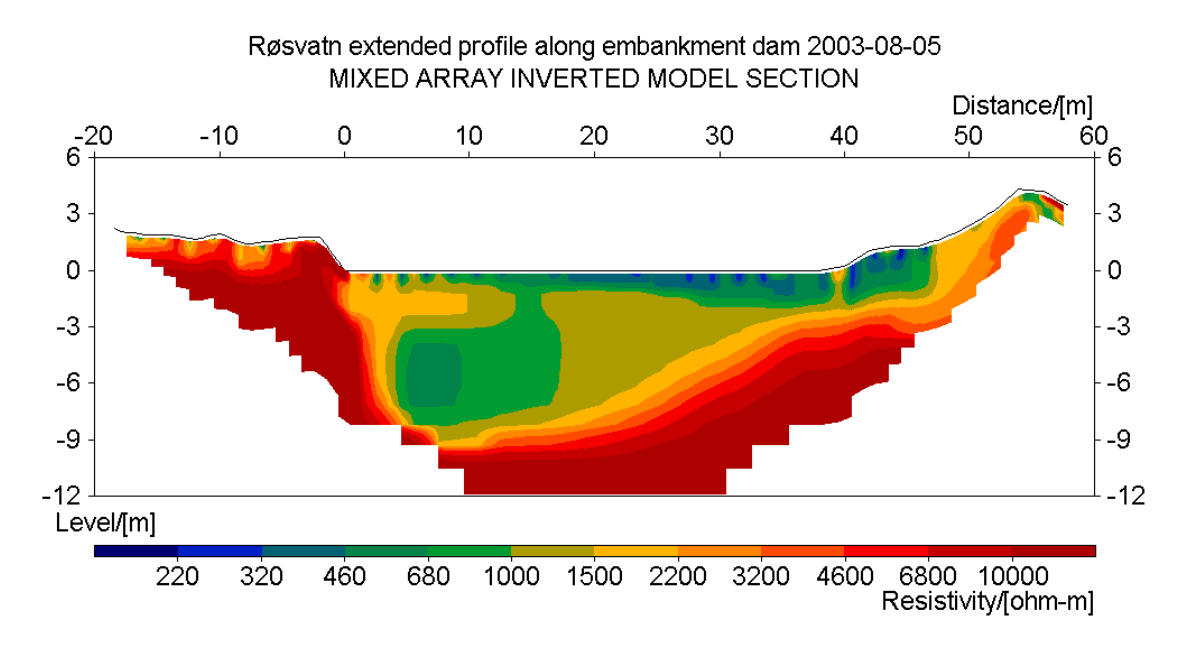


Figure 9-2 Inverted resistivity sections based on combined gradient array and Wenner data from extended line measured at empty reservoir (filling #6).

### 9.3 Resistivity measuring results

Resistivity and IP was measured at a number of different reservoir water levels, going from empty to full reservoir. The corresponding inverted resistivity sections exhibit large contrasts, and significant change in resistivity is evident as a result of changes in water level. The section in Figure 9-3a is based on data measured with the reservoir empty, and the one in Figure 9-3b with the reservoir water at the maximum level. Due to limited sensitivity towards the ends of the electrode layout, the depth section is automatically trimmed off at depth on each side. The diagrams in Figure 9-4a and Figure 9-4b are also based on low and high reservoir data, but the inversion included additional data and the model extended to larger depths and closer to the edges. Although the resolution is lower at the lower edges the sections clearly show the high resistive rock at the base, with a shape that agrees quite well with the one in Figure 9-2.

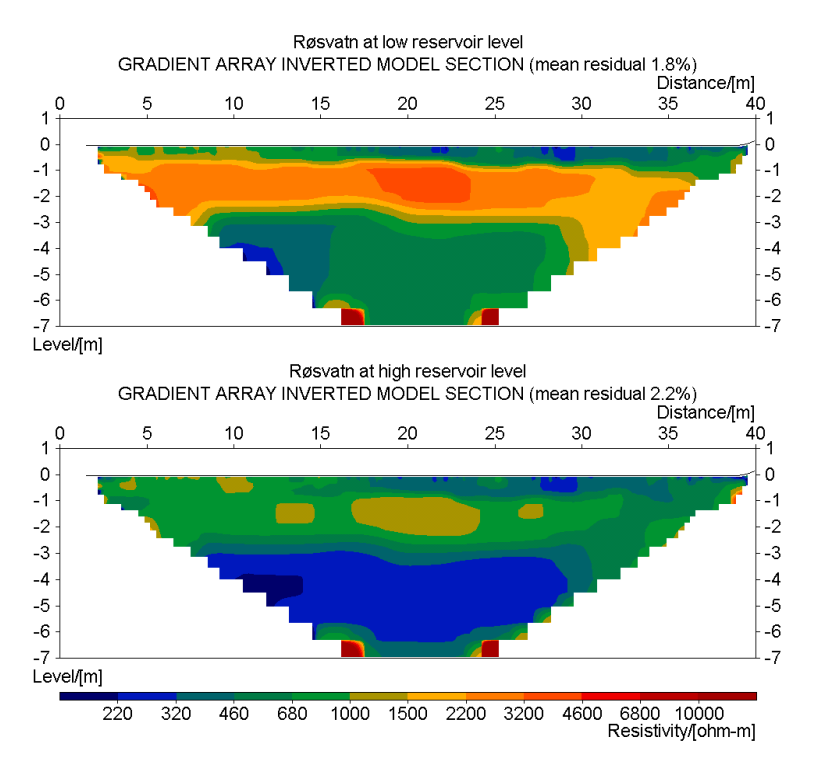


Figure 9-3 Inverted resistivity sections based on: a) gradient array at empty reservoir (between filling #1 and #2), b) gradient array at high reservoir level (filling #4).

The resistivity in the dam itself has an apparent layered structure, going from bottom and upwards from low, via high/intermediate to low/intermediate. The low resistivity in the bottom layer is probably showing the combined effect of the clay layer used to seal the bottom, plus the water saturated core, filter and rock fill at the lower levels. The method's resolution does not make it possible to discriminate between these parts with the electrodes placed along the top of the core alone. At section 5-7m in Figure 9-3 and Figure 9-4 a high resistive anomaly is visible at 2-3 metres depth, which may be associated with a leakage zone according to the expectations.

Furthermore, at section  $\approx$ 22m a high resistivity anomaly is located at rather shallow depth (Figure 9-3a Figure 9-4a). All anomalies, low resistive or high resistive, indicate inconsistent material properties and may therefore be associated with leakage zones. However, as higher resistivity is assumed in the defect material high resistive anomalies in the core are the most probable.

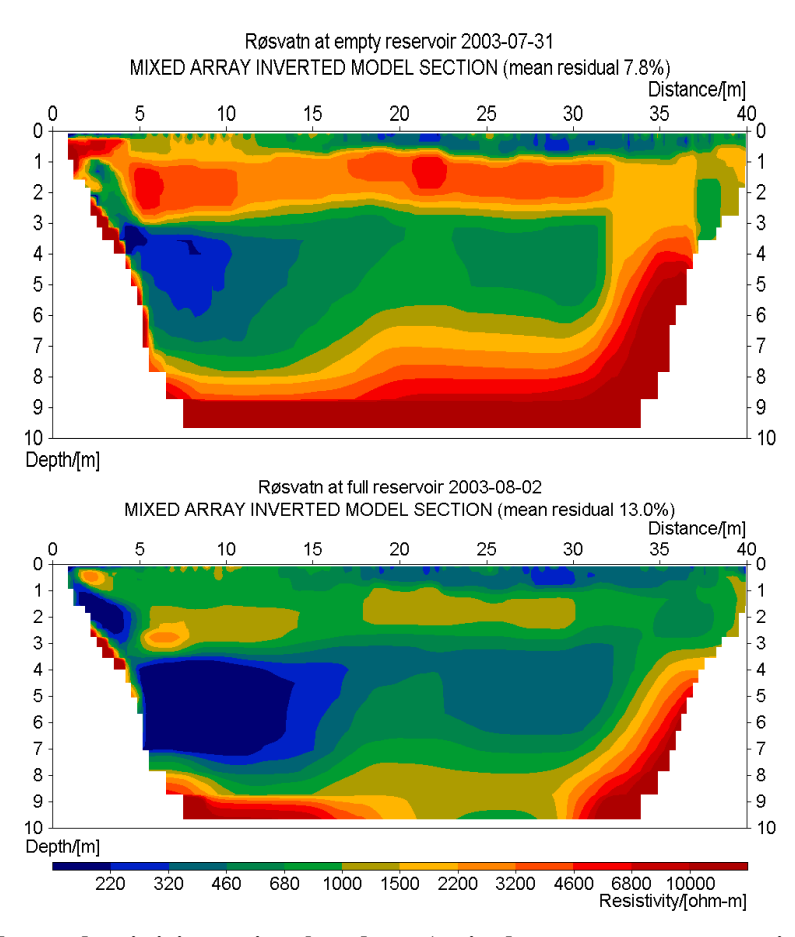


Figure 9-4 Inverted resistivity sections based on: a) mixed array at empty reservoir (between filling #1 and #2), b) mixed array at high reservoir level (filling #4).

A way of enhancing anomalous zones, in cases where there is a strong variation in resistivity with depth but less pronounced horizontal variation, is to subtract the average resistivity of each depth level from the inverted model section. Such processing of the inverted sections was carried out and an example is shown in Figure 9-5, but all sections turned out to have a rather similar appearance although there are differences in the details. Prominent zones of high values are seen around section 7m (depth 2-3m), section 22m (depth 0.5-2.5m) and in the interval 28-35m (depth 2.5-5m). The latter zone also seems to tie up with a shallower zone around section 27m. These zones may be interpreted as zones with less fine particles in the dam core and thus potential zones of anomalous leakage. The variation at the very bottom of the section is disregarded as an artefact caused by the very high contrast between the high resistive bedrock and the fine-grained material of the dam core and the clay sealing at the bottom of the dam. The high resistivity left part of the top

layer is an effect cause by the lower right part of the shallowest part of the dam (Figure 9-3), which is probably caused by different grain size distribution and/or different moisture content.

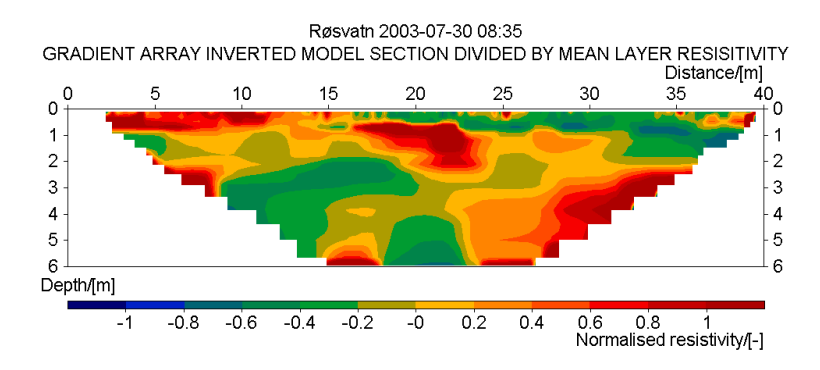


Figure 9-5 Inverted resistivity section presented as relative deviation from average resistivity for each depth level, based on gradient array at low reservoir level.

# 9.4 Relative difference versus water level

The data sets recorded at the different reservoir levels were analysed via time-lapse inversion, where the data set recorded before the first attempt to fill the reservoir started was used as reference data set. Time-lapse inversion is a relatively new feature in the inversion software, and the mixed electrode array data sets gave high model residuals and apparently problems to handle the large changes in resistivity associated with the changes in reservoir water level in a stable way. Due to this, and the fact that the mixed array data sets were measured over much longer time as discussed below, the following presentations will only include gradient array data.

The results are presented in Figure 9-6 as difference sections showing the change relative to the initial resistivity, where negative values indicate decrease in resistivity and positive values increase in resistivity. As the data sets using the gradient array (shown here) were taken right after (within 1-3 hours) the rise of the reservoir level it is likely that a leakage zone that respond quicker to a higher reservoir level would stand out as a zone with a high relative change in the figures shown.

The section in Figure 9-6a shows the change resulting from the drop from the water level at the start of the experiment to the completely empty reservoir after filling #1 (the first attempt to fill it that failed). There is not a big change in resistivity between these sections, possibly a slight drop in resistivity in the upper 3 metres which may be caused by increased moisture content resulting from the higher water level, and slight increase at the lower levels. Exceptions from this trend are zones centred around 7-8 metres and 29-30 metres at the mid-lower parts of the section with a slightly larger drop in resistivity. The latter might be indicative of anomalous material properties and possible leakage that would give a faster breakthrough of higher moisture content and increased temperature. The increase in resistivity at the deeper levels may be a result of the drop in reservoir water level.

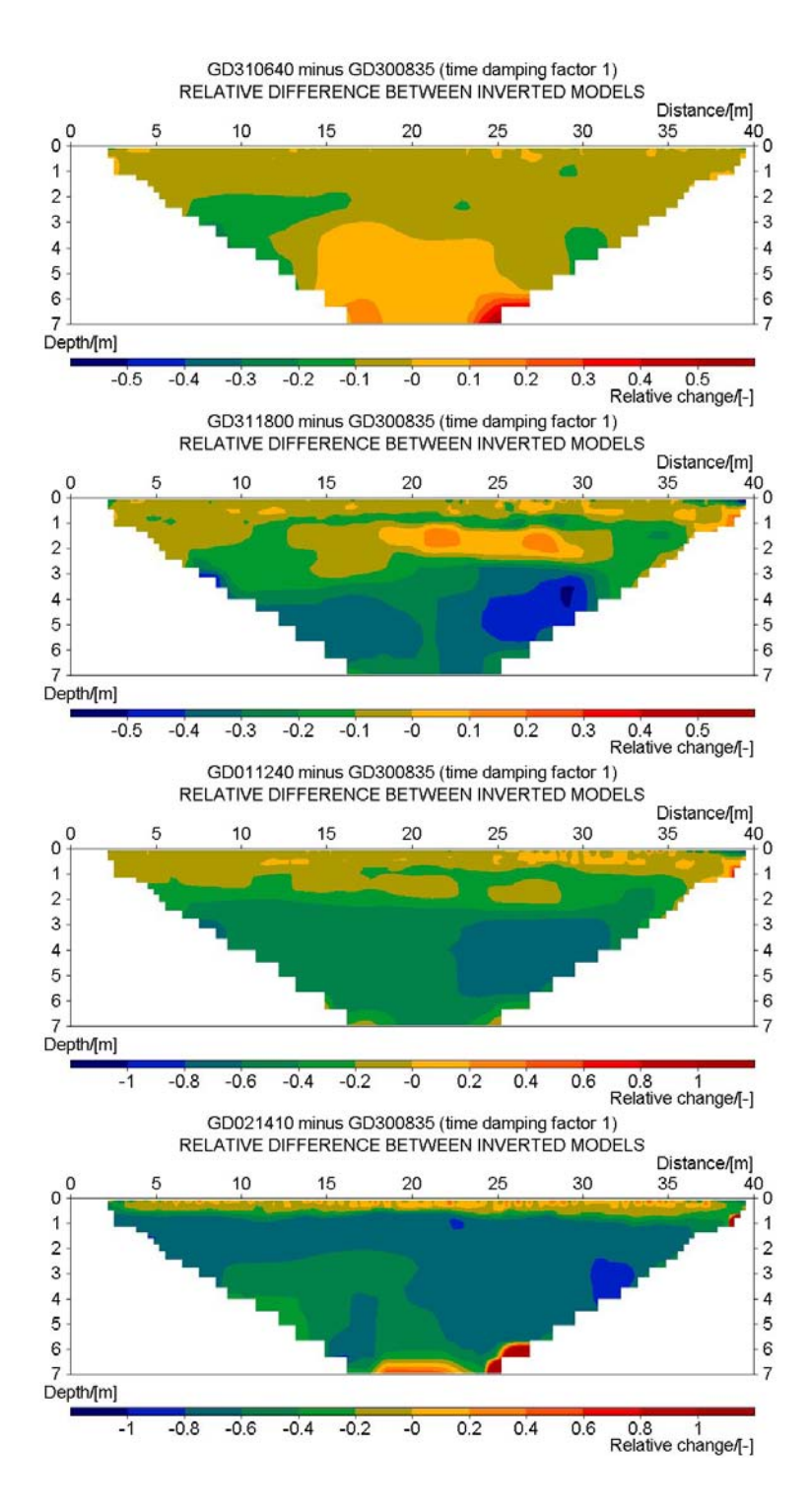


Figure 9-6 Difference in inverted resistivity sections based on gradient array: a) at low reservoir level, b) at reservoir level between filling1# and #2, c) at reservoir level +3.5m (filling #3), b) at high reservoir level (filling #4). Note difference in scale between the sections.

After filling #2 (increasing the reservoir water level to +2m again), most of the dam section below 2m below the crest exhibits a drop in resistivity of 10-20% (Figure 9-6b), except in a zone centred around section 27 metres and another zone around section 7-8 m where the drop is over 40%. The latter may be interpreted as potential leakage zones. Two zones at 1-2m depth centred around section 22m and 27m, corresponding to earlier identified high resistive zones (Figure 9-3 and Figure 9-4), show an unexpected increase in resistivity.

Filling #3 (rising the water to +3.5m) leads to a 40-50% decrease in resistivity, compared to the start conditions, for model depths below 2m below dam crest (Figure 9-6c). Again areas around section 8m and section 27m stand out with a larger decrease (>60%).

Filling #4 (the final rise in water level) leads to a resistivity drop of more than 60% in most of the depth section below 0.5m depth (Figure 9-6d), except between section 10-15m where the drop is between 40-50% at depth. Furthermore, at the centre of the dam (section 20m) there is hardly any increase at the bottom of the section, a tendency that can also be observed in the previous two time steps.

# 9.5 Relative difference versus time

A number of measurements were made at the same water filling level but at different times. This included measurement before filling the reservoir and after draining it, which can be expected to show changes in resistivity as a result of for example change in water saturation and temperature in the core. Similarly, measurements were taken on filling level #3 (+3.5m) both when filling and emptying the reservoir. In addition, two sets of measurements were taken at maximum reservoir level (filling #4) with a few hours in between. These data sets were analysed via time-lapse inversion, and the result presented as relative difference.

The result for the empty reservoir is shown in Figure 9-7a, and a decrease in resistivity of around 40-60% in the shallow part (0.5-3m depth) is clear. This change is quite even, except around section 7m and 16m where the change is >60%. The overall change is interpreted as caused by increased moisture content following wetting of the embankment dam when the water level increased, and the zones with larger change may indicate zones of anomalous material properties. Below 2.5-3m depth the resistivity has increased, indicating that the moisture content was already high in that part (as discussed above for Figure 9-6a), except in the rightmost part (notably from section 24m and up) where there is a decrease in resistivity.

One explanation for the increase in resistivity could be the type of change in resistivity that has been documented in the laboratory, since the core was built from compacted moraine a few days earlier this process is likely to have been in progress. Another possible explanation for the increase in resistivity could be if the core material contained excess ions at the construction that have been washed out. Excess ions could be derived from the natural sources such as groundwater, or human activities, where the material was taken. If this is the case the resistivity would increase after a while when the original pore water has been washed out by the reservoir water that is lower in ion content. With this scenario, the

high change spots at the bottom and right edge could be due to washout of ions and possibly fine particles. So far, however, there is no information from the site to support this interpretation. Other options could be other time dependent changes in the electro-chemical system, possibly affected by change in pore water pressure.

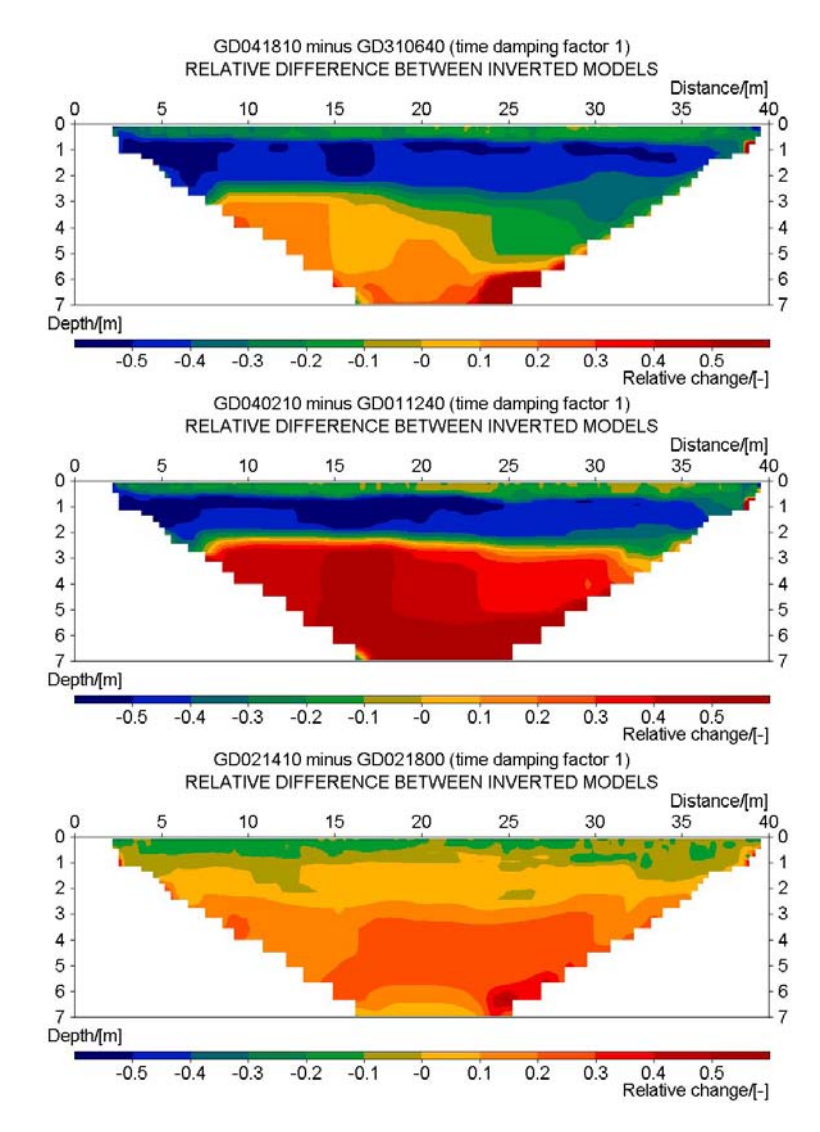


Figure 9-7 Difference in inverted resistivity sections based on gradient array data: a) at empty reservoir before and after rising water level, b) at filing #3 vs. #5, c) at high reservoir level (filling #4) 1<sup>st</sup> recording vs. 2<sup>nd</sup> recording.

The pattern described for the empty reservoir is largely seen also for the results from the two data sets recorded at filling level #3, i.e. with the reservoir water 1.6m below the dam crest (Figure 9-7b). One major difference, however, is that the resistivity has increased throughout the lower part of the inverted section.

#### **ELFORSK/BC Hydro**

The overall pattern is quite similar for the difference between the recording made immediately after filling #4 (the rise of the reservoir to the top level), and the one made a few hours later, i.e. a decrease in resistivity in the very top and an increase below. The decrease in the top part is interpreted as an increase in water saturation in the core during the hours following the fill-up, whereas the explanation for the increase in the lower part could be due to any of the mechanisms discussed above.

It should be pointed out that recording of one section takes some time, typically around 45 minutes for the gradient array sections presented here, and that the resistivity measurements were not initiated immediately after filling up to a new level since SP monitoring was in progress then. This means that fast changes cannot be recorded, so it is very likely that the differences recorded after filling #4 would have been larger if the recording had started immediately and measuring been done faster. Measuring would have been significantly faster if resistivity but no IP effects were measured. It is also reasonable to expect that a gradual increase in resistivity would have been detected if monitoring had continued with the water at filling level #4 for a day or more.

The fast change in resistivity that is recorded, evident for e.g. the two data sets with a few hours in between at the maximum reservoir level, is a complication for evaluating data combined from different electrode arrays. It took a few hours to measure a full combined data set comprising the gradient, dipole-dipole and pole-dipole arrays. These types of effects are specific to this experiment, and would normally not be of any concern for monitoring of embankment dams.

#### 9.6 Induced polarisation results

The induced polarisation (IP) data was analysed preliminarily, and we cannot at this time give an exhaustive physical explanation to the results. Judging from the correlation with the other methods, however, it appears to contain some information that can be of use for leakage detection, which motivates a brief presentation. There are significant IP effects in the dam, and the estimated chargeability does vary very significantly with reservoir water level and time, as evidenced by the examples shown in Figure 9-8.

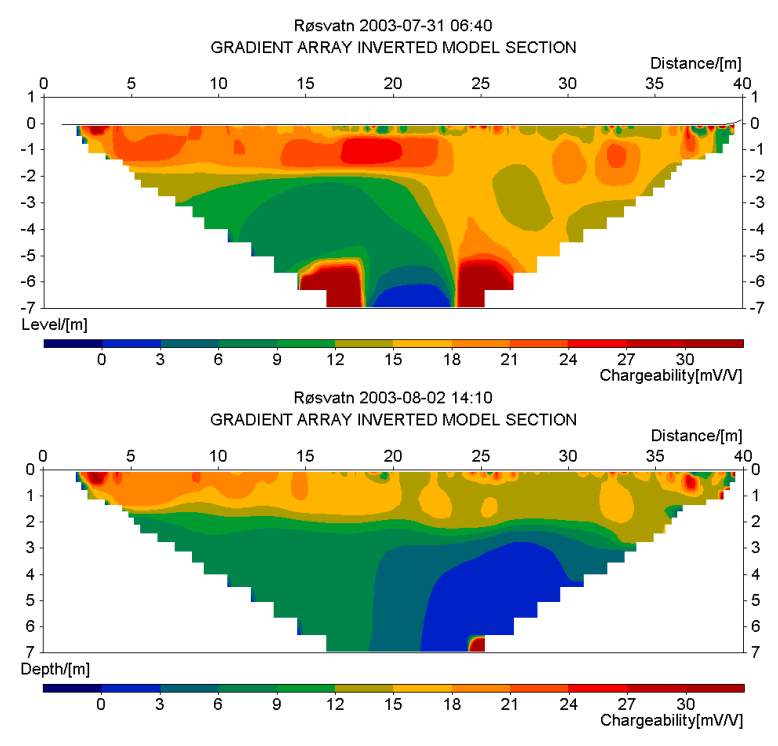


Figure 9-8 Inverted induced polarisation (IP) sections based on gradient array data recorded at:
a) minimum reservoir level (between filling #1 and #2), b) maximum reservoir level (filling #4).

It should be noted that time-lapse inversion is not yet available for IP data, and the inversions have thus been carried out separately for each data set without any time-lapse constrains. This makes the difference sections more sensitive to noise, which is enhanced by the higher noise sensitivity of IP measuring, and several of the difference sections bear signs of this. An example of change in chargeability with time is shown in Figure 9-9, showing the difference between data sets recorded at reservoir filling level +3.5m (filling #3 and filling #5). There are zones of decreasing as well as increasing chargeability. Notable zones of decrease are found centred around section 6m (2-3m depth), section 16m (0.5-1.5m depth), section 21m (0.5-1.5m depth), section 28m (3-4m depth) and section 35m (depth 2-3m). Zones of increase are most prominent in the mid and lower parts of the difference section.

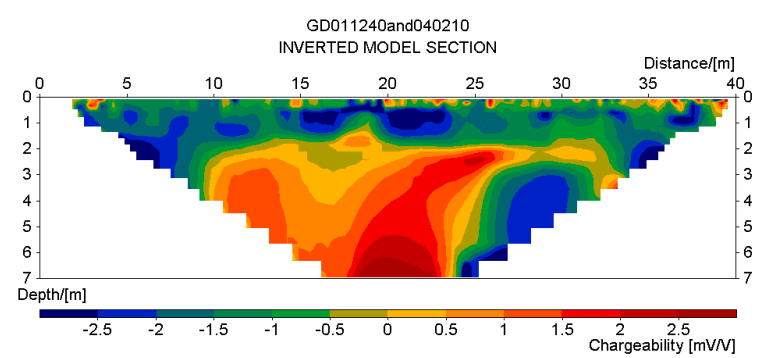


Figure 9-9 Difference in inverted induced polarisation (IP) sections based on gradient array data recorded at reservoir level +3.5m (filling #) going up vs. going down.

The chargeability, or IP effect, in a porous media such as a soil depends on the interaction between surface conduction on the walls of the pore spaces and the ions in the pore water. If ions are absent in the pore water no interaction can take place, and no IP effects will occur. If a suitable amount of ions are present the interaction can take place and significant IP effects may occur, with magnitudes that will depend on factors such as type of minerals causing the surface conduction, water saturation, type and concentration of ions in the pore water, size of pore spaces etc.. If the ion content of the pore water gets high enough the fluid conduction of the formation will dominate and eventually damp out the IP effects (e.g. Sumner 1976; Olhoeft 1985; Scott and Barker 2003).

The change in chargeability recorded at the Røsvatn site is probably caused mainly by changes in water saturation and ion concentration. Thus, zones with larger decrease in chargeability can be interpreted as zones with more rapid change for these parameters, which in turn is an indication of increased seepage. The increase of chargeability in some zones may have some relation to the increase in resistivity that is seen in the sections in Figure 9-7, it is actually seen in parts of the section at depths that correlates quite well with the increase in resistivity, and there is generally a relation between the magnitude in resistivity and the IP effects (Slater and Lesmes 2002). A tentative interpretation could be that there has been an exchange in ions in the lower parts that increase the resistivity but do not decrease the IP effects, except for zones with higher seepage rates where enough ions have been removed to cause a decrease in IP effects.

# 9.7 Detected defects

A number of suspected defect areas have been identified, mainly based on analysis of the changes in resistivity with reservoir levels and time, as summarised in Table 9-1 below.

Table 9-1. Summary of detected and possible defects by geoelectrical imaging.

Dam	Observed	Resistivity	Level	Comment
section		evaluation	(m)	
(m)		method		
7 (5-8)	Several	Resistivity at	367-368	Higher resistivity
	levels	each time		Faster/larger decrease in res.
		alone and		Decrease in IP
		difference		
		between levels		
22 (20-24)	All levels	Resistivity at	368-369	Higher resistivity
	and filling	each time		Faster/larger decrease in res.
	#4	alone and		Decrease in IP
		difference		
		between levels		
27 (25-29)	Filling #2	Difference	365-367	Faster/larger decrease in res.
	and	between levels		Decrease in IP
	filling #3	and between		
		time steps		
	t less certain re			
16 (15-17)	After fill-up	Difference	369	Faster/larger decrease in res.
	and drainage	between time-		Decrease in IP
		steps		
27 (26-28)	Several	Resistivity at	369	Higher resistivity
	levels	each time		
		alone		
36 (35-37)	After fill-up	Difference	367-368	Decrease in IP
	and drainage	between time-		
		steps		

## 10 SP - field measurements

Two distinct types of measurements were performed in this project: time-series measurements and repeated one-time measurements. The time-series measurement set-up was similar to that of a long-term monitoring experiment. The repeated one-time measurements supplement the time-series experiment and were carried out as ordinary manual SP surveys.

#### 10.1 Time-series measurements

# 10.1.1 Measurement layout and procedure

For the time-series measurements 49 electrodes were installed along the upstream edge of the exposed dam core. Based on the results from the pre-study the electrode line was originally to be placed at the downstream side of the crest about 2 meters from the centre of the core. This proved to be impossible in practice. It was only possible to place the electrodes securely on the dam core itself. According to the pre-study the downstream edge of the might exhibit slightly higher anomaly amplitudes than the upstream edge, but the upstream edge is recommended as the primary location in the "CEA SP Field Manual" (Corwin, 2002). The numerical modelling in the pre-study required several parameters that we could only estimate, and the results rely heavily on these estimates. Because of this uncertainty we decided to follow the recommendation in the SP-manual and place the electrodes at the upstream edge of the dam crest.

The electrodes were stationary during the measurement period to minimize effects caused by soil-electrode contact variation and small-scale disturbances. Measurements always commenced before changing the reservoir water level to establish a baseline from which changes can be observed. During all measurements telluric variation was be recorded and corrected for.

The distance between electrodes was 0.8 metres and the profile covers section 0 to 38.4 metres. The electrodes were non-polarizable Cu-CuSO<sub>4</sub> electrodes manufactured by Tinker&Rasor Inc. The voltage measurements were performed with the same multi-electrode measuring system that was used for the resistivity measurements (see section 9.1)

All SP measurements were done simultaneously with 2 or 3 reference electrodes (or, to be precise, with a time lag of approximately 2 minutes, i.e. the time required to complete a measurement on all 49 electrodes). The first reference electrode was placed 145 metres downstream of the dam at section -400m. The second reference electrode was situated at the dam at section 19.2m. The third reference electrode was located at section -10.5 metres.

During the period 2003-07-30 to 2003-07-31 the first two electrodes were used. Between 2003-08-01 and 2003-08-02 (12:00) we used electrodes 2 and 3. For the rest of the time all three reference electrodes were used. We decided to add the third electrode because the telluric disturbances were so strong that it was unsure whether the telluric correction

procedure would work. The far electrode should have been added to the measurement setup at 2003-08-01 but it mistakenly replaced the far electrode instead of being added. This mistake was observed and corrected at 2003-08-02 12:00.

# 10.1.2 Processing

From the results of the pre-study we expected the SP anomalies to be very small, generally less than 10mV. During the measurements we also learned that the telluric disturbances in the area were large. Measured along the whole dam they could amount to several tens of millivolts.

In order to extract information from these noisy data we employed a three-step procedure:

- 1. Telluric correction. The telluric variation was measured simultaneously with the observations on the dam and the results were used to predict the telluric disturbance for each electrode. The predicted disturbance was the subtracted from the observed value.
- 2. Spike removal filtering. The filter works by suppressing values that deviate more than a given fraction from a 20-point sliding median.
- 3. Moving median filtering. A time window of about 90 minutes was used.

Figure 10-1 shows an example of the effect of the processing steps on the longest time series recorded. The data series shown was recorded at electrode #12 located at section 29.6m on the dam. Note that the beginning and the end of the time series are disturbed by edge effects from the filtering procedure.

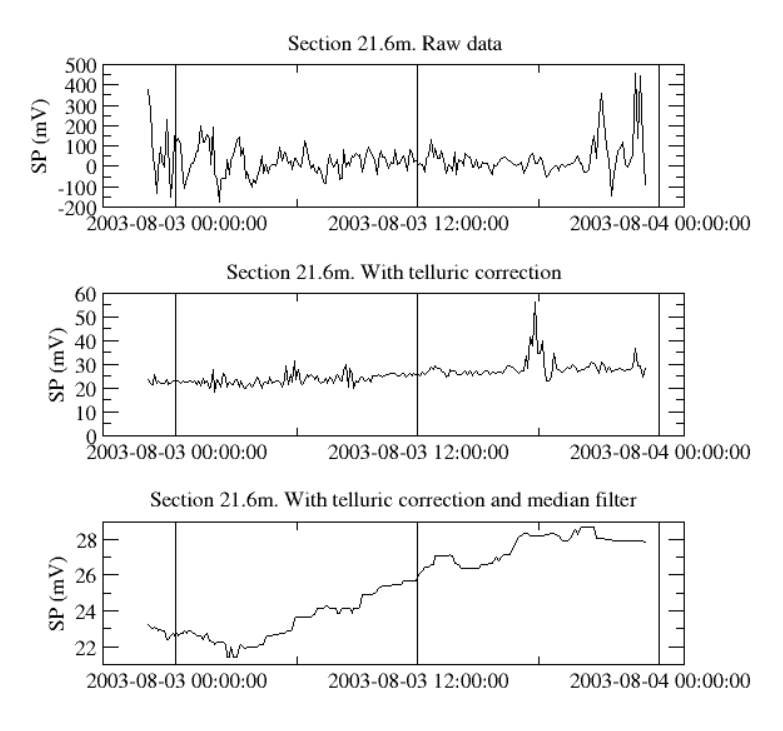


Figure 10-1 Processing of time series recording for electrode #12 (section 29.6m.)

#### 10.1.3 Results

Generally influx areas acquire a negative charge and outflux areas acquire a positive charge. For a simple dam geometry model this means that the upstream side will exhibit negative SP anomalies and the downstream side has positive anomalies for a given water level. Ignoring resistivity effects an increase of the water level would simply increase the amplitude on both sides. A time-series recording on the up-stream edge of the core would show negative correlation with the water level. Now, in reality things are more complicated and resistivity changes must also be accounted for. The numerical modelling made in the pre-study takes into account a realistic dam geometry as well as the effect on the resistivity caused by the variation in the volume of the upstream water body. All material resistivities were, however, assumed to be constant. For this case it appears that anomalies on the upstream side may be both negative and positive depending on the depth to the defect area (cf. Figure 5-1 to Figure 5-4). Adding to this the fact that we have observed large resistivity variations in the dam it becomes difficult to predict the behaviour of seepage-induced anomalies. Therefore any area with high SP variation over time should be considered as possible defect location.

The time series recording in Figure 10-1 shows a well-defined SP increase that correlates fairly well with a drop in reservoir water level. This is one of the clearer examples though, and it was found that inspection of the time-series recordings one by one is not really feasible. To easier detect changes we chose to work with median filtered profiles, which can be seen as snapshots in time of the SP along the profile. One should note however that due to the nature of the median filter each SP-value in the profile is not taken at exactly the same point in time. The point-to-point comparison inherent in the viewing of a profile plot facilitates the detection of anomalous areas.

Figure 10-3 to Figure 10-7 show the processed SP profiles before and after a reservoir level change together with the difference between them. The idea behind this kind of display is that disturbed areas in the dam should correspond to sections where the difference between the before/after profiles is large. Keeping in mind that the anomalies we discuss here are very small and detected in a area with considerable telluric disturbances one can still identify some areas of large variation possibly corresponding to defects in the core.

Figure 10-2 shows the change in SP going from water level 365.4 to 368.2 metres. This was the first filling after the dam construction was completed. Between sections 0 and 12 metres the SP has decreased. Between section 20 and 38.4m there is no appreciable change in SP. In the intermediate zone the SP changes smoothly from one extreme to another. Possibly interesting short wavelength anomalies are found at sections: 2.4, 12.8 (weak), 24.8, 28.0 (weak) and 34.4m (weak) metres.

After the first water level change one of the rubber packers in the drainage pipe failed and the reservoir was emptied. The second level change is then a repetition of the first although the final water level was about a meter less. Figure 10-3 shows the SP change going from level 365.14 to 367.32 metres. There is a weak increase in SP going towards higher section

numbers. Areas with considerable change in SP occur around sections: 14.4, 24.8 and 27.2 metres.

Figure 10-4 shows the change in SP when the reservoir water level changes from 367.16 to 368.43 metres. One prominent feature of the difference plot is the bipolar character of the section 12.2 to 17.6 metres (approximately). This is quite difficult to explain as it implies the presence of closely spaced anomaly sources. For now we will consider the whole section anomalous. Other interesting anomalies occur at sections: 2.4, 22.4, 27.2 and 32 (weak) metres.

Figure 10-5 shows the effect of changing the reservoir level from 368.46 to 369.63 metres. Anomalous areas appear around sections: 2.4, 12.8, 20.0 and 24.8 (weak) metres.

Figure 10-6 shows SP changes during the lowering of the water level from 369.63 to 368.47 metres. This is the longest continuous recording of SP. The rate of change of the water level is much lower than for the other level changes. The reason for this was the limited capacity of the drainage pipes. The SP changes are small overall. Weak but possibly relevant anomalies occur around sections: 3.2, 17.6, 24.0 and 31.2 metres.

Figure 10-7 shows SP changes during the final emptying of the reservoir. The rate of change in water level was higher than in the previous level change because we could now remove the rubber packers from the sealed drainage pipes. Changes in SP are small. Weak anomalies can be found around sections: 2.4, 24.8 and 33.6 metres.

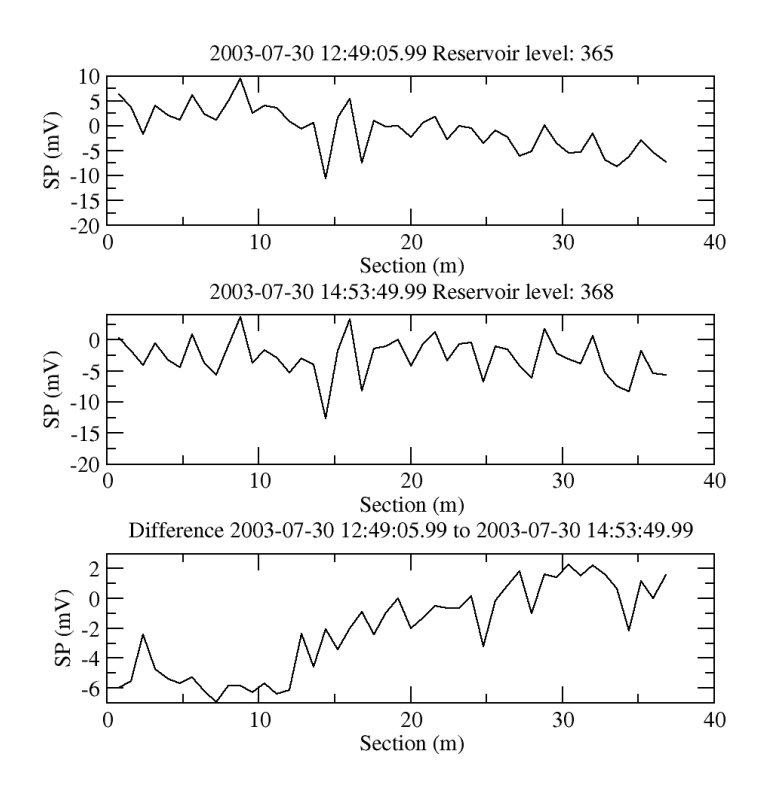


Figure 10-2 Processed profiles before (top) and at (middle) filling #1. Bottom pane shows difference.

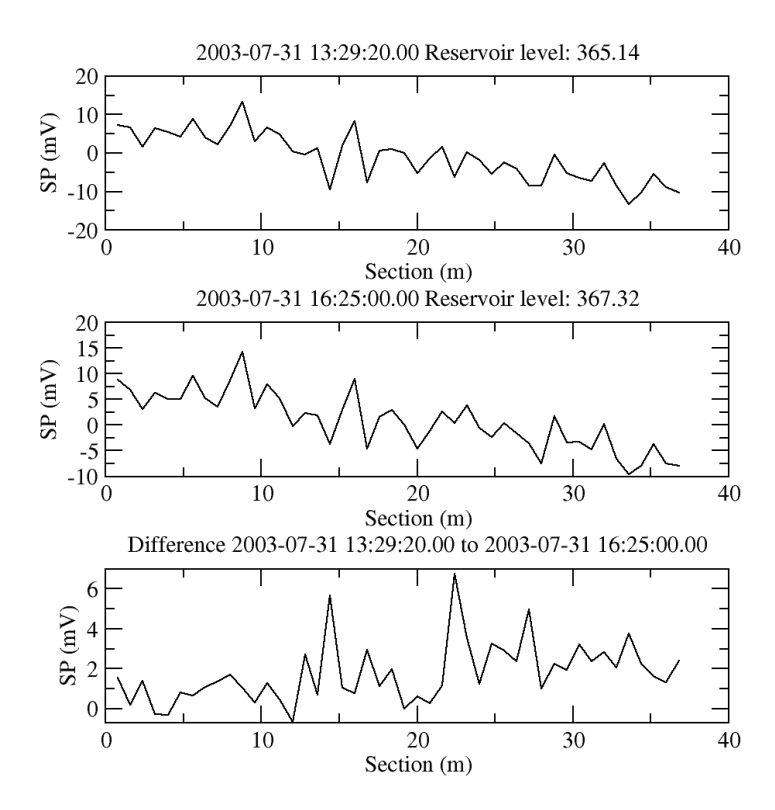


Figure 10-3 Processed profiles before (top) and at (middle) filling #2. Bottom pane shows difference.

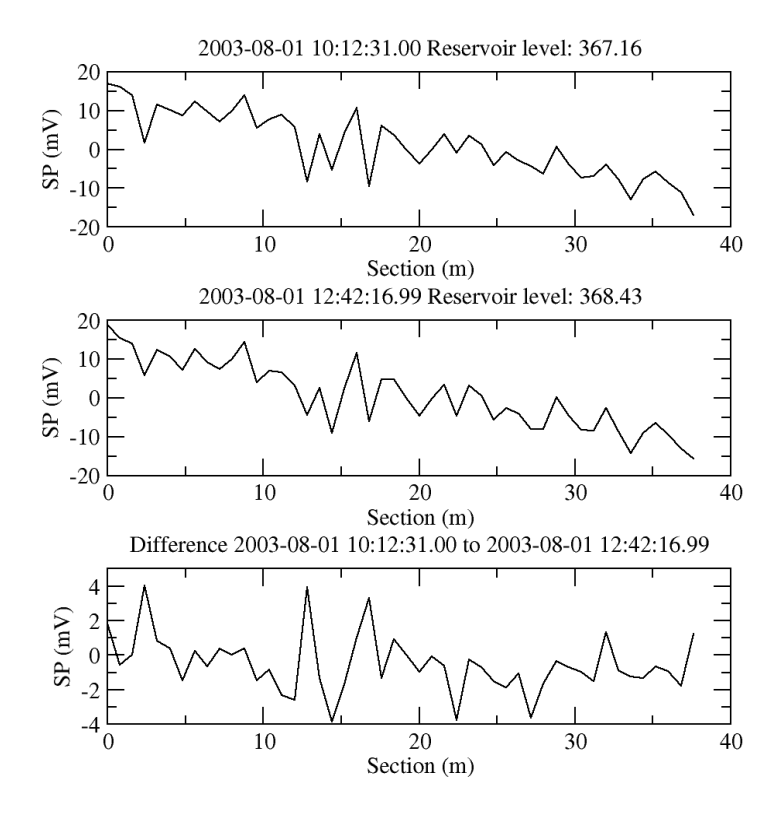


Figure 10-4 Processed profiles at fillings #2 (top) and #3 (middle). Bottom pane shows difference.

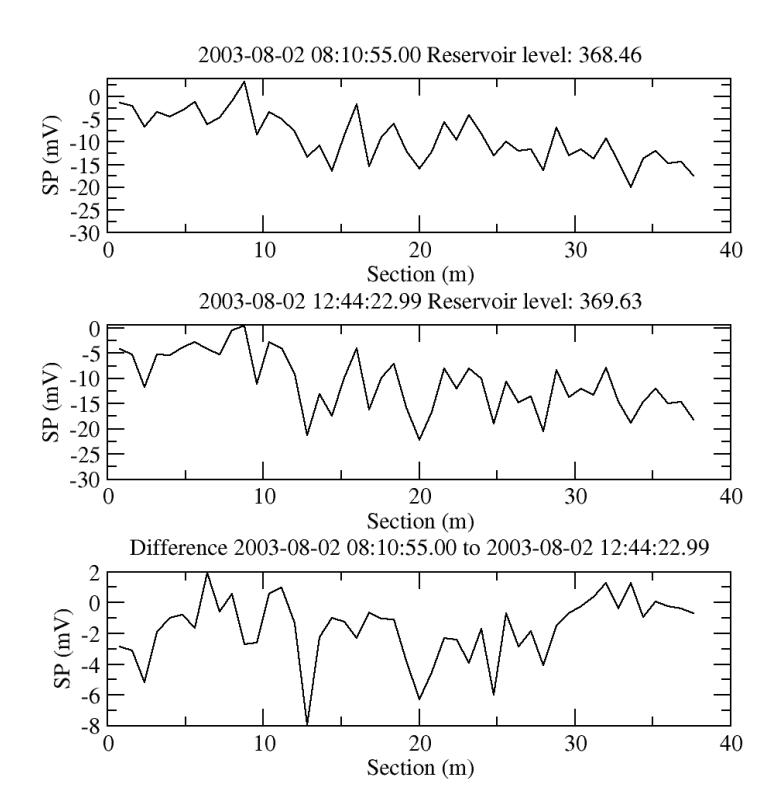


Figure 10-5 Processed profiles at fillings #3 (top) and #4 (middle). Bottom pane shows difference.

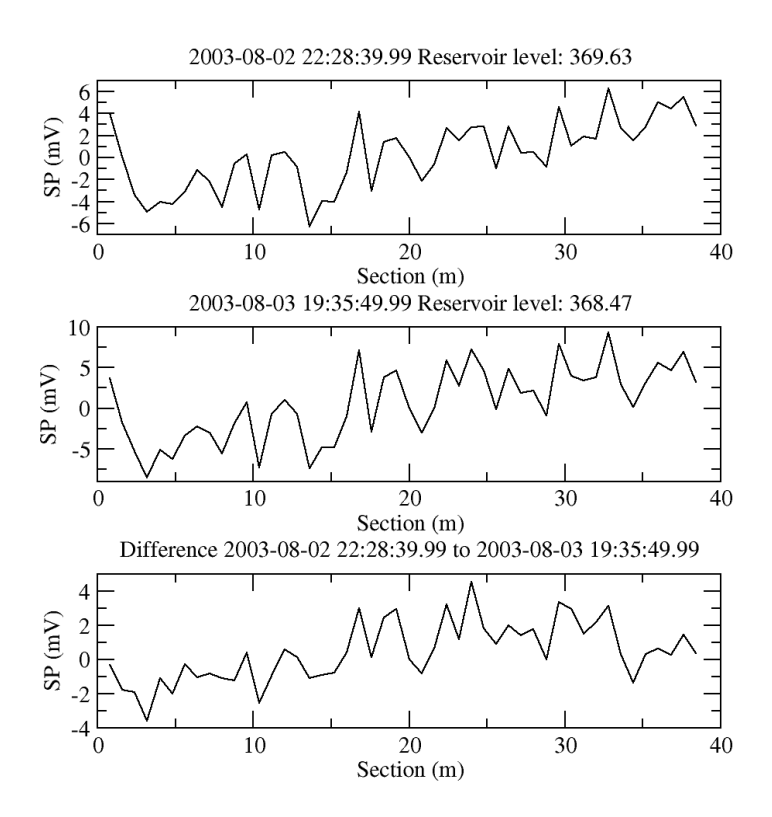


Figure 10-6 Processed profiles at fillings #4 (top) and #5. Bottom pane shows difference.

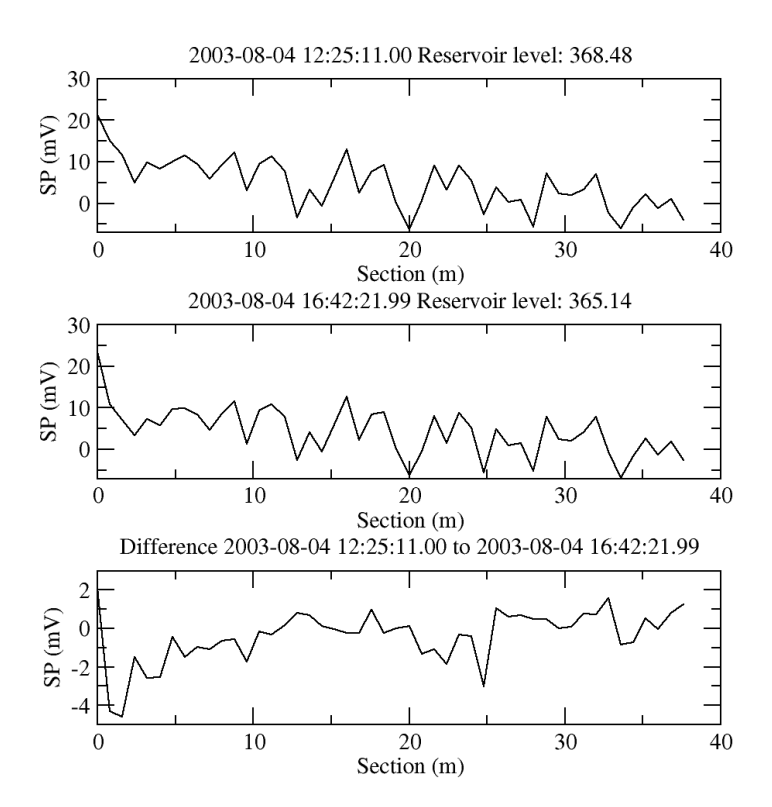


Figure 10-7 Processed profiles at fillings #5 (top) and #6 (middle). Bottom pane shows difference.

Table 10-1 summarises the anomalous areas identified above. If we ignore the areas that are defined by weak anomalies only (indicated by grey background in the table) the following interesting sections remain: 2.4, 12.8-14.4 and 20.0-24.8. These are interpreted as possible defect locations.

Table 10-1 Location of SP anomalies (defects).

Dam	Anomaly	Weak Anomaly	
section (m)	Observed at filling #	Observed at filling #	
2.4	1, 3, 4, 6		
3.2		5	
12.8	4	1	
14.4	2		
17.6		5	
20.0	4		
22.4	3		
24.0		5	
24.8	1, 2, 6	4	
27.2		2, 3	
28.0		1	
32.0		3, 5	
34.4		1, 6	

# 10.2 Resistivity effects

Resistivity variation impacts the amplitude of the SP anomalies directly. If there is an overall decrease in resistivity the SP anomalies will decrease approximately portion to the resistivity decrease. Figure 10-8 shows how the mean resistivity has varied during the measurement series. The mean resistivity here is a mean of the cell resistivities taken from the inverted sections based on gradient array data. Since cell size increases with depth this method gives higher weight to near-surface variation. It should nevertheless serve to give a coarse picture of the overall variation. At the highest water level the resistivity has decreased by approximately 50% and this is the order of reduction of SP one would expect. For example, the SP anomaly will be approximately constant if a water level increase will double the gradient and reduce the resistivity to the half. Consequently, the larger anomalies one would expect at higher water levels due to larger hydraulic potential gradients are to a large extent offset by this decrease in resistivity.

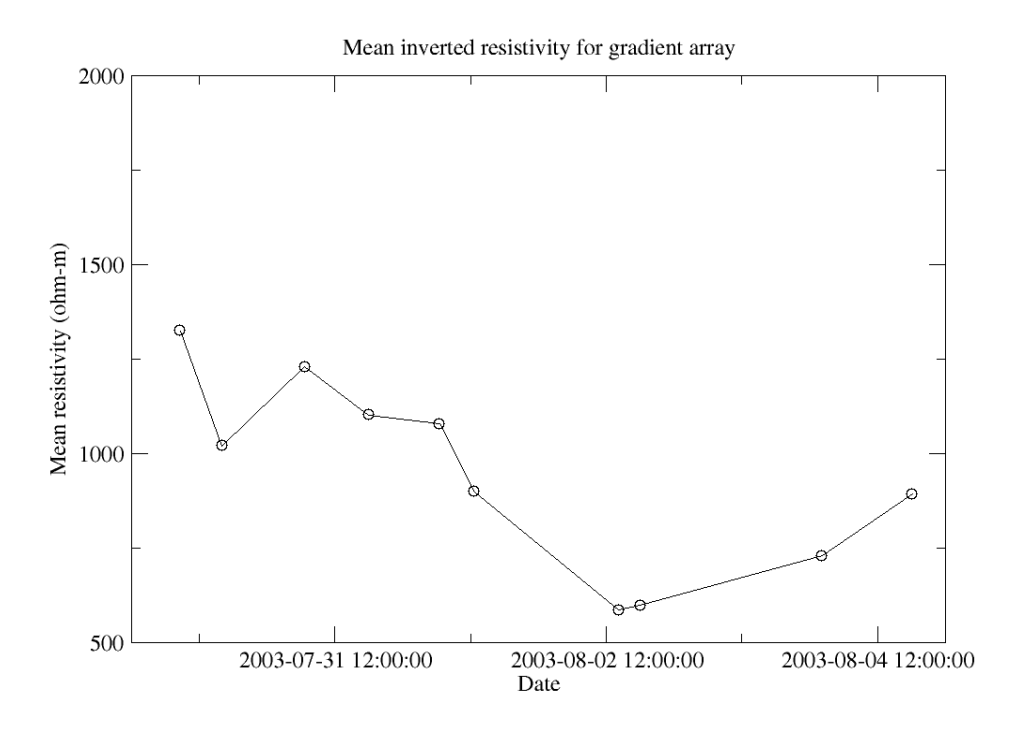


Figure 10-8 Variation of mean resistivity with time. Data are taken from inverted sections based on the gradient array.

### 10.3 One-time measurements

We performed a number of small SP survey measurements while monitoring data was collected. These data probably have lower resolution than the monitoring data and should be regarded as a supplement to the time-series measurements. The measurements were made with the total potential method employing a base electrode at the dam crest at section 37 m. The electrodes used were non-polarizable Cu-CuSO<sub>4</sub> electrodes. Voltage measurements were made with a portable high input-impedance A/D converter (Lawson

Labs). The very high input impedance (circa  $10^{13} \Omega$ ) of this device facilitates reliable observations even when the contact resistance between ground and electrode is high.

A loss of synchronisation between the measurement system computers used means that no real-time telluric correction is possible. The results must therefore be interpreted with caution. High frequency tellurics have been filtered out by the measuring procedure, however, and low frequency telluric components have been checked by making repeated observations on one of the electrodes in each profile. In all cases the drift observed during the measurement period was less than 10 mV. For the shoreline measurements the observed drift was less than 5 mV. These figures should give some indication as to the reliability of the observations.

# 10.3.1 Shoreline measurements

A number of profiles were measured along the upstream shoreline. A small vessel carrying the moving electrode was towed in the water. Note that this procedure means that the profile will move towards the crest of the dam as the reservoir water level increases. Figure 10-9 shows plots of the observed SP-anomalies. Apart from some disturbances at the beginning of the profile measured at reservoir level 369.63 metres the noise levels are low. Repeated measurements at the first electrode station show that the drift during measurements is less than 5 mV, well below the amplitude of the anomalies. Since this sort of drift control relies on the assumption that the drift is linear with time it is not absolutely sure that there have been no low-frequency telluric disturbances during the measurement. The similarity between the profiles, however, indicates that such disturbances have not likely influenced the observations.

All three anomalies appear slightly bowl shaped possibly reflecting the depth to the bedrock foundation. The most interesting feature, however, is the strong minimum that occurs at section 30 metres as the reservoir level is increased. Such a minimum would be expected where there is a concentration of influx of water into the core. It should be noted, however, that strong resistivity variations have been observed during the filling of the reservoir, and it is not impossible that this variation contributes significantly to this anomaly.

An equivalent point source interpretation of the depth to the anomaly source shows that the source should lie about 2-3 metres below (or more correctly distant from; the source need not lie directly below the profile) the profile. This means that the source should be located at a level of about 366-367 m.

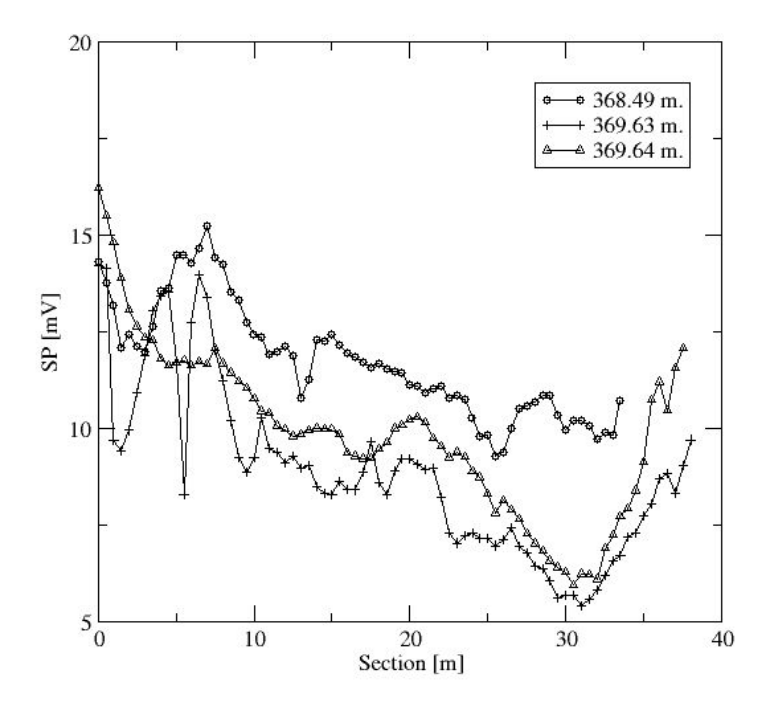


Figure 10-9 SP-profiles along the upstream shoreline measured at different reservoir levels as shown in the legend.

# 10.3.2 Cross profiles

A number of profiles perpendicular to the dam crest were measured at sections 10, 21, and 31m; these are shown in Figure 10-10, Figure 10-11 and Figure 10-12. The profiles are quite noisy and it is difficult to draw any strong conclusions from them. One would expect the anomalies to increase going downstream. This seems to be the case with the profiles at sections 10 and 21m, although the strong positive tails in sections 10 and 21m are probably caused by the observation point moving closer to the concrete foundation that lies under part of the dam. The fact that the anomaly decreases going downstream at section 31m if also difficult to explain, but the observation strengthens the observation in the preceding that the part of the dam around section 30m is anomalous.

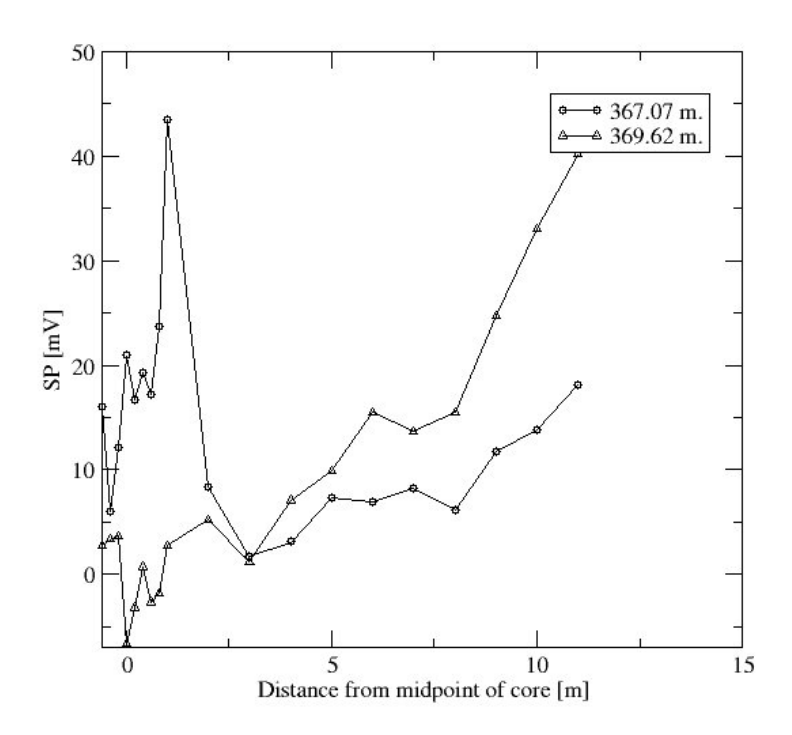


Figure 10-10 Cross-profile at section 10m.

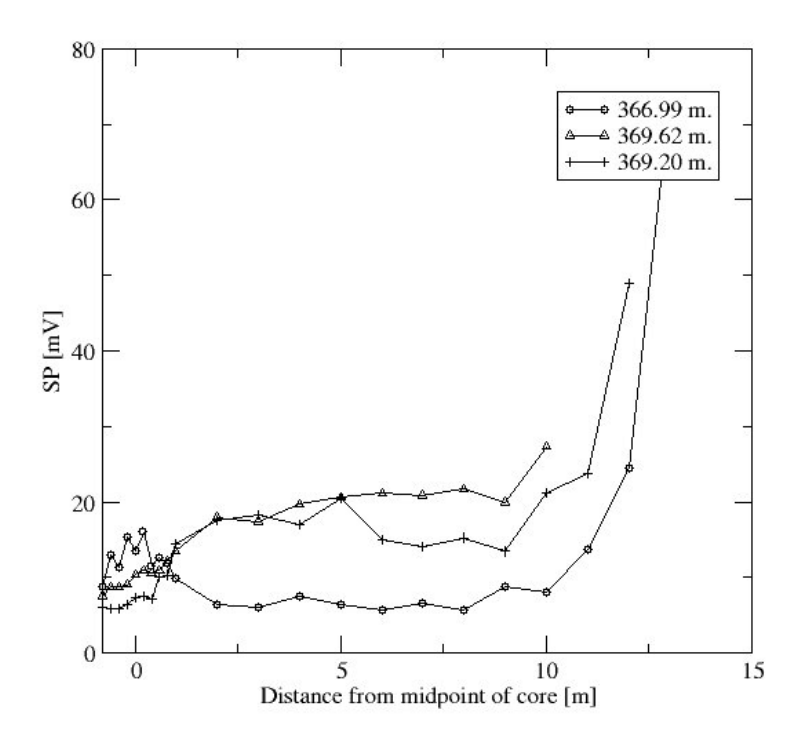


Figure 10-11 Cross-profile at section 21m.

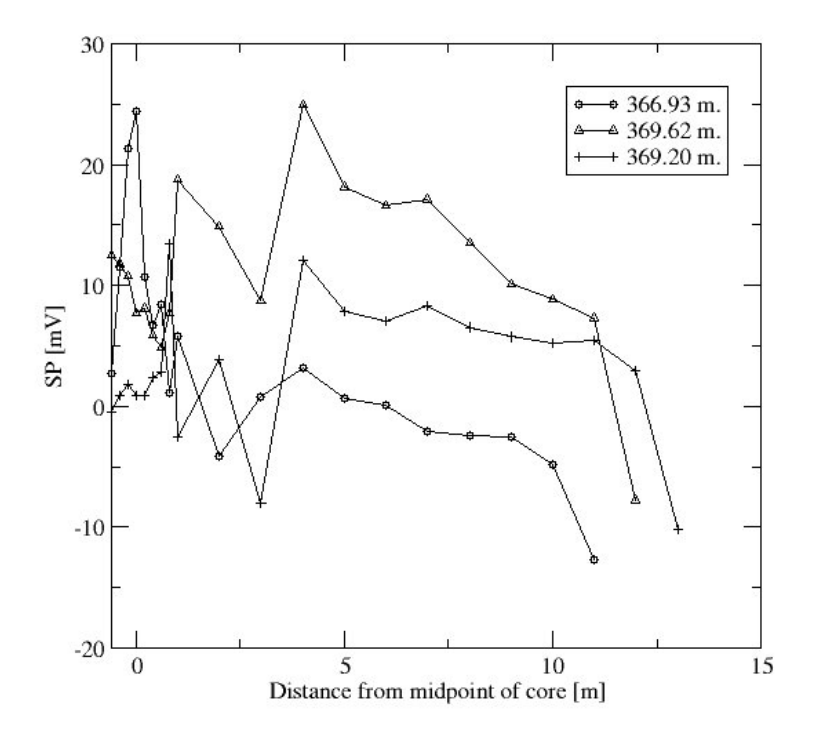


Figure 10-12 Cross-profile at section 31m.

#### 10.4 Conclusions

The SP-data were difficult to interpret because of several factors:

- The telluric disturbances were high
- The resistivity variation was higher than expected
- Observations were made during strongly transient conditions.

Despite the problems the SP time-series measurements have isolated three possible defect areas at sections: 2.4-3.2, 12.8-14.4 and 20.0-24.8m. It was not possible to estimate the source depth for these anomalies. The first of the anomalies is probably caused by seepage along the transition between the dam and the foundation and is probably not a designed defect.

There are also a number of weaker anomalies that one would not dare interpret as possible defects areas based on SP alone. Section 27.2-28m is one such example. It is very weakly defined in the SP data but temperature data, resistivity data, and visual inspections have indications in this area.

The survey profiles add little information. The shoreline profiles are the most interesting ones where a distinct anomaly occurs around section 30m. The estimated source depth of this anomaly is 2-3 metres.

## 10.5 Detected defects

The detected potential defects are shown in the table below. Evaluation of the defect elevations are estimated on the filling levels, except for the defect at section 30m, which is evaluated as a point source.

Table 10-2 Location of detected potential defects. Weak observations are indicated by (w).

Dam section (m)	Observed at	Comments	
2.4-3.2	Filling 1, 3, 4, 6 5 (w)	<368m	
12.8-14.4	Filling, 2, 4 1 (w)	<368m	
20.0-24.8	Filling 3, 4, 5 (w)	<368.5m	
27.2-28.0	Filling 1(w), 2(w), 3(w)	<368m, very tentative result	
30	Shoreline profile	367m	

# 11 Visual observations

#### 11.1 General

During the installation of the electrodes a preliminary visual inspection was done. A thick steel plate was found on the crest (Figure 11-1), but originally only a few cm could be seen on the surface. The plate was removed. Two cables were also found on the crest and removed. One "U-beams" was found on the downstream slope, which unfortunately could not be removed. The dam toe was visually inspected regularly.



Figure 11-1 Steel plate found on the crest.

# 11.2 Dam toe observations at filling #1

No routine observations were made during filling #1, on July 30. A leakage at section 27m was detected around 14:00, just after the filling started. Water started also to overflow the weir at the same time.

# 11.3 Dam toe observations at filling #2

On July 31, the entire dam toe was dry until 13:43 (at water level about 366m) when a water outflow was found at section 27m, about 1.5m above the dam toe. The outflow area was about 0.5m wide and about 0.3m high, but the seepage was concentrated to two small outflow leakage areas. The rest of the dam toe was dry until the water started to fill up the area upstream the weir. No other wet areas could be observed during the afternoon.

A heavy rain during the evening saturated the dam toe that was still wet the following morning. Inundating water caused by the weir was observed from sec 23m to the end of the dam with depths up to about 5cm. A leakage was observed at the left abutment concentrated to connection to the rock, causing standing water up to sec 2m.

# 11.4 Dam toe observations at filling #3

Filling #3 caused slowly increasing flow at both of the previously observed leakage areas. After some ours, standing water was also found between section 4 and 5m. Around 14:00 some outflow was found from the rock on the left side. A very moist area was observed around section 18m. Water was also flowing under the concrete bar. All seepage from the dam will not be measured by the seepage weir. Water was also flowing along the drainage pipes (section 8.5m), embedded in clay below the dam.

Generally, the same situation was found in the afternoon (around 16:30). Affected areas were increasing, and the soil also became more or fully saturated. Standing water was found at section 21 and 23m.

At about 21:00 very moist/wet areas was found between section 12 and 19m, and almost saturated around section 22-23.5m. The leakage flows at the old leakage areas were stable.

## 11.5 Dam toe observations at filling #4

Due to the rain the entire dam toe was wet before filling #4 started. An increasing flow with clear water was observed at the left abutment. Muddy water was found at section 2-4m at 11:30. The entire area between section 12-19m was saturated, and water was standing from section 22m to the end of the dam, and between section 6 and 11.5m. This may also be sign of a small leakage in this area.

## 11.6 Detected leakages

In summary, several areas with larger outflow were found by visual inspection. Due to the various water levels, some indications were achieved about the inflow level of the defects. These indicated levels are more distinct at high leakage than at low leakage due to the time for the water to pass the dam. Small and diffuse water outflow is further more difficult to detect and estimate, especially at rainy weather. Note also that we can't be sure that the outflow and defect are located in the same section.

Table 11-1 Summarised result from visual observations.

Dam	Observed at	Outflow	Inflow	Extension	Estimated
section		level	level		Seepage flow
		(m)	(m)		(1/s)
Sec 0-2m	Filling #1 and	Dam toe	367		
	#2	+0.5m			
	(Morning after	(Seepage			
	lowering the	face in			
	reservoir)	silty clay)			
Sec 4-6m	Filling #3	Dam toe	368.5	1-2m wide	
	_				
Sec 6-	Filling #4	Dam toe	369.5	3-5 m wide	
11.5m					
Sec 8.5m	Filling #3	Dam toe	368	Around the	0.2
		– 1m		pipe	
Sec 18,	Filling #3	Dam toe	368	2-3m wide	
21-23m					
Sec 27m	Filling #1 and	Dam toe	366.5	0.5x0.3m	0.1-0.3
	#2	+1.5m			

## 12 Field measurement - Discussion

# 12.1 Real conditions versus assumptions in the Pre-study

Real transient processes in the field were found to be more complicated than what was foreseen in the Pre-study. The transient thermal impact was close to expected, but the short time temperature changes (due to changed weather) were not considered. The additional variation was however useful.

The conditions for resistivity measurements were favourable in terms of electrode contact, which in combination with the short electrode separations resulted in very good data quality. The electrode distance was 2/3 of a metre for the measurements, which is an improvement over the 1 metre spacing used for modelling in the Pre-study.

The resistivity of the reservoir water was lower than assumed in the pre-study, which will affect the contrast between materials so that water saturated defect zones will have less contrast against surrounding core material than anticipated.

The resistivity of the unwashed downstream support fill was probably lower than expected in the Pre-study. The clay used for sealing on the rock foundation was not anticipated in the Pre-study. This clay is expected to have a very low resistivity and if it was extensively used it would constitute a very conductive layer at the bottom of the dam and thereby create difficulties for the method in handling the very high contrasts in resistivity compared to the rock. This will definitely decrease the resolution of the method in this zone.

Further consideration is required for the change in resistivity with time in the core material, as documented in laboratory tests and in the field measurements. One explanation for the increase in resistivity could be the type of change in resistivity that has been documented in the laboratory. Since the core was built from compacted moraine a few days earlier, a similar process is likely to have been in progress in the dam during the measuring period. Another possible explanation for the increase in resistivity could be if the core material contained excess ions at the construction that have been washed out. Excess ions could be derived from the natural sources such as groundwater, or human activities, where the material was taken. If this is the case the resistivity would increase after a while when the original pore water has been washed out by the reservoir water that is lower in ion content. Yet another mechanism that may be contributing to the increase in resistivity is washout of fines in the upstream support fill, it was observed during the filling of the reservoir that fine material migrated out into the reservoir water. Other options could be other time dependent changes in the electro-chemical system, possibly affected by change in pore water pressure. In any case, it is most likely that such effects will only occur during a short period after the construction of a dam, and would not be an issue for existing dams.

The conditions for the SP measurements were found to be more complicated than was assumed in the pre-study. The resistivity of the core material and the reservoir water was lower than expected. This means that any SP anomalies will be attenuated in comparison

with the pre-study. Before the laboratory measurements of the streaming potential cross-coupling coefficient are finished we cannot say whether the assumptions about this parameter were reasonable. One should however note that in general the cross-coupling coefficient will decrease as the resistivity decreases. The reason is that the electric double-layer will be compressed when the ionic strength of the electrolyte increases. Still, this effect is probably insignificant since the electrolytes (water) here are quite diluted.

#### 12.2 Results

Defect areas have been identified by all methods in different ways. The only method that can identify the defect location both in dam section and level is resistivity (assuming 2D conditions). From previous studies we know that we should compensate for the 3D-reality. The same conditions may also be valid for IP that also is showed.

SP-measurement can normally be used to estimate the depth, provided the shape of the anomaly can be accurately determined. The very small anomaly amplitudes together with the rather large electrode polarization offsets make this unrealistic in this case. The levels for defects observed by SP have therefore been estimated based on water level information and only the maximum highest extension is showed in the figures.

The agreement between resistivity and IP is good, where a resistivity anomaly is followed by a decrease in IP, except for one defect that is observed by resistivity only (Figure 12-1). Good agreement is also achieved between resistivity and SP around section 22m and maybe at section 27m. The location of the other defect areas differ some metres between the methods.

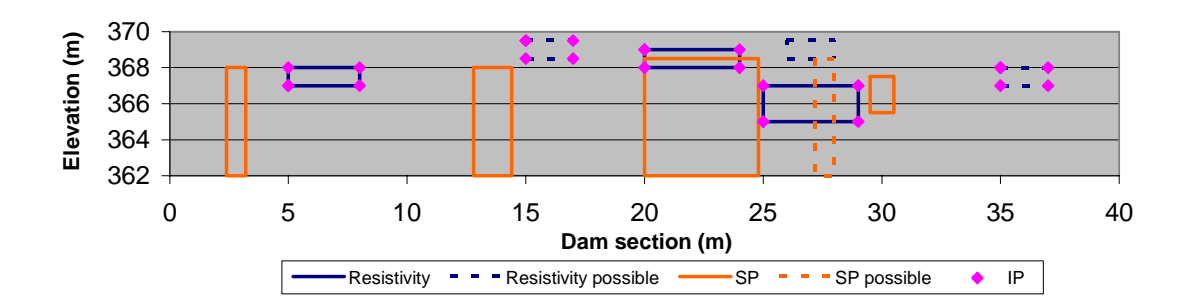


Figure 12-1 Result from all electrical methods. Note that the defect elevations for SP are based on water level information.

The levels of the defects observed by temperature and visual inspections have as SP been estimated based on water level information and just the maximal highest extension is showed in the Figure 12-3. The temperature measurements give however some additional information that allows an estimation of the lower limit. Both these methods use information from the dam toe, i.e. not in the core where the defects are located. The two methods agree well. It seems as the temperature gives a more distinct location of the defect

at the dam toe, which may be explained by a more sensitive response and less affected by standing water etc.

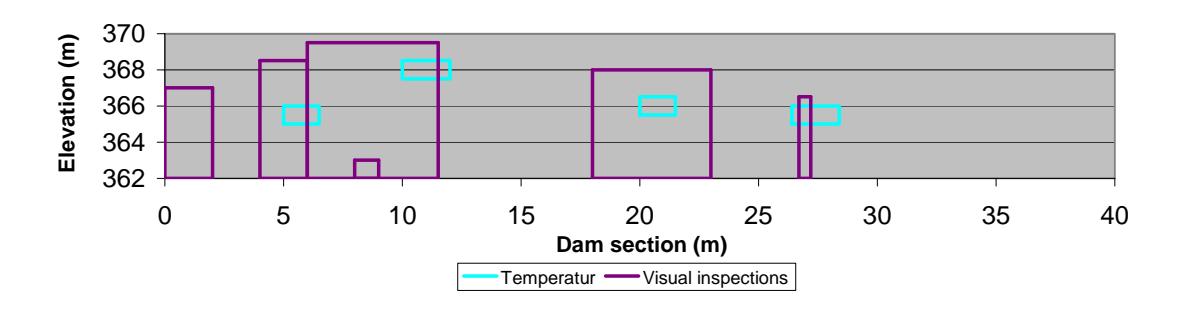


Figure 12-2 Result from temperature measurements and visual inspections at the dam toe. Note that the elevations for the defects are based on water level information.

The collected final information from all methods shows three main defect areas (Figure 12-3). The most significant defect is found around section 22m, which is shown by all methods. The elevation is more uncertain varying from elevation 365 to 368m.

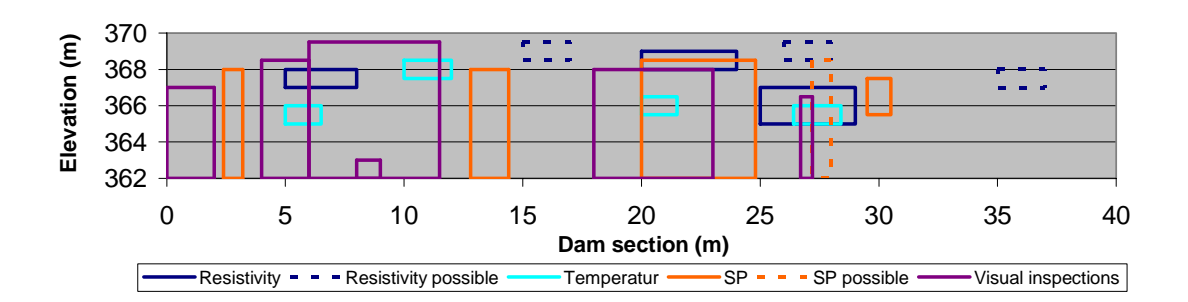


Figure 12-3 Summarized result from all methods. Note that the elevations for the defects are based on water level information for all methods except resistivity. The height is also set constant to 1m for all methods except resistivity.

A second significant defect is observed at section 27m at elevation 365-367m. The SP anomaly is however weak and interpreted only as possible defect.

A third area is probably somewhere around section 5m, and at any level between 365 and 369m. This defect is probably more diffuse and also located closer to the abutment where the detection and resolution capabilities of the methods are reduced.

Some single "SP defects" and "possible resistivity defects" can also be seen which don't agree with any other method. This is not unexpected because no method is infallible. This fact supports the recommendation to use several methods when feasible.

#### 12.3 Field scale versus other scales

# 12.3.1 Scale factors for temperature

The temperature variation measured at the dam toe can be described in dimensionless form (Johansson 1997) using a dimensionless temperature T' and the dimensionless distance x', assuming concentrated seepage flow in a limited area with a constant height, H. They are defined as:

$$T' = \frac{T_{\text{max},0} - T_{\text{min},0}}{T_{\text{max},1} - T_{\text{min},1}}$$

and

$$x' = \frac{\lambda_0 x}{C_0 v_T H^2}$$

Assuming a constant dimensionless temperature the result will be equal for all x' i.e. 10 times larger distance (x) will need 10 times larger seepage (expressed by the thermal velocity,  $v_T$ ).

# 12.3.2 Scale factor considerations for resistivity imaging

In transferring the results to full-scale dams it must be considered that the resolution capability of resistivity imaging reduces with increasing depth. On the other hand, monitoring will increase the resolution capability through the seasonal variation in temperature and TDS of the reservoir water, which acts as a natural tracer. Furthermore, seasonal temperature variation will affect the resistivity not only in a defect area itself, but also in a zone around it thus increasing the size of the "target".

#### 12.3.3 Scale factor considerations for SP

The present investigation was performed on a scaled down embankment dam. How do the results apply to a full-scale investigation? We can assume that the material properties, i.e., resistivity, hydraulic conductivity and cross-coupling coefficient do not depend on the scale of the experiment. If the linear dimension scale factor is n, the following observations apply:

- The hydraulic potential is proportional to *n*.
- The hydraulic gradient does not change.
- For a given set of current sources the electric potential scales as 1/n.
- The cross-sectional area of an isolated seepage zone scales as  $n^2$ .

Consider here the simplified model used in the pre-study. For this case the anomaly amplitudes are determined by the strength of the streaming current discontinuities at the ends of the seepage zone. The streaming current density is proportional to the hydraulic

#### **ELFORSK/BC Hydro**

gradient, and hence not affected by scaling. The total streaming current is the product of the streaming current density and the cross-sectional area of the seepage zone and consequently scales as  $n^2$ . The SP anomaly can be viewed as the scaled up effect of equivalent current sources and thus scales as  $(1/n) \cdot n^2 = n$ .

The consequence of the above is that as the size of a dam increases the relative size of the seepage zone decreases if the SP is constant. In the pre-study, for example, we saw that to be detectable the seepage zone had to be about 1 m<sup>2</sup>. If we increase the linear scale of the dam 10 times the result is that the SP anomaly increases by a factor 10 also, but for this case the seepage zone then has an unrealistic area of 100 m<sup>2</sup>. If the SP anomaly was to be unchanged the area of the seepage zone need only be 10 m<sup>2</sup>, still large but not completely unrealistic.

# 13 Proposed next steps

This test site at Røsvatn is unique and the result from the field test must be evaluated carefully in order to take out all information before planning new tests. The presentation in this report is so far made as a typical dam investigation, but there is still material that can be further evaluated.

It is important to allow an extensive evaluation of the measuring results from the test dam and compare the result with the known defects before taking any further steps. This should be carried out as far as possible. However, some suggestions about following steps are presented below. The extent for each step must of course be modified due to the detection ability for the methods used.

# 13.1 First step - Collection of experience

The main objective for this step is to understand why the result was "good or bad". This includes:

- Collect real material at a (lab test) especially permeability, porosity, soil gradation, resistivity, cross coupling coefficient and compare this with assumed input data in the "Pre-study",
- Identify all kind of relevant data that was not included or discussed in the "Pre-Study" (such as clay above the bedrock, water quality),
- Discuss the influence transients effects in temperature, saturation, and water conductivity,
- Repeat some parts of the pre-study with real data and compare the result; and,
- Simulate the real defects using the modelling tools and try to match measured and simulated data using input from laboratory test.

This step should be done by the "monitoring group" extended with Megan Sheffer and Dr. Bob Corwin, together with the "defect design group", and presented as Part 3 in this project.

# 13.2 Second step – Transferring result to other scales

The main objective for this step is to extend the knowledge to other scales, especially to full scale dams, both for investigation and monitoring aspects. The modelling tools used in the first step may be sufficient (the result is so far unknown) otherwise the tools have to be improved.

• Study how the field test specific situation will apply for the real situation in full scale, and for the laboratory scale,

#### **ELFORSK/BC Hydro**

- Use field data from Hällby, Sädva, Mica ... as reference cases and add artificial defects to check the result from the up-scaling,
- Repeat and improve the "Parameter study"; and
- Investigate other methods, especially IP.

This step should also be done by the "monitoring group" extended with Megan Sheffer and Dr. Bob Corwin, together with the "defect design group". Independent laboratory test could be carried out somewhere else, perhaps as Ph.D-projects.

# 13.3 Third step - Repeated or new tests in different scales

The main objective for this step is to extend the knowledge to verify previous result from different scale in a systematic and scientific way. The ambition should be higher than what's normally necessary for dam owners, and for practical applications. Other methods may also be included.

- Identify defects that could be studied systematically and isolated in laboratory scale.
- Model simulations for laboratory scale and field test scale.
- Measurements in the field tests scale.
- Compare simulated and measured result in laboratory and field.

The entire part, or at least the first two points above, is appropriate within a Ph.D-project, preferably supervised by the "monitoring group". The project must however be made in close contact with both the "defect design group" and the "monitoring group".

# 14 Conclusions

All these conclusions are drawn without any knowledge of the real location of the defect. Some of the conclusions may therefore not be valid in full, when the real defect locations are revealed, and the result may have to be re-evaluated.

The result from the field test should be further evaluated before planning any new tests in laboratory and in the field. It is also important to compare the result with the known defects before taking any further steps.

There is a good agreement between the results of the different methods tested, and the methods support each other in the composite evaluation. Geophysical methods should as far as possible be used together in order to improve the quality and reliability of the evaluation.

Visual inspection and photo documentation is important and can give valuable input for the composite evaluation of the geophysical results. Documentation from the dam construction in the form of drawings of e.g. depth to foundation can be valuable, and may be used as input in the inverse model interpretation of the geophysical data to enhance the resolution and reduce ambiguities. That was not an option in this case, but the data may be reevaluated using such input. It should be pointed out, however, that such options are still in their infancy in available software and will require further research and development.

The test with Induced Polarisation (IP) measurements showed an agreement with resistivity measurements and IP should be further tested also for seepage detection in embankment dams. The measurements at Sädva could be extended with IP in the near future. More basic research is also needed to get a better understanding of the method.

Field tests, as well as earlier experience from dam monitoring, show that single measurements are difficult to evaluate since too many variables are unknown or uncertain. Repeated measuring (or better, regular monitoring) is strongly recommended. As demonstrated in this study repeated measurements at different reservoir water levels give valuable information on the variation in properties in the dam.

Temperature measurement at the dam toe may be a good complement to visual inspections for seepage outflow detection at the dam toe, and can be performed also during the rainy season. The sensors (or preferably an optic fibre) should be buried close to the seepage face or deeper (preferable about 1 m below the surface). The method can be applied also for large dams.

# 15 Acknowledgement

This project has been challenging in several ways and we are grateful to all support given by the sponsors as well as the interest shown by the design group and the reference group.

We appreciate and acknowledge the support given by Frank Tverrå, Edvin Lorenzen, and the staff at Statkraft at Korgen during the field measurements.

Finally, we would also like to express our gratitude to Dr. Bob Corwin for sharing his deep and unique experience in SP monitoring and modelling, despite his limited health. Bob, we wish that these results will inspire you in your recovery.

# 16 References

- Archie, G.E. (1942) The electrical resistivity log as an aid in determining some reservoir characteristics, *Petroleum Transactions of the AIME*, **146**, p 54-62.
- Bergström, J. (1998) Geophysical Methods for Investigating and Monitoring the Integrity of Sealing Layers on Mining Waste Deposits, Licentiate thesis, Luleå University of Technology, ISSN 1402–1757, ISBN LTU-LIC--98/24—SE, 77p.
- Corwin, R.F. (2002) CEA SP Field Manual Self Potential Data Acquisition in Support of Dam Seepage Investigations, CEATI Report No T992700-0205.
- Friborg, J. (1997), Experimental and theoretical investigations into the streaming potential phenomenon with special reference to applications in glaciated terrain, Ph.D. thesis 1997:02 L, Luleå University of Technology.
- Johansson, S. and Dahlin, T. (1996) Seepage monitoring in an earth embankment dam by repeated resistivity measurements, *European Journal of Engineering and Environmental Geophysics*, vol 1, no 3, p 229-247.
- Johansson, S. (1997) Seepage Monitoring in Embankment Dams, Doctoral Thesis, TRITA-AMI PHD 1014, ISBN 91-7170-792-1, Royal Institute of Technology, Stockholm.
- Johansson, S., Claesson, J., Dahlin, T., Friborg, J., Hellström, G., Bing, Z., (2001) A Parameter Study For Internal Erosion Monitoring. Still not released from CEA.
- Loke, M.H. (2001) Constrained time-lapse resistivity imaging inversion. *Procs. SAGEEP* 2001 (Symposium on the Application of Geophysics to Engineering and Environmental Problems), Denver, Colorado, March 4-7 2001.
- Loke, M.H., Acworth, I and Dahlin, T. (2001) A comparison of smooth and blocky inversion methods in 2-D electrical imaging surveys, *Procs. ASEG 15<sup>th</sup> Geophysical Conference and Exhibition, August 2001, Brisbane.*
- Olhoeft, G. R. (1985) Low-frequency electrical properties, *Geophysics*, 50(12), 2492-2503.
- Scott, J. and Barker, R. (2003) Determining pore-throat size in Permo-Triassic sandstones from low-frequency electrical spectroscopy, *Geophysical Research Letters*, **30(9)**, 1450, 3-1 3-4.
- Schön, J., (1996) Physical Properties of Rocks: Fundamentals and Principles of Petrophysics, Handbook of Geophysical Exploration: Vol. 18, Redwood Books, Trowbridge. Schopper, J.R., 1982. Electrical conductivity of rocks containing electrolytes. In: Landolt-Börnstein, Group V, Physical Properties of Rocks, 16: 276-291, Springer-Verlag.
- Sjödahl P., Dahlin, T., Zhou, B. and Johansson S. (2002) Monitoring of Leakage in Embankment Dams through Resistivity Measurements A 2.5D Modelling Study, *Procs. 8th EEGS-Meeting, Aveiro, Portugal, 8-12 September 2002*, 4p
- Slater, L. and Lesmes, D. (2002) IP interpretation in environmental investigations, *Geophysics*, **67(1)**, 77-88.

#### ELFORSK/BC Hydro

- Sumner, J.S. (1976) *Principles of induced polarization for geophysical exploration*, Developments in economic geology 5, Elsevier, Amsterdam, 277p.
- Zhou, B. and Greenhalgh, S.A. (2001) Finite element three-dimensional direct current resistivity modelling: accuracy and efficiency considerations. Geophys. J. Int. 45, 679-688.



# **ELFORSK**

SVENSKA ELFÖRETAGENS FORSKNINGS- OCH UTVECKLINGS – ELFORSK – AB Elforsk AB, 101 53 Stockholm. Besöksadress: Olof Palmes Gata 31 Telefon: 08-677 2530. Telefax 08-677 2535 www.elforsk.se